IDENTIFICATION OF ADAM17 SUMOYLATION, EXAMINATION OF ITS EFFECT ON PROTEIN STABILITY, AND CONFIRMATION OF CAS9 POST-TRANSLATIONAL MODIFICATIONS BY PROXIMITY LIGATION ASSAYS

by

Özgecan Ayhan

B.S., Mathematics Teacher Training Education, Marmara University, 2010

M.Sc., Molecular Biology and Genetics, Boğaziçi University, 2014

Submitted to the Institute for Graduate Studies in
Science and Engineering in partial fulfillment of
the requirements for the degree of
Doctor of Philosophy

Graduate Program in Molecular Biology and Genetics

Boğaziçi University

2024

ACKNOWLEDGEMENTS

I never expected that writing the acknowledgments would be the most challenging part. There are countless people I am deeply grateful for, and I could write an entire thesis on them.

I am deeply grateful to my thesis supervisor, Dr. Umut Şahin, for his unwavering guidance, endless patience, and invaluable insights that have been instrumental in shaping this research endeavor. I would also like to express my sincere gratitude to my thesis committee members, Dr. Nurhan Özlü and Dr. Batu Erman, for their thoughtful feedback and encouragement throughout this process. Additionally, I am deeply grateful to Dr. Necla Birgül İyison and Dr. Nesrin Özören for their valuable time and insightful contributions in evaluating this thesis. I extend my profound gratitude to Dr. Tolga Sütlü for his invaluable guidance and unwavering encouragement and support, both in academic matters during my thesis progress and in the lab, as well as on a personal level. I am also deeply grateful to Dr. Stefan Fuss for his valuable guidance during the confocal training, as well as for his supportive advice and enduring friendship. I would also like to express my sincere gratitude to Dr. Tolga Emre and Dr. Ulduz Sophi Afshar for their valuable contributions to this study. Finally, I would like to thank my master's thesis advisor, Dr. Aslı Tolun, who introduced me to the field of molecular biology and genetics, inspired me to pursue this academic path, and who has consistently believed in my abilities.

I am deeply grateful to all the current and previous members of the SUMO Lab. I would especially like to thank Tunahan Ergünay for his valuable contributions to this work, his consistently positive attitude, his support and assistance in the experiments, and his excellent friendship and companionship. I am deeply grateful to Bahriye Erkaya and Yusuf Tunahan Abacı for their valuable teachings, guidance, and assistance in the lab. I also appreciate Arda Baran Çelen's contribution to this work and his instruction on AP Assays. I am also deeply grateful to my interns Selin Bereketli, Kumru Kaleli, Göksu Bayrak, Özge Özdemir, and Ata Kulalı for their invaluable assistance in the experiments. In particular, Selin and Kumru's exceptional efforts were instrumental in enabling a significant part of this

study. Teaching them was a rewarding experience from which I learned a great deal. Additionally, I am deeply grateful to Egemen Şahin for his steadfast support and tireless efforts to assist me in the lab. His patience in addressing my problems and his dedication to finding solutions have been invaluable. Furthermore, I am thankful to the other members of the SUMO Lab, including Emre Pekbilir, Duygu Yeşildağ, Harun Öztürk, Sezgi Canaslan, and Panagiota Georgiadou, for their constant support and help in the lab.

I would like to extend my deep gratitude to all the members of the MBG group. I am particularly thankful to Dr. Davod Khalafkhany for his invaluable contributions, including thought-provoking brainstorming sessions, insightful guidance on experimental procedures, and his wonderful companionship during our late-night shifts in the lab, where he would often provide uplifting musical accompaniment with his guitar. I am also deeply grateful to Dr. Yiğit Kocagöz for his warm friendship and companionship during the long hours spent working at the confocal microscope facility, as well as for his patience and unwavering support in my personal life. It is a pleasure to acknowledge Elif Darbuka Tula for her valuable assistance with cell culture, her consistently supportive and joyful attitude, and her wonderful friendship and companionship, especially during the challenging times of the COVID-19 pandemic. I am also grateful to Barbaros Düzgün for his valuable troubleshooting and experimental support. I would also like to extend my sincere gratitude to all the members of the AKİL and Sütlü Labs, including Özen Kaya, İlke Suder, Efe Elbeyli, Hilal Ok, Öykü Çakır, Elif Çelik, Mert Kaya Aras, Cevriye Pamukçu, and Zeyneps, for their valuable contributions and support.

I am deeply thankful to the professors and administrators at the Department of Molecular Biology and Genetics at Boğaziçi University for creating an environment conducive to academic growth and providing the necessary resources and infrastructure for this research. I am deeply grateful to Ümit Bayraktar and Aslı Gündoğdu for their help and support during the difficult times.

Finally, I am deeply grateful to my family, friends, and loved ones for their unwavering support, constant encouragement, and unconditional love throughout this journey. Their steadfast belief in me was essential to the successful completion of this work.

My mother, Medine Ayhan, and my brother Umutcan Ayhan have been amazing in supporting me and guiding me through the tough parts of this whole process. Their unwavering emotional support and invaluable guidance were instrumental in helping me navigate the challenges of this endeavor. Although my father, Ahmet Ayhan, passed away before he could witness this; his love, compassion, and support have remained a constant source of inspiration to me, and his presence continues to be felt in my life. I am deeply grateful to my cats Şapşik, Misscat, and Afrodit for their unconditional love and for teaching me patience. Also, I would like to thank my chosen family, my dear friends, Eyüp Yazıcı and Sercan Kaba, for their unwavering love, support, and encouragement throughout this endeavor. I am also deeply grateful to my spiritual guide, Vajracaksu Dharmachari, for his invaluable guidance and for helping me find inner peace and balance during the most stressful times of this journey. Finally, I am deeply grateful to Orhan Arslan for his valuable support and encouragement while writing this thesis. His presence and moral support in my defense were invaluable, helping me navigate this important milestone with confidence and composure.

I dedicate this work to my mother, Medine Ayhan, a breast cancer survivor whose resilience and unwavering spirit have been a constant source of inspiration, demonstrating the remarkable power of the human spirit to overcome adversity.

This research was made possible by the crucial financial support of TÜBİTAK (121C230), for which I am deeply grateful. Without this funding, this project would not have been feasible.

ABSTRACT

IDENTIFICATION OF ADAM17 SUMOYLATION, EXAMINATION OF ITS EFFECT ON PROTEIN STABILITY, AND CONFIRMATION OF CAS9 POST-TRANSLATIONAL MODIFICATIONS BY PROXIMITY LIGATION ASSAYS

Post-translational modifications, such as SUMOylation and ubiquitylation, are essential regulatory mechanisms that modulate various cellular processes, including gene expression, protein function, and signaling. These modifications can alter the stability, localization, and interactions of target proteins, thereby regulating a broad range of biological activities. This study investigated the roles of SUMOylation and ubiquitylation on CRISPR-associated Cas9 and the metalloprotease ADAM17.

Understanding the regulation of Cas9 through post-translational modifications is critical for improving the efficiency and specificity of CRISPR-based genome editing. In this study, a powerful and ultra-sensitive technique called proximity ligation assay (PLA) was employed to further verify that Cas9 is both SUMOylated and ubiquitylated. The PLA experiments also confirmed the major SUMO conjugation site of Cas9. Furthermore, PLAs have shown that Cas9's SUMOylation and ubiquitination modulate its subcellular localization by competing for the same lysine residue and acting antagonistically.

The regulation of ADAM17 activity by post-translational modifications is a critical area of research, as ADAM17 is a key enzyme that cleaves and releases numerous cell surface proteins, including cytokines, growth factors, and their receptors. This study showed for the first time that ADAM17 is subject to both SUMOylation and ubiquitylation and that these modifications have opposing effects on ADAM17 stability. However, further research is needed to identify the specific SUMOylation sites and their impact on ADAM17 stability, localization, and shedding activities.

ÖZET

ADAM17 SUMOYLASYONUNUN TESPİTİ, PROTEİN STABİLİTESİ ÜZERİNDEKİ ETKİSİNİN İNCELENMESİ VE CAS9 POST-TRANSLASYONEL MODİFİKASYONLARININ YAKINLIK LİGASYON ANALİZLERİ ILE DOĞRULANMASI

Post-translasyonel modifikasyonlar, SUMOlasyon ve ubikitinasyon gibi, gen ekspresyonunu, protein fonksiyonunu ve sinyalleşmeyi de içeren çeşitli hücresel süreçleri düzenleyen temel düzenleyici mekanizmalarıdır. Bu modifikasyonlar, hedef proteinlerin stabilitesini, lokalizasyonunu ve etkileşimlerini değiştirebilir ve böylece geniş bir biyolojik aktivite yelpazesini düzenler. Bu çalışmada, SUMOYlasyon ve ubikitinasyonun CRISPR ile ilişkili Cas9 ve metalproteaz ADAM17 üzerindeki rolleri araştırılmıştır.

Cas9'un post-translasyonel modifikasyonlar aracılığıyla düzenlenmesini anlamak, CRISPR tabanlı genom düzenleme verimliliğini ve özgünlüğünü artırmak için kritiktir. Bu çalışmada, Cas9'un hem SUMOylasyona maruz kaldığını hem de ubikitinasyon uğradığını doğrulamak için güçlü ve ultra-hassas bir teknik olan Yakınlık Ligasyon Analizi (YLA) kullanılmıştır. YLA deneyleri ayrıca Cas9'un ana SUMO bağlama bölgesini doğrulamıştır. Dahası, YLA deneyleri Cas9'un SUMOylasyonunun ve ubikitinasyonun aynı lizin için rekabet ederek ve antagonistik bir şekilde çalışarak Cas9'un hücresel lokalizasyonunu modüle ettiğini göstermişlerdir.

ADAM17, birçok hücre yüzey protezini kesip serbest bırakan kritik bir enzimdir ve post-translasyonel modifikasyonlar tarafından düzenlenmesi, önemli bir araştırma alanını oluşturur. Bu çalışma, ADAM17'nin hem SUMOylasyon hem de ubikuitinasyon tarafından düzenlendiğini ve bunların ADAM17 stabilitesi üzerinde karşıt etkilere sahip olduğunu ilk kez göstermiştir. ADAM17'deki spesifik SUMOylasyon bölgelerinin ve bu bölgelerin enzimin stabilitesi, lokalizasyonu ve ektobölge kesimi aktiviteleri üzerindeki etkilerini belirlemek için daha fazla araştırmaya ihtiyaç vardır.

TABLE OF CONTENTS

LIST OF FIGURES

LIST OF TABLES

LIST OF SYMBOLS

A	Amper
A	Alanine
bp	Base pair
cm^2	Centimeter square
D	Aspartic acid
g	Gram
g	Gravity
h	Hour
K	Lysine
kDa	Kilodalton
M	Molar
mg	Milligram
mL	Milliliter
mM	Millimolar
mm	Millimeter
ng	Nanogram
R	Arginine
V	Volt
α	Alpha
β	Beta
µg	Microgram
µL	Microliter
µM	Micromolar
^oC	Degree Celsius

LIST OF ACRONYMS/ABBREVIATIONS

ADAM	A Disintegrin and Metalloproteinase
AP	Alkaline Phosphatase
BB94	Batimastat
CRISPR	Clustered Regularly Interspaced Palindromic Repeats
DMEM	Dulbecco's Modified Eagle Medium
EGFR	Epidermal Growth Factor Receptor
ER	Endoplasmic Reticulum
FBS	Fetal bovine serum
gRNA	guide RNA
HBS	HEPES-buffered saline
HDR	Homology-directed repair
IP	Immunoprecipitation
iRhoms	Rhomboid-like pseudoproteases
iTAP	iRhom Tail Interacting Protein
KO	Knock-out
LB	Luria Bertani
MMP	Matrix Metalloproteinase
NEM	N-ethylmaleimide
NHEJ	Nonhomologous End Joining
NLS	Nuclear Localization Signal
PBS	Phosphate-buffered Saline
PCR	Polymerase Chain Reaction
PDI	Protein Disulfide Isomerase
PIC	Protease Inhibitor Cocktail
PKC	Protein Kinase C
PLA	Proximity Ligation Assay
PMA	Phorbol 12-myristate 13-acetate
PTM	Post-translational modification
RIPA	Radioimmunoprecipitation assay buffer

SDM	Site directed mutagenesis
SEM	Standard error of the mean
SENP	Sentrin-specific protease
SIM	SUMO-interacting motif
STUbL	SUMO-targeted Ubiquitin ligase
SUMO	Small Ubiquitin-like modifier
TALEN	Transcription activator-like effector nuclease
TBS	Tris-buffered Saline
TIMP3	Tissue Inhibitor of Metalloproteinases-3
TNFα	Tumor Necrosis Factor Alpha
ZFN	Zinc-finger Nuclease

1. INTRODUCTION

1.1. Post-translational Modifications

Post-translational modifications (PTMs) are critical regulatory mechanisms that contribute enormously to proteome complexity by controlling the abundance, function, localization, and interactions of proteins, without altering gene expression. These modifications can occur through the addition of various chemical groups, such as phosphate, methyl, acetyl, or small protein moieties, to specific amino acid residues on the target proteins. Alternatively, post-translational modifications can also involve controlled proteolytic cleavage, where specific peptide bonds are selectively cut, leading to the generation of mature, active protein forms (Figure 1.1). Together, this diverse array of post-translational modifications allows for the fine-tuning and dynamic regulation of protein properties, enabling cells to respond rapidly to changing environmental and developmental cues. (Spoel, 2018).

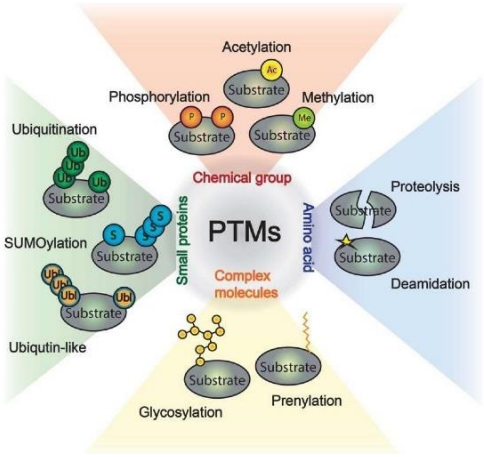

Figure 1.1. Approaches for post-translational modifications (PTMs) of proteins. Post-translational modifications can be categorized as chemical group modifications (red part), amino acid modifications (blue part), addition of complex molecules (yellow part), and additions of small proteins (in green). The figure is reprinted from Salas-Lloret and González-Prieto, 2022.

1.2. SUMOylation and Ubiquitylation

One of the well-studied post-translational modifications is SUMOylation, which involves the covalent attachment of Small Ubiquitin-like Modifier (SUMO) proteins to target lysine residues on the substrate. As the name suggests, SUMO is a modifying protein slightly larger than 10 kDa and shows 18% amino acid similarity to Ubiquitin (Bayer et al., 1998). SUMO is a member of the ubiquitin-like protein family, and its conjugation processes are very similar to the ubiquitin pathway. Like ubiquitin, SUMO requires the sequential action of E1 activating enzymes, E2 conjugating enzymes, and E3 ligases to covalently attach to target proteins. This multi-step enzymatic process allows for the reversible and dynamic regulation of protein function through SUMOylation (Celen and Sahin, 2020; Sahin et al., 2022).

SUMO peptides and the SUMOylation process have many similarities with ubiquitin and ubiquitylation, respectively. A classical "ββαββαβ" ubiquitin fold is the core of SUMO1. Both mature ubiquitin and SUMO proteins contain a C-terminal diglycine motif (-GG), which forms a covalent isopeptide bond with the target lysine on protein substrates. Both ubiquitin and SUMO attachment to the proteins lead to changes in substrate stability, and those attachments can be reversed by specific proteases (Sahin et al., 2022).

Although SUMO peptides share many features with ubiquitin, they also have some crucial differences, leading to unique biochemical and cellular functions associated with SUMO. The unique surface charge distribution of SUMO not only enhances the solubility of SUMO peptides but also facilitates the formation of binding interactions with a wide range of diverse proteins. Moreover, SUMO has an N-terminal extension that is not present in ubiquitin, which is likely a key factor in why SUMOylation has different cellular functions compared to ubiquitylation (Sahin et al., 2022). The similarities and differences between SUMO and ubiquitin are summarized in Figure 1.2.

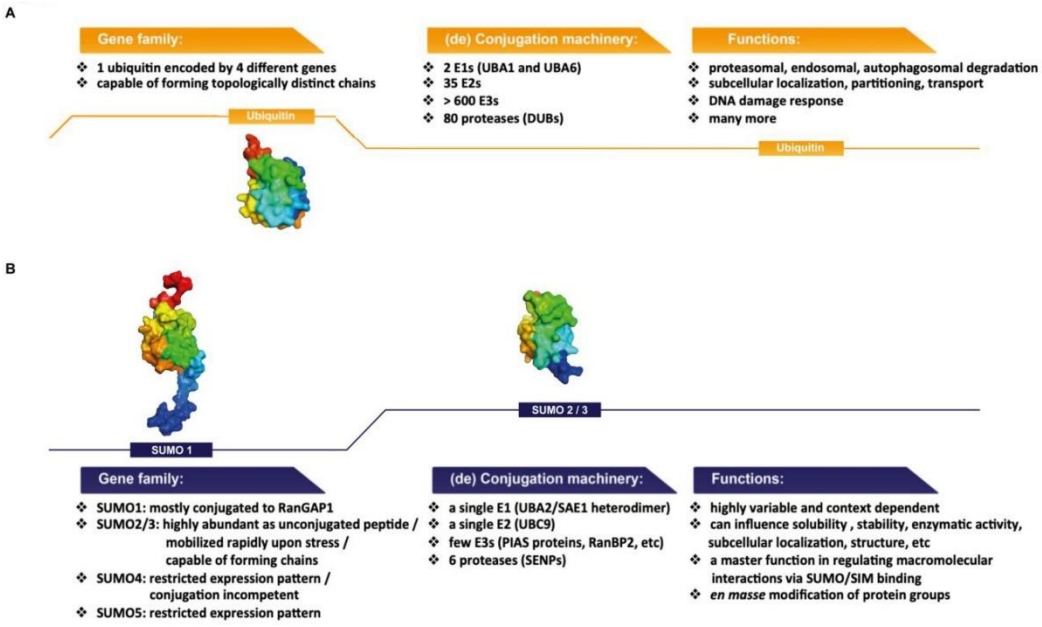

Figure 1.2. The similarities and differences between ubiquitin (A) and SUMO (B). Although SUMO1 and ubiquitin share only 18% sequence similarity, they have similar 3D structures, with the characteristic of a central ubiquitin core folded into a "ββαββαβ" pattern. However, a flexible N-terminal extension that protrudes from this central core gives SUMO1 a unique structural feature. The figure is reprinted from Sahin et al., 2022.

SUMO isoforms are conjugated to lysine amino acids within a specific consensus motif on target proteins. Mammals have five SUMO paralogues: SUMO1, SUMO2, SUMO3, SUMO4, and SUMO5. Due to the 97% sequence similarity between SUMO2 and SUMO3 in humans, it is challenging to distinguish them using antibodies. Consequently, they are often collectively referred to as SUMO2/3 in the literature. Among these, SUMO1 and SUMO2/3 have been the most extensively characterized SUMO paralogues in previous studies, and they share 50% sequence similarity (Sahin et al., 2022). SUMO1 and SUMO2/3 are ubiquitously expressed, while the expression of SUMO4 and SUMO5 is limited to a few tissues, such as the kidney, spleen, and placenta for SUMO4 and the testes and leukocytes for SUMO5 (Sahin et al., 2022). The different SUMO isoforms, despite their similarities, can have distinct functional roles and target different subsets of proteins for SUMOylation. Nonetheless, the core SUMOylation pathway, involving the sequential action of E1 activating enzymes, E2 conjugating enzymes, and E3 ligases, is generally consistent across

all SUMO peptides. Figure 1.3 summarizes this SUMO pathway and the wide-ranging effects of SUMOylation on SUMO substrates, cellular processes, and overall organismal health (Celen and Sahin, 2020).

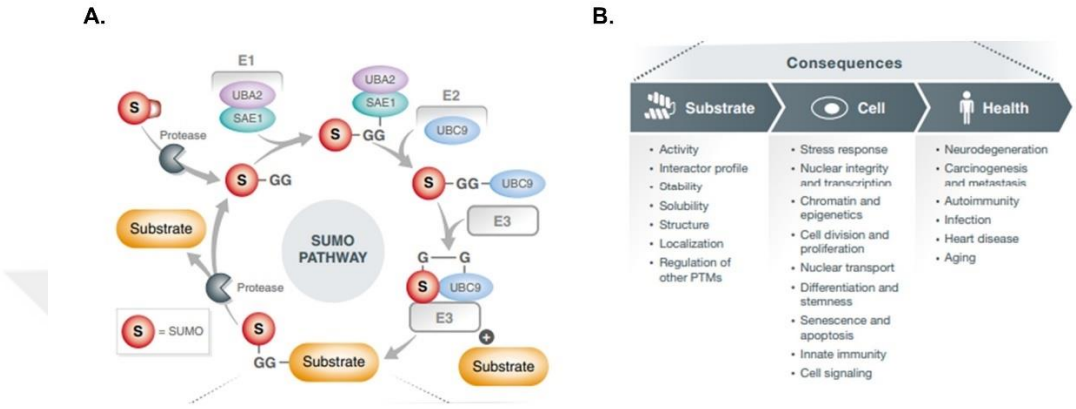

Figure 1.3. The SUMO Pathway and Its Multifaceted Effects. (A). The SUMO pathway is outlined schematically, depicting the step-by-step process of SUMO maturation, activation, conjugation, and deconjugation. (B). This post-translational modification plays a crucial role in fine-tuning cellular responses to various environmental and developmental cues. The figure is reprinted from Celen and Sahin, 2020.

As shown in Figure 1.3.A, the precursor SUMO peptide first becomes mature by exposing diglycine with the help of proteases. The mature SUMO is then transferred to the E1 SUMO-activating enzyme complex (SAE1/UBA2), and subsequently to the global E2 SUMO-conjugating enzyme UBC9, in an ATP-dependent process (Gareau and Lima, 2010). From this E2-SUMO intermediate, the SUMO moiety is finally conjugated to the target lysine residue on the substrate protein, either directly by UBC9 or with the assistance of SUMO E3 (Celen and Sahin, 2020).

While there are many E2 conjugases in the ubiquitin pathway, the only E2 conjugase in the SUMO pathway is UBC9, and inactivation or knockdown of *UBC9* is sufficient to inhibit the entire SUMO pathway. Furthermore, knockout of *UBC9* in mouse reproductive cells proves to be embryonically lethal, resulting in disruptions to the structure and

organization of cell nuclei (Nacerddine et al., 2005). UBC9 plays a crucial role in the SUMOylation pathway, acting as both a conjugating enzyme and a ligase. It can bind SUMO directly to target substrates or conjugate SUMO peptides to E3 ligases, providing more specific substrate selection. The SUMOylation process can occur on a single lysine residue (mono-SUMOylation) or on multiple different residues (multi-SUMOylation), and in some cases, more than one SUMO peptide can be attached to the same residue (poly-SUMOylation). SUMO peptides bind to the lysine amino acid within the SUMO consensus motif ψKxD/E (ψ: Hydrophobic amino acid, K: target lysine, x: any amino acid, D / E: negatively charged aspartic acid or glutamic acid) to specifically target proteins for SUMOylation. Additionally, SUMO-interacting motifs (SIMs) found on certain proteins facilitate non-covalent interactions with some SUMOylated proteins. Furthermore, the SUMO peptide covalently bound to a SUMOylation site on a protein can also interact with a SIM motif on the same protein, potentially altering the folding and function of the target protein. The SUMO pathway and SUMOylation of target proteins have been implicated in a wide range of cellular functions, including transcriptional regulation, cell cycle progression, DNA repair, chromatin remodeling, and the stress response (Figure 1.3.B) (Celen and Sahin, 2020).

SUMO-specific proteases, known as sentrin-specific proteases (SENPs), play a crucial role in reversing the SUMOylation process. These proteases cleave the covalent bond between the SUMO peptide and the target substrate, effectively removing the SUMO modification and restoring the original state of the substrate (Drag and Salvesen, 2008). This deconjugation process is essential for the dynamic and reversible regulation of SUMOylated proteins, allowing cells to fine-tune their responses to various environmental and developmental stimuli. The dynamic and reversible nature of SUMOylation, along with its ability to modulate diverse cellular processes, has made it an area of intense research interest (Huang et al., 2015).

Given that SUMOylation alters the characteristics of target proteins, including stability, solubility, activity, interaction profiles, structure, localization, and regulation of other post-translational modifications, it plays a crucial role in vital cellular processes. These include stress response, nuclear integrity, chromatin structure and epigenetics, division and

proliferation, differentiation and stemness, senescence and apoptosis, innate immunity, and cell signaling. Consequently, it is unsurprising that SUMOylation is actively involved in important pathological processes such as neurodegeneration, carcinogenesis, metastasis, aging, autoimmune diseases, infections, and heart diseases (Celen and Sahin, 2020). Considering the multifaceted effects of SUMOylation on cellular function and its implication in various disease states, it is essential to understand the regulatory mechanisms governing this post-translational modification.

Interestingly, although SUMOylation is an exclusively eukaryotic process, SUMO peptides often regulate and neutralize viral or bacterial proteins to prevent intracellular pathogen infection. However, some pathogens have established counterregulatory mechanisms to hijack or block the SUMO-dependent host innate immune response pathways (Celen and Sahin, 2020; Sahin et al., 2022).

1.3. CRISPR/Cas9 System

The CRISPR-Cas9 system is a widely used and transformative tool in the field of genome editing, gene regulation, diagnostics, and imaging. This revolutionary technology has rapidly gained prominence due to its simplicity, cost-effectiveness, and versatility (Cong et al., 2013). Cas9 is a bacterial protein that is part of the adaptive immune system of bacteria, protecting them against invading genetic elements such as bacteriophages and plasmids (Barrangou et al., 2007). In this system, CRISPR RNA-based DNA recognition and Cas nuclease-mediated DNA cleavage result in double-strand breaks (DSB), allowing for precise genome modification (Jinek et al., 2012).

CRISPR stands for **C**lustered **R**egularly **I**nterspaced **S**hort **P**alindromic **R**epeat, referring to the arrays of conserved short palindromic repeats interspaced by non-repetitive sequences, where the spacers are derived from genetic elements of viruses and plasmids (Bolotin et al., 2005; Mojica et al., 2005; Pourcel et al., 2005). In combination with CRISPR-associated genes (cas), CRISPR locus provides an acquired immune system for bacteria. After infection, Cas nucleases cut the invading DNA into small fragments, which are then

incorporated into the CRISPR array as spacers. These spacers serve as templates to guide Cas in destroying foreign DNA sequences. This allows bacteria to acquire immunological memory for future infections, effectively protecting them from subsequent viral or plasmid attacks. (Jiang and Doudna, 2017). The working principle of the CRISPR-Cas9 system is shown in Figure 1.4.

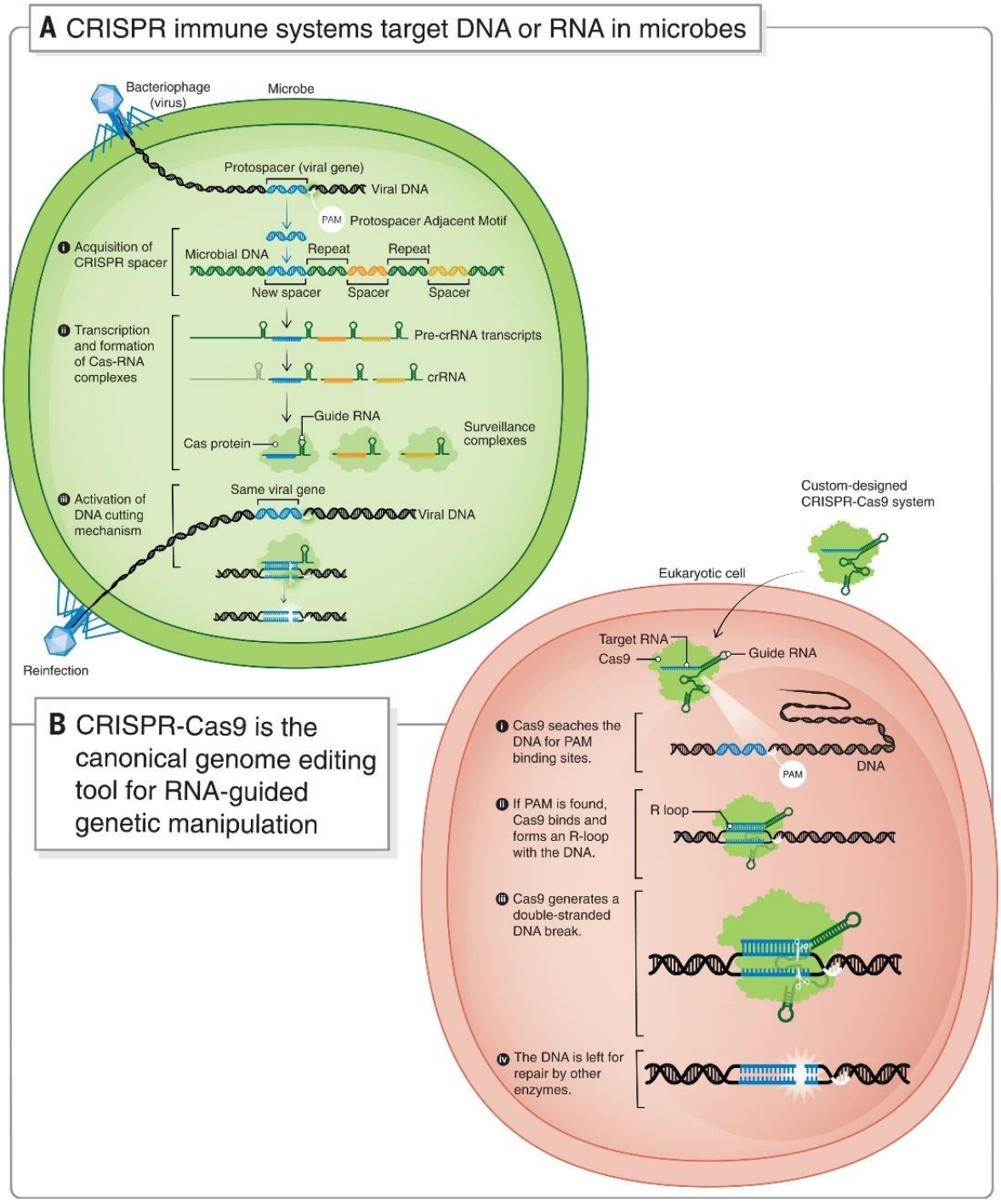

Figure 1.4. The CRISPR-Cas system provides a programmable tool for genome editing. (A). CRISPR immune systems in microbes acquire genetic sequences matching an invading agent, then assemble them into Cas-RNA complexes to identify and destroy the target. (B). Cas9 enzymes are directed by guide RNAs to create double-strand breaks in DNA for repair. The figure is reprinted from Wang and Doudna, 2024.

1.4. Structural Basis of Cas9-Mediated DNA Cleavage

Cas9 consists of two lobes: the alpha-helical recognition (REC) lobe, which facilitates interactions with nucleic acids, and the nuclease lobe, which contains the conserved HNH and split RuvC catalytic nuclease domains. (Jinek et al., 2014). The HNH nuclease domain of Cas9 cleaves the single DNA strand, enabling complementary base pairing between the guide RNA and the target strand, a crucial step for Cas9 binding to DNA (Anders et al., 2014; Jinek et al., 2014; Nishimasu et al., 2014; Jiang et al., 2015). On the other hand, the RuvC catalytic core of Cas9 cleaves the non-target DNA strand after the formation of an RNA:DNA hybrid. The flexibility of the Cas9 HNH domain plays a crucial role in enabling its catalytic activity. As the HNH domain binds to the DNA, it undergoes a transformation from an inactive to an active state, which allows it to reach and cleave the target DNA strand. (Jinek et al., 2014; Jiang et al., 2015). Several positively charged residues within the HNH domain have been shown to facilitate interactions with the target DNA strand, enabling the enzyme to effectively dock at the cleavage site (Jiang et al., 2015; Slaymaker et al., 2016; Palermo et al., 2018; Wilkinson et al., 2019).

1.5. Applications of CRISPR/Cas Systems in Biology and Biomedicine

The ability of the CRISPR/Cas system to generate double-strand breaks in the invading genome led to the discovery that this same technique could be used for host-independent genome editing (Cong et al., 2013; Mali et al., 2013). Unlike earlier genome editing technologies such as zinc finger nucleases (ZFNs) and transcription activator-like effector nucleases (TALENs), which require altering the nuclease structure itself, the target specificity in the CRISPR/Cas system is primarily determined by the separately provided guide RNA (Jinek et al., 2012). This allows for greater flexibility and ease of use compared to the more complex engineering required for ZFNs and TALENs (Robb, 2019).

The CRISPR/Cas systems are classified into three major types (I, II, and III) based on the sequences and structures of the Cas proteins. While the type I and type III CRISPR/Cas systems require the coordinated activity of a multisubunit complex to cleave the target DNA,

the type II CRISPR/Cas system, which includes the widely used Cas9 nuclease, needs only a single multidomain endonuclease to carry out the DNA cleavage process. This simplified structure of the type II CRISPR/Cas system contributes to its widespread adoption and versatility in genome editing applications (Makarova et al., 2015, 2017).

The working principle of the CRISPR-Cas9 system, with its ability to precisely target and modify DNA sequences, has revolutionized various fields of biology, including genetics, cell biology, and medicine, by enabling researchers to manipulate genomes with unprecedented efficiency and precision. For example, the CRISPR-Cas9 system has been used for gene knockout, gene knockin, genome-wide screening, therapeutic gene editing, and even rewriting genetic codes (Wang and Doudna, 2024). Beyond its use in genome editing, the CRISPR-Cas9 system has been repurposed for diverse applications, such as gene regulation, epigenetic modifications, live-cell imaging, and diagnostics (Villiger et al., 2024). Figure 1.5 summarizes the evolution of CRISPR technology.

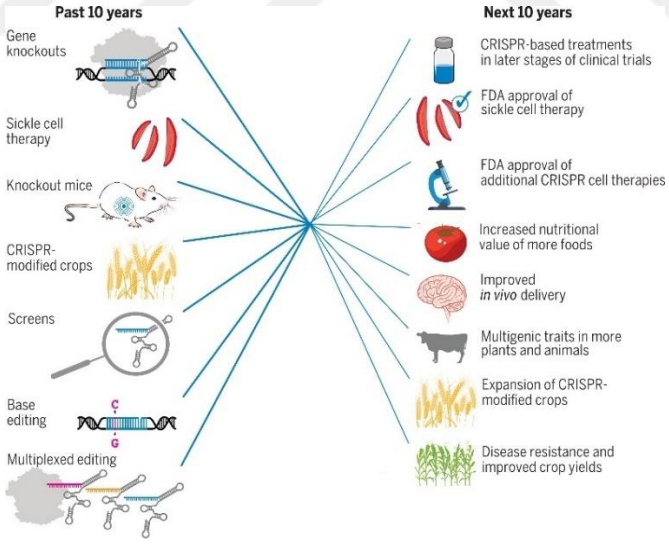

Figure 1.5. The Evolution of CRISPR Technology: From the Past to the Future. Over the past decade, CRISPR technology has been developed to create essential tools for gene knockout, animal models, genetic screening, and multiplexed editing. The figure is reprinted from Wang and Doudna, 2024.

1.6. Cas9: A Target for SUMOylation and Ubiquitylation

There are intensive studies on developing strategies to make Cas9's effects on the target (on-target effects) more sensitive and efficient, as well as to reduce its off-target effects (Slaymaker et al., 2016). Our previous lab member Arda Çelen had shown that Cas9 is ubiquitylated (Çelen, 2019).

In this study, the aim is to elucidate whether Cas9 is SUMOylated in eukaryotic cells mainly by proximity ligation assay (PLA), to our knowledge, constitute the first post-translational modifications (PTMs) on this protein will be reported to date. Also, the consequences of two different PTMs, Ubiquitylation and SUMOylation, on Cas9 are aimed to discover. The studies presented here are a part of our newly published article: "Sumoylation of Cas9 at lysine 848 regulates protein stability and DNA binding" (Ergünay et al., 2022). Elucidating how the Cas9 enzyme is controlled through post-translational modifications is essential both for an in-depth understanding of the working mechanism of the CRISPR pathway and for developing new and better Cas9 variants for genome editing.

1.7. Protein Ectodomain Shedding and ADAM17

The proteolytic cleavage of the extracellular domains of the membrane proteins (protein ectodomain shedding) is one of the irreversible post-translational modifications that control the function of hundreds of membrane proteins. When membrane proteins are cleaved by proteases located nearby on the same or another cell membrane, the extracellular domain (ectodomain) is released into the extracellular space while the remaining portion stays attached to the membrane. The extracellular domain released into the extracellular space is frequently responsible for signal transduction by binding to relevant receptors in other cells. Without ectodomain shedding, membrane-bound ligands are restricted to juxtacrine or autocrine signaling. However, proteolytic cleavage of these ligands is crucial for enabling paracrine signaling to distant target cells. Additionally, receptor interactions with extracellular protein domains can regulate their activation or inactivation. Ectodomain shedding may also generate soluble decoy receptors that sequester ligands, thereby

modulating their availability. In this way, the intracellular level, activation, and inactivation processes of many proteins are controlled by mechanisms such as the release of membrane-bound growth factors and cytokines into the extracellular space, as well as the degradation of cell surface receptors and cell adhesion proteins (Blobel, 2005). Therefore, ectodomain shedding plays a crucial role in many developmental and physiological processes, as it regulates the availability of signaling molecules, cell surface receptors, and cell adhesion proteins. Disruption of this process can lead to the development of various diseases, including cancer, Alzheimer's disease, and inflammatory disorders, highlighting the importance of tightly controlled ectodomain shedding for maintaining homeostasis and normal cellular function (Lichtenthaler et al., 2018). The ectodomain shedding process and the various signal transduction pathways it regulates are illustrated in Figure 1.6.

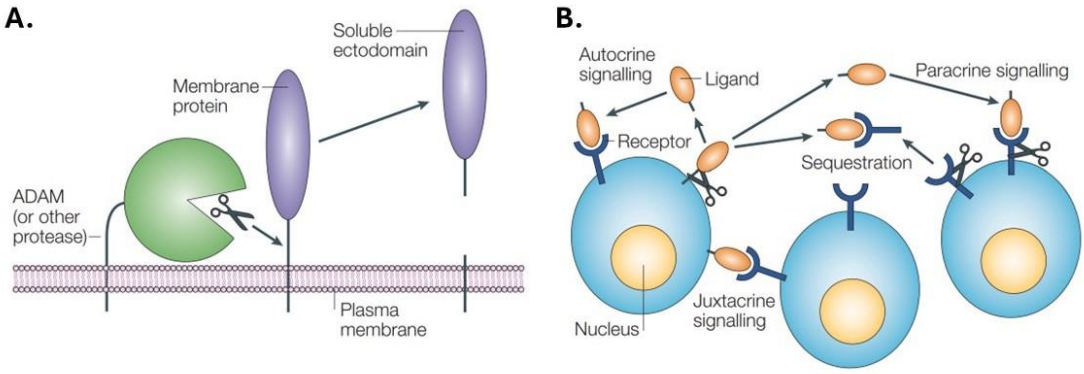

Figure 1.6. Ectodomain shedding and its effects on signaling. (A). The schematic illustration of membrane protein cleavage by ADAM or other proteases, releasing soluble extracellular domains. (B). Potential functions of protein ectodomain shedding include autocrine, juxtacrine, or paracrine signaling, and ligand sequestration. The figure is reprinted from Blobel, 2005.

1.8. ADAM (A Disintegrin and Metalloproteinase) Protein Family and Protein Ectodomain Shedding

The most well-known sheddases involved in ectodomain shedding are ADAM (**A** **D**isintegrin **a**nd **M**etalloproteinase) protein family group and MMPs (Matrix

Metalloproteinases). ADAM protein family consists of 21 members whose 13 members are active (Düsterhöft, Lokau, et al., 2019). ADAM10 and ADAM17 are two of the most active and well-studied members of the ADAM protein family. As the name "metalloproteinase" implies, the proteolytic activity of both ADAM10 and ADAM17 is attributed to the zinc ion located at the center of their protein structure, which is essential for their catalytic function (Kato et al., 2018).

ADAM10 and ADAM17 show approximately 30% sequence homology and they are both ubiquitously expressed in mammalian cells. ADAM10 plays a key role in development, as it cleaves Notch receptor proteins and is a critical component of the Notch signaling pathway, which regulates cell fate decisions during embryogenesis and adult tissue homeostasis (Blobel, 2005). In contrast, ADAM17 has diverse functions. It regulates the first line of immune defense by releasing the proinflammatory cytokine Tumor Necrosis Factor Alpha (TNFα), thereby promoting inflammation in response to tissue damage and infection. Additionally, ADAM17 controls cell proliferation and embryonic development by shedding ligands of the epidermal growth factor receptor (EGFR), which activates signaling pathways that drive cell growth and differentiation (Matthews et al., 2017).

Although the Notch signaling pathway is primarily controlled by ADAM10, Notch is also one of the ADAM17 substrates, with both ADAM10 and ADAM17 regulating its activity (Murthy et al., 2012). The crucial importance of these two ADAM proteins is highlighted by the fact that mice with *ADAM10* gene knockouts exhibited central nervous system and cardiovascular disorders and survived only until day 9.5 of embryogenesis. (Hartmann et al., 2002). Similarly, *ADAM17* knockout mice died between day 17.5 of embryonic development and the first day after birth, with most developing open eyelids, underscoring their pivotal roles in embryonic development and tissue homeostasis (Peschon et al., 1998).

1.9. ADAM17-mediated Ectodomain Shedding and Its Relevance with Diseases

ADAM17 was initially named as the tumor necrosis factor-alpha (TNFα) converting enzyme (TACE), as it was first discovered to be responsible for shedding and releasing the proinflammatory cytokine TNFα into the extracellular space (Black et al., 1997). Today, ADAM17 is known to have more than 90 substrates, including a diverse array of ligands, proteins, and receptors that play crucial roles in various cellular processes. These substrates include growth factors such as epidermal growth factor (EGF), transforming growth factor α (TGFα), heparin-binding EGF-like growth factor (HB-EGF), and amphiregulin (AREG), which are important for development and differentiation (Düsterhöft, Lokau, et al., 2019; Sahin et al., 2004). ADAM17 also cleaves vascular endothelial growth factor receptor-2 (VEGFR-2), proteins involved in cell adhesion like L-Selectin and ICAM-1, and ligands or receptors that contribute to immune function, such as tumor necrosis factor α (TNFα) and the interleukin 6 receptor (IL6R) (Düsterhöft, Babendreyer, et al., 2019). Additionally, ADAM17 processes signaling molecules like amyloid precursor protein (APP) and prion protein, which are associated with neurodegenerative diseases (Düsterhöft, Lokau, et al., 2019). The wide range of ADAM17 substrates highlights its pivotal role in regulating various biological processes, such as immunity, regeneration, and development. Its cleavage targets include growth factors, adhesion proteins, immune mediators, and signaling molecules involved in diverse cellular functions.

Genetic studies have revealed that a homozygous deletion in the *ADAM17* gene can cause inflammatory skin and bowel disease (Blaydon et al., 2011). Beyond gene mutations, disruptions in *ADAM17* gene expression or ADAM17 protein activation have also been linked to a variety of diseases, including lung cancer, breast cancer, colorectal tumors, carcinomas, brain tumors, rheumatoid arthritis, inflammatory bowel disease, stroke, cardiovascular diseases, chronic kidney disease, respiratory diseases, metabolic disorders, Alzheimer's disease, and Parkinson's disease (Arribas and Esselens, 2009). The critical role of ADAM17 in activating EGFR ligands through shedding makes it an important drug target, particularly for cancer types driven by alterations in EGFR signaling (Sahin et al., 2004).

1.10. The Function, Structure, and Regulatory Mechanisms of ADAM17

Since ADAM17 plays a significant role in a wide range of critical biological processes, the level and activity of ADAM17 within the cell are tightly controlled through various post-translational modifications (PTMs). In a study by Yoda et al. (2013), overexpression of the ADAM17 gene did not lead to an increase in the proteolytic activity of the ADAM17 protein. The researchers attributed this to the strict regulatory mechanisms governing the ADAM17 protein, such as post-translational modifications (PTMs) (Yoda et al., 2013).

Indeed, many mechanisms keep the ADAM17 protein inactive and prevent its proteolytic activity in the absence of specific stimuli. The best-known inhibitory mechanism is the presence of a highly conserved prodomain (amino acids 18-214) at the N-terminus of the ADAM17 protein, just behind the signal sequence. This prodomain contains cysteine amino acids that coordinate the zinc ion in the active site, thereby preventing substrate entry (Milla et al., 1999). Cleavage of this prodomain by furin-like proprotein convertases is necessary for the activation and maturation of ADAM17. This cleavage removes the inhibitory prodomain, allowing the enzyme to become catalytically active. The resulting active form, called mature ADAM17, is then translocated to and localized on the cell membrane where it can engage in its proteolytic functions (Schlöndorff et al., 2000).

The mature ADAM17 protein is 610 amino acids in length, formed by the cleavage of the first 214 amino acids from the 824 amino acid proform. This N-terminal prodomain not only keeps ADAM17 proteolytically inactive, but also acts as a chaperone, facilitating the proper folding of ADAM17 within the endoplasmic reticulum (ER) (Leonard et al., 2005). The metalloprotease domain serves as the catalytic center, carrying out the proteolytic cleavage of ADAM17 substrates. The disintegrin region works with integrins and contributes to the activation of ADAM17. The membrane-proximal domain and CANDIS region recognize and bind ADAM17 substrates, which also play a role in the enzyme's activation. The transmembrane region anchors ADAM17 to the cell membrane and plays a role in its intracellular localization and transport. Finally, the cytoplasmic region is associated with the activation of ADAM17 through phosphorylation and various

intracellular interactions. The domains of ADAM17 protein and their corresponding functions are summarized in Figure 1.7.

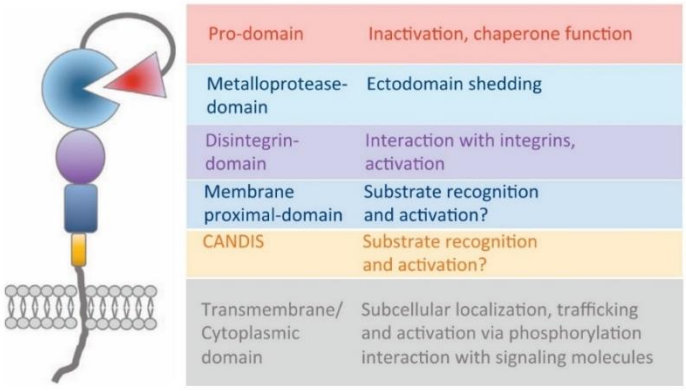

Figure 1.7. The schematic illustration of ADAM17 domains and their functions.The ADAM17 protein is composed of several functional domains that regulate its activity and function. The figure is reprinted from Zunke and Rose-John, 2017.

After the expression of the *ADAM17* gene, the 814-amino-acid ADAM17 protein, known as the proform, is folded in the endoplasmic reticulum (ER) with the assistance of its prodomain. This prodomain acts as a chaperone, helping the ADAM17 proform to properly fold and assume its correct three-dimensional structure. Then, the membrane-proximal domain (MPD) of ADAM17 interacts with inactive Rhomboid-like pseudoproteases (iRhoms), also present in the ER. This interaction is necessary for the transport of ADAM17 from the ER to the Golgi apparatus, and the subsequent maturation of ADAM17 through the removal of the prodomain (Adrain et al., 2012).

Rhomboids are intramembrane serine proteases that were first found in the Drosophila melanogaster, where they play an active role in developmental processes by cleaving the Epidermal Growth Factor Receptor (EGFR). Vertebrates have two iRhoms: iRhom1 and iRhom2, and they are highly conserved across species. While iRhom1 is mainly responsible for the regulation of ADAM10, iRhom2 (RHBDF2) is mainly responsible for the regulation of ADAM17 (Matthews et al., 2017). One of the key proteins involved in this regulation is iTAP (iRhom tail interacting protein), which binds to the cytoplasmic tail of iRhom and

enhances the iRhom-ADAM17 interaction (Oikonomidi et al., 2018). This interaction is crucial for the proper localization, trafficking, and maturation of ADAM17 within the cell.

The proform ADAM17, transported from the endoplasmic reticulum to the Golgi apparatus by the iRhom and iTAP proteins, is then cleaved by furin-like proteases in the Golgi, resulting in its maturation. This mature ADAM17 is then transported to the cell membrane, with continued assistance from the iRhom and iTAP proteins. Although ADAM17 reaches the cell membrane in its mature state, it must still be released from the iTAP-iRhom complex to become fully active. This release is achieved through phosphorylation, which is also a PTM. Specifically, the cytoplasmic domain of the iRhom protein is phosphorylated by 14-3-3 proteins, triggering the dissociation of ADAM17 from the iTAP-iRhom complex. Once released, the mature ADAM17 enzyme becomes active on the cell membrane (Cavadas et al., 2017; Grieve et al., 2017). This complex process of ADAM17 maturation, trafficking, and activation is summarized in Figure 1.8.

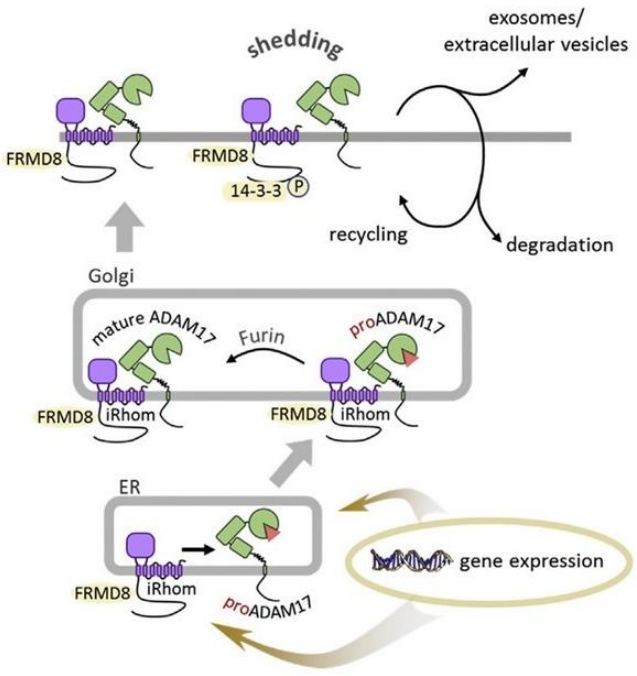

Figure 1.8. The process of maturation, transport to the cell membrane and activation of the ADAM17 protein.The figure is reprinted from Düsterhöft, Babendreyer, et al., 2019.

Although ADAM17 on the cell membrane is mature, its activity is tightly regulated by several mechanisms that can either inhibit or activate it. Mechanisms that inhibit ADAM17 activity include its interaction with the α5β1-integrin, which can keep ADAM17 in an inactive state (Gooz et al., 2012). Furthermore, after ADAM17 undergoes dimerization, it can interact with TIMP3 (Tissue Inhibitor of Metalloproteinases-3), a natural protease inhibitor that blocks its catalytic activity (Xu et al., 2012). Another inhibitory mechanism involves a conformational change in ADAM17 induced by the isomerization with protein disulfide isomerase (PDI) (Düsterhöft et al., 2013). Figure 1.9 summarizes the mechanisms controlling ADAM17 on the cell surface.

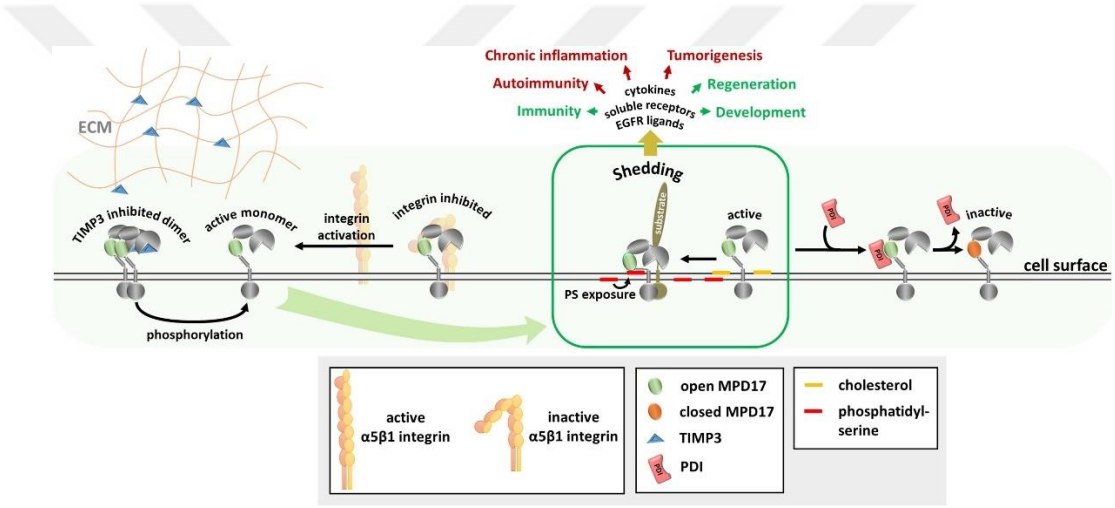

Figure 1.9. Schematic representation of the mechanisms that regulate ADAM17 on the cell surface. Interaction with integrins, Tissue Inhibitor of Metalloproteinases-3 (TIMP3), and protein disulfide isomerase (PDI) are the inhibitory mechanisms of mature ADAM17 protein while phosphatidylserine (PS) exposure is needed for its activation on the cell membrane. The figure is reprinted from Grötzinger et al., 2017.

TIMP3 inhibition is removed by phosphorylation of the cytoplasmic domain of ADAM17. On the other hand, for ADAM17 to become fully active, it must translocate from the cholesterol-rich regions of the cell membrane to areas where phosphatidylserine (PS) is exposed (Grötzinger et al., 2017). Once in these membrane regions, ADAM17 can bind to the cell membrane through its MPD and CANDIS domains, allowing it to more effectively cleave its substrates (Sommer et al., 2016). This complex regulation ensures that ADAM17 activity is tightly controlled and only occurs in the appropriate cellular contexts.

One of the mechanisms controlling ADAM17 intracellular level and activity is phosphorylation, a PTM previously mentioned in TIMP3 inhibition. As we know, enzymes responsible for protein phosphorylation are kinases, and kinases such as ERK and MAPK are crucial for the regulation of key cellular processes like cell survival, growth, and proliferation (Anjum and Blenis, 2008). In a study conducted by Díaz-Rodríguez et al. in 2002, it was shown that the cytoplasmic region of mouse ADAM17 is phosphorylated at the 735th threonine amino acid by the ERK kinase (Díaz-Rodríguez et al., 2002). Subsequent studies have further demonstrated that ERK-MAPK signaling pathways are activated after growth factor stimulation and phosphorylate ADAM17 at multiple sites within its cytoplasmic domain (Fan et al., 2003; Killock and Ivetić, 2010; Schwarz et al., 2014; Xu and Derynck, 2010).

In addition, ADAM17 can also be stimulated by PMA (phorbol-12-myristate-13-acetate), a synthetic analog of diacylglycerol (DAG) that is widely used to activate ADAM17. The stimulation of ADAM17 by PMA occurs through the activation of Protein Kinase C (PKC), which in turn leads to the activation of the ERK and p38 MAPK pathways (Düsterhöft, Babendreyer, et al., 2019). While numerous studies have demonstrated the importance of ADAM17 cytoplasmic domain phosphorylation for its activation, there are also reports suggesting that ADAM17 activation can occur independently of its cytoplasmic region and phosphorylation (Hall and Blobel, 2012; Le Gall et al., 2010; Reddy et al., 2000; Schwarz et al., 2013). Further research is needed to fully elucidate the complex mechanisms underlying ADAM17 regulation and activation.

1.11. The Cytoplasmic Tail of ADAM17 and Its Role in ADAM17 Regulation

The role of ADAM17's cytoplasmic domain in regulating its activity remains elusive. In previous studies where the cytoplasmic domain was partially or completely deleted, Reddy et al. found that this domain, and its phosphorylation, were not required for PMA stimulation or shedding of interleukin-1R-II and p55 TNFR (Reddy et al., 2000). The finding that ADAM17 can be stimulated in the absence of its cytoplasmic domain was unexpected since it is very well known that intracellular protein kinases are activated by PMA stimulation resulting in phosphorylation of cytoplasmic domain of ADAM17 and subsequent

activation of ADAM17. The authors concluded that the cytoplasmic domain can be responsible for the regulation of ADAM17 by other stimulatory or inhibitory agents (Reddy et al., 2000).

Another explanation can be related to the roles of the cytoplasmic domain of ADAM17 on its substrate recognition. A few years later, other studies pointed out similar results indicating that phosphorylation of T735 is dispensable for ADAM17 activity (Horiuchi et al., 2007; Hall and Blobel, 2012). However, in another study conducted by Schwarz *et al*., PMA-stimulated ADAM17-mediated TNFα shedding was completely lost when the cytoplasmic domain of ADAM17 was completely deleted (ADAM17ΔCT) although there was no change in trafficking, cell surface levels, catalytic activity, dimer formation, furin cleavage, and iRhom2 binding of ADAM17 (Schwarz et al., 2013).

1.12. ADAM17 and SUMOylation

Although it is known that ADAM17-mediated protein ectodomain shedding is regulated by numerous mechanisms, many aspects of this regulation still remain unclear and require further investigation. Moreover, whether ADAM17-mediated ectodomain shedding is controlled by SUMOylation, a crucial post-translational modification, has not been explored previously.

Previous studies have demonstrated that many membrane proteins are subject to SUMOylation (Wasik and Filipek, 2014). However, no link has yet been established between the crucial processes of SUMOylation and protein ectodomain shedding. In this context, it remains unknown whether ADAM17, a well-known regulator of ectodomain shedding for numerous vital proteins and itself controlled by various post-translational modifications, is also regulated by SUMOylation. So, it was aimed to investigate whether ADAM17-mediated ectodomain shedding is controlled by SUMOylation, and if so, to elucidate how this post-translational modification affects ADAM17's proteolytic activity. The findings from this study will shed light on an additional layer of regulation in the vital process of ADAM17-dependent ectodomain shedding, ultimately enabling a better understanding of the diseases

that arise due to dysregulation of ADAM17 activity and paving the way for future targeted therapeutic approaches.

2. AIM OF STUDY

The overall aim of the study was to elucidate the post-translation modifications, specifically SUMOylation and ubiquitylation of two distinct proteins, Cas9 and ADAM17. Also, the effects of SUMOylation and ubiquitylation on the localization, stability, and function of those enzymes were studied.

The first aim was to verify SUMOylation and ubiquitylation of Cas9 in eukaryotic systems by proximity ligation assays. The proximity ligation assays also showed the localization of those post-modifications in human cell lines. To verify the SUMOylation site of Cas9, cell lines stably expressing Cas9 and SUMOylation-defective Cas9 variants were also generated. Elucidating the regulation of Cas9 by post-translational modifications such as SUMOylation and ubiquitylation is crucial for optimizing and enhancing the efficacy of this genome editing tool. Understanding how these modifications impact Cas9's localization, stability, and functional activity will enable researchers to fine-tune and improve the performance of the Cas9 system for diverse genomic engineering applications.

The second aim was to identify SUMOylation and ubiquitylation of ADAM17 and investigate the effects of the changes in global SUMOylation on ADAM17 stability and ADAM17-mediated ectodomain shedding. Understanding the post-translational mechanisms of ADAM17, the primary sheddase of numerous ligands and a key player in a wide range of diseases, can enable the identification of potential therapeutic targets. These targets may be related to ADAM17 regulation, shedding activity, or downstream signaling cascades that could be modulated to treat disease pathologies associated with aberrant ADAM17 function.

3. MATERIALS

3.1. Cell Culture

HEK293 cells were kindly provided by Dr. Tolga Sütlü from Acıbadem University.

3.2. Plasmids and Primers

Plasmids and primers used in this study are listed in Table 3.1. and Table 3.2, respectively.

Table 3.1. Plasmids.

Construct	Origin	Backbone, #Addgene ID
GFP-SUMO1	Provided by Dr. Hugues De Thé, College de France	pcDNA3.1
GFP-SUMO2	Provided by Dr. Hugues De Thé, College de France	pcDNA3.1
GFP-Ubc9	Provided by Dr. Hugues De Thé, College de France	pcDNA3.1
His-Ubiquitin	Provided by Dr. Hugues De Thé, College de France	pcDNA3.1
pCW-FLAG-Cas9	Addgene, USA	pCW, #50661
pRK5F-TACE	Addgene, USA	pRK5, #31713
psPAX2	Addgene, USA	psPAX2, #12260
pCMV-VSV-G	Addgene, USA	Na, #8454

Table 3.2. Sequences and Applications of the Primers.

Primer	Sequence (5'-3')	Application
Cas9-D850A-Forward	CTGAAGGACGCCTCCATCGACAAC	Site-directed mutagenesis
Cas9-D850A-Reverse	GTTGTCGATGGAGGCGTCCTTCAG	Site-directed mutagenesis
ADAM17-K188R-Forward	GTGGTTATTTAAGAGTGGATAATG	Site-directed mutagenesis
ADAM17-K188R-Reverse	CATTATCCACTCTTAAATAACCAC	Site-directed mutagenesis
ADAM17-K697R-Forward	GTGTGGATAAGAGATTGGATAAAC	Site-directed mutagenesis
ADAM17-K697R-Reverse	GTTTATCCAATCTCTTATCCACAC	Site-directed mutagenesis
ADAM17-K753R-Forward	GCAGCTCCAAGACTGGACCAC	Site-directed mutagenesis
ADAM17-K753R-Reverse	GTGGTCCAGTCTTGGAGCTGC	Site-directed mutagenesis
ADAM17-SDM-F1	TTGCCTTTCTCTCCACAGGT	Sanger sequencing of SDM products
ADAM17-SDM-F2	GACAGAGAACCACCTGAAGA	Sanger sequencing of SDM products
ADAM17-SDM-F3	AACATGATCCGGATGGTCTA	Sanger sequencing of SDM products
ADAM17-SDM-F4	GAGGAAAGGAAAGCCCTGT	Sanger sequencing of SDM products

3.3. Consumables and Devices

The consumables and devices used in this study are listed in Table 3.3 and Table 3.4, respectively.

Table 3.3. Consumables.

Name	Supplier
Cell Culture Dishes (60 mm, 100mm)	TPP, Switzerland
Cell Culture Flasks (75cm^2)	TPP, Switzerland
Cell Scraper	TPP, Switzerland
Cryovial Tubes (2ml)	CAPP, Denmark
Microfuge Tubes	CAPP, Denmark
Multichannel Pipette	Thermo Scientific, USA
Multichannel Pipette Tips	Thermo Scientific, USA
Multiwell Plates	TPP, Switzerland
Nitrocellulose Blotting Membrane (0.2um)	GE Life Sciences, England
Petri Dishes	Fırat Plastik, Turkey
Pipette Tips (Filtered)	BioPointe Scientific, USA
Pippette Tips (Bulk)	CAPP, Denmark
Protein A Resin Captiva	Repligen, USA
Syringe Filter Units (0.22 µm, 0.45 µm)	EMD Millipore, USA

Table 3.4. Devices.

Device name	Brand
Autoclaves	Midas 55, Prior Clave, UK AS260T, Astell, UK
BD Accuri	BD, USA
Carbon dioxide tank (cell culture)	Genç Karbon, Turkey
Cell culture incubator	WTC, Binder, Germany
Centrifuges	Allegra X-22, Beckman Culture, USA
Cold room	Birikim Elektrik Soğutma, Turkey
Confocal microscope	Leica SP8, USA
Documentation system	Gel Doc XR system, Bio-Doc, USA

Table 3.4. Devices (cont.).

Device name	**Brand**
Fluorescent microscope	Axio Observer.Z1, Zeiss, Germany
Freezers and refrigerators	4 °C: Uğur, USS 374 DTKY, Turkey -20 °C: Uğur, UFR 370 SD, Turkey -80 °C: ULT deep freezer, Thermo, UK
Heat block	Block Heater Analog, VWR, USA
Ice flaker	AF20, Scotsman Inc., Italy
Laminal flow cabinet	Class IIB, Tezsan, Turkey
Micropipettes	Finnpipette, Thermo, USA
Microwave oven	Arçelik, Turkey
Nanodrop	ND-1000, Thermo Fisher, USA
Oven	Gallenkamp, 300, UK
pH meter	Hanna Instruments, USA
Pipettor	S1 Pipet Filler, Thermo Fisher, USA
Power supply	EC XL 300, Thermo Fisher, USA
PikoReal Real-Time PCR system	Thermo Fisher, USA
Rotator-mixer	Grant Instruments, UK
Shaker	Analog Orbital Shaker, VWR, USA
Software	ImageJ, NIH, USA PyMOL, USA Syngene-Genetools, UK Leica LAS X, USA
Sonicator	Sonoplus, Bandelin, Germany Q800, QSonica, USA
Vortex	Silverline, VWR, USA
Water purification	WA-TECH UP Water Purification Sys., Germany
Western blot documentation system	G-BOX Chemi XX6, Syngene, UK

3.4. Reagents, Kits, Enzymes and Chemicals

The reagents, kits, and enzymes used in this study are listed in Table 3.5. Chemicals are listed in Table 3.6.

Table 3.5. Reagents kits and enzymes.

Product	**Supplier**
Complete Mini Protease Inhibitor Cocktail	Roche, Switzerland
DNA Ladder (1kb)	NEB, USA
Duolink® In Situ Detection Reagents Orange	Sigma-Aldrich, USA
Duolink® In Situ PLA® Probe Anti-Rabbit MINUS	Sigma-Aldrich, USA
Duolink® In Situ PLA® Probe Anti-Rabbit PLUS	Sigma-Aldrich, USA
dNTP mix	NEB, USA
DpnI enzyme	NEB, USA
ECL	Advansta, USA
HiPerFect Transfection Reagent	Qiagen, Netherlands
NucleoSpin Gel and PCR Clean-up kit	Machery-Nagel, Germany
Nucleospin MiniPrep Kit	Machery-Nagel, Germany
PageRuler Prestained Protein Ladder	Thermo, USA
Plasmid MidiPrep Kit	Machery-Nagel, Germany
Q5 High-Fidelity DNA Polymerase	NEB, USA
Sirius	Advansta, USA

Table 3.6. Chemicals.

Chemical	**Brand**
2-mercaptoethanol	Merck, Germany
4’6-diamidino-2-phenylindole (DAPI)	Sigma-Aldrich, USA
Acetic acid	Sigma-Aldrich, USA
Acrylamide	Bio-Rad, USA
Ammonium persulfate (APS)	AppliChem, Germany
Ampicillin	Merck, Germany
Bromophenol blue	Sigma-Aldrich, USA
Calcium chloride dehydrate	Sigma-Aldrich, USA
cOmplete^{TM}, EDTA-free Protease Inhibitor Cocktail	Roche, Switzerland
Cycloheximide	Sigma-Aldrich, USA
Dimethyl sulfoxide (DMSO)	Sigma-Aldrich, USA
Doxycycline hyclate	Merck, Germany
Dulbecco’s Modified Eagle Medium (DMEM)	Gibco, Fisher Scientific, USA
Ethanol	Merck, Germany
Ethylenediaminetetraacetic acid (EDTA)	Wisent Bioproducts, Canada
Fetal Bovine Serum (FBS)	Gibco, Fisher Scientific, USA
Glycerol	MP Biomedicals, USA
Glycine	NeoFroxx, Germany
HEPES buffered saline (HBS)	Lonza, Switzerland
Hydrochloric acid	Sigma-Aldrich, USA
Interferon-α (human)	Roche, Switzerland
Isopropanol	Sigma-Aldrich, USA
Kanamycin	Gold Biotechnology, USA
Luria-Bertani (LB) Agar	Caisson Laboratories, USA
Luria-Bertani (LB) Broth	Caisson Laboratories, USA

Table 3.6. Chemicals (cont.).

Chemical	**Brand**
Methanol	Merck, Germany
MG132	Calbiochem, Germany
ML792	Medkoo Biosciences, USA
N-ethylmaleimide (NEM)	Sigma-Aldrich, USA
Nonidet P-40	Sigma-Aldrich, USA
Paraformaldehyde (PFA)	Santa Cruz Biotechnology, USA
Penicillin/Streptomycin (100X)	Lonza, Switzerland
Phenol-chloroform-Isoamyl alcohol	Sigma-Aldrich, USA
Sodium chloride	Merck, Germany
Sodium Deoxycholate	Sigma-Aldrich, USA
Sodium dodecyl sulfate (SDS)	Merck, Germany
Sodium hydroxide	Merck, Germany
Technical Ethanol	Çakır Kimya, Turkey
Tetramethylethylenediamine (TEMED)	Sigma-Aldrich, USA
Tris-base	Biofroxx, Germany
Triton X-100	VWR, USA
Trypsin-EDTA (0,05%, 0,25%)	Gibco, Fisher Scientific, USA
Tween 20	Merck, Germany

3.5. Buffers and Antibodies

Buffers and solutions used in this study are shown in Table 3.7. Antibodies with their concentrations used in the experiments are shown in Table 3.8.

Table 3.7. Buffers.

Buffer name	Ingredients
1,10-Phenanthroline stock solution	1 gr 1,10-Phenanthroline in 10 ml absolute ethanol. Stored at -20^{0}C.
10X SDS Western blot running buffer	1% (w/v) SDS, 3.03% (w/v) Tris base, 11.41% (w/v) glycine in ddH_2O
10X SDS Western blot transfer buffer	3.03% (w/v) Tris base, 11.41% (w/v) glycine in ddH_2O
4X Laemmli buffer	200 mM Tris-HCl (pH 6.8), 8% SDS, 40% glycerol, 4% 2-mercaptoethanol, 50 mM EDTA, 0.08% bromophenol blue in ddH_2O
5% Stacking gel (Western Blot)	0.125 mM Tris-HCl (pH 6.8), 0.1% (w/v) SDS, 4% (w/v) acrylamide:bisacrylamide, 0.05% (w/v) APS,0.0075% (w/v) TEMED in ddH_2O
8% Resolving gel (Western blot)	375 mM Tris-HCl (pH 8.8), 0.1% (w/v) SDS
AP Assay Buffer	100 mM Trizma base, 20 mM MgCl2, 100 mM NaCl. pH adjusted to 9.5.
AP Lysis Buffer	1% Triton-X, 1:100 1,10-phenanthroline stock solution, 1:500 0.5 M EDTA (final 1 mM EDTA) in PBS
AP Substrate Solution	50 mg/mL p-NPP in ddH_2O
AP Working Solution	1:25 AP Substrate Solution in AP Assay Buffer
BB94 stock solution	1 mM BB94 dissolved in DMSO. Stored at -20^{0}C and protected from light.
Immunoprecipitation (IP) lysis buffer	2% SDS, 50 mM Tris-HCl (pH 8.0), 20 mM NEM, Protease inhibitor cocktail, in ddH_2O

Table 3.7. Buffers (cont.).

Buffer name	Ingredients
Ponceau S stain	5% Glacial acetic acid, 0,1% Ponceau S, in ddH_2O
Radioimmunoprecipitation (RIPA) buffer	50 mM Tris-HCl, 300 mM NaCl, 1% NP-40, 10% glycerol, 0,1mM EDTA (pH:8) in ddH_2O (pH 7.4)
Western blot blocking & antibody solution	5% (w/v) non-fat dry milk in TBS-T
NEM Stock solution	0,5M NEM in EtOH
NEM Working solution	400ul NEM Stock in 10ml PBS
1X TBS-T	50mM Tris HCl pH:7.4, 150mM NaCl, 0,05% Tween-20
PBS-T	0,05% Tween-20 in 1X PBS
PLA Permeabilization buffer	0,5% TritonX-100 in 1X PBS
PLA Blocking buffer	1% BSA, 0,05% TritonX-100 in 1X PBS
PMA stock solution	0,1 mg/mL Phorbol 12-myristate 13-acetate (PMA) in DMSO. Stored at -20^{0}C and protected from light.

Table 3.8. Antibodies.

Antibody	Supplier	Source	Dilution
6X Histidine (#sc-57598)	Santa Cruz Biotech, USA	Mouse	WB (1:1000)
β-Actin (#MA1115)	BosterBio, USA	Mouse	WB (1:1000)
ADAM17 (#sc-390859)	Santa Cruz Biotech, USA	Mouse	WB (1:1000) PLA (1:250)
ADAM17 (#ab39162)	Abcam, UK	Rabbit	WB (1:1000) PLA (1:1000)

Table 3.8. Antibodies (cont.).

Antibody	Supplier	Source	Dilution
Anti-Mouse IgG HRP (#7076S)	CST, USA	Goat	WB (1:10000)
Anti-Rabbit IgG HRP (#7074S)	CST, USA	Goat	WB (1:10000)
Cas9 (#844301)	BioLegend, USA	Mouse	PLA (1:100)
FLAG (#F1804)	Sigma Aldrich, USA	Mouse	WB (1:1000)
FLAG (#14793S)	CST, USA	Rabbit	WB (1:1000) PLA (1:400)
HA (16B12)	BioLegend, USA	Mouse	WB (1:1000)
SUMO1 (#4930S)	CST, USA	Rabbit	WB (1:1000) PLA (1:150)
SUMO2/3 (#ab3742)	Abcam, UK	Rabbit	WB (1:1000) PLA (1:150)
UBC9 (#ab75854)	Abcam, UK	Rabbit	PLA (1:150)
Ubiquitin FK2 (#ST1200)	Sigma Aldrich, USA	Mouse	WB (1:1000) PLA (1:1000)

4. METHODS

4.1. Cell Culture

HEK293 and HeLa cells were maintained in Dulbecco's Modified Eagle Medium (DMEM) supplemented with 10% Fetal Bovine Serum and 1% Penicillin/Streptomycin. The cells were cultured in 75 cm^2 cell culture flasks in a humidified incubator maintained at 37°C and 5% CO_2. Passaging was performed every 2-3 days when the cells reached 90% confluency. Briefly, the medium was discarded, and the cells were washed with 1X PBS. They were then incubated with 0.005% trypsin solution for 3-4 minutes in the incubator. Next, a volume of DMEM equal to twice the volume of trypsin was added to deactivate the trypsin. The cells were collected into 15 ml falcon tubes, centrifuged at 300 x g for 5 minutes, resuspended in fresh medium, and seeded into new flasks at a 1:3 to 1:5 ratio.

4.2. Treatments

Doxycycline (2 μM) was added directly to the cell culture medium to the cells transfected with the pCW-Cas9 plasmid or Cas9-expressing HEK293 cells the day before the experiment to induce Cas9 expression.

To inhibit global SUMOylation in the AP Assays and ADAM17 stability assays, the cells were treated with 2 μM of ML792 for 18-24 hours, by changing the medium 6 hours following transfection.

MG132, a proteasome inhibitor, was added to the cell medium at a concentration of 10 μM for 6 hours or 2 μM overnight before the start of the experiment to inhibit proteasomes. Since MG132 is dissolved in DMSO, control cells were treated with an equivalent volume of DMSO as a mock treatment.

Cycloheximide (CHX), a protein synthesis inhibitor, was added to the cell culture medium at a concentration of 50 µg/ml, 18 hours after transfection. The treatment was then continued for 4, 8, and 12 hours, allowing for different time points to be preserved during the experiment.

For the AP Assays, the ADAM17 enzymatic activities were activated or inhibited by preparing a fresh medium containing 25 ng/mL Phorbol 12-myristate 13-acetate (PMA) or 2 µM batimastat (BB94), which was then vortexed. Next, the medium containing constitutive shedding was collected into clean 1.5 mL tubes and replaced with the PMA- or BB94-containing medium under the laminar flow hood in the dark. The cells were then incubated for 1 hour in the incubator maintained at 37°C and 5% CO2.

4.3. Transfection

The day before transfection, HEK293 cells were seeded in 6-well, 12-well, or 10 cm2 plates at a density of 70,000 cells/cm2. Once the cells reached 70% confluency the next day, calcium phosphate transfection was performed. Briefly, plasmid DNA was resuspended in ddH_2O, and 2 M $CaCl_2$ was added dropwise to achieve a final concentration of 125 mM. After incubating the DNA- $CaCl_2$ complex at room temperature for 5 minutes, 2X HBS was added dropwise and mixed well. This final solution was then incubated at room temperature for 10 minutes before being added dropwise to the cells. The DNA amounts and chemical volumes are provided in Table 4.1.

Table 4.1. Materials and the amounts used in transfection.

Material	12-well plates	6-well plates	10 cm plates
ddH_2O (µL)	54,7	109,4	Up to 438
DNA (µg)	1 to 2	2 to 4	10 to 15
2 M $CaCl_2$	7,8	15,6	62,5
2X HBS	62,5	125	500
Total (µL)	125	250	1000

4.4. Proximity Ligation Assay (PLA)

The proximity ligation assay (PLA) is an ultrasensitive and powerful method to detect protein-protein interactions and protein quantifications (P. Wang et al., 2021). This method was recently developed to detect post-translational modifications such as ubiquitylation and SUMOylation on proteins (Sahin et al., 2016). The PLA method, in which all processes are performed on a microscope slide, derives its strength from the combination of two sensitive techniques, immuno-fluorescence and PCR (polymerase chain reaction). In this method, the cells are fixed, as in the immunofluorescence method, and then treated with primary antibodies. Since the PLA kit contains anti-mouse and anti-rabbit secondary antibodies conjugated with specific oligonucleotides, one of these primary antibodies must have been developed in the mouse and the other in the rabbit. These secondary antibodies, which are special production, have oligos that are complementary to each other and if the two proteins are within 14 nm of each other, the oligos are hybridized to form a circle. After ligation of this 'oligo-circle' by T4 ligase, a rolling circle amplification is started via PCR, also on the same microscope slide. The amplified oligo-circles can be detected as a fluorescent signal under a confocal microscope using the fluorescent dNTP mixture. The detection sensitivity of this method is at the single molecule level, each signal points to a single protein-protein interaction (Sahin et al., 2016). The method is summarized in Figure 4.1.

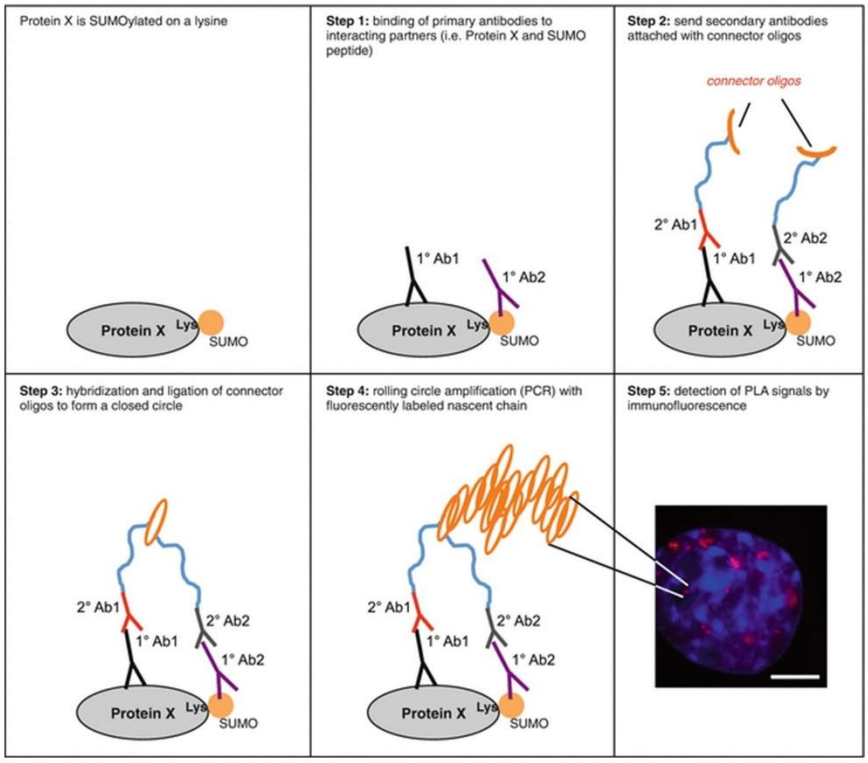

Figure 4.1. Detection of SUMOylated protein forms by proximity ligation assay (PLA) is summarized schematically. Secondary antibodies conjugated with complementary oligos are readily available in PLA kits. This figure is reprinted from Sahin et al., 2016.

HEK293 or HeLa cells were seeded on 20 mm round glass coverslips in 12-well plates at a density of 35,000 cells/cm^2. Once the cells reached 30% confluency, they were washed with PBS and fixed with 500 µL of 4% paraformaldehyde (PFA) in PBS, incubating for 15 minutes at 37°C. The PFA was then removed, and the cells were washed with PBS three times for 5 minutes each. Next, the cells were permeabilized with a 0.5% Triton-X100 containing permeabilization buffer at room temperature for 30 minutes. Blocking was then performed using a 1% BSA and 0.05% Triton-X100 containing blocking buffer, either at room temperature for 1 hour or at 4°C overnight. Since the PLA kit uses anti-mouse and anti-rabbit oligos, one primary antibody should be raised in mouse and the other in rabbit. The primary antibodies were then diluted in the blocking buffer and incubated on the cells for 1 hour at room temperature. This was followed by washing the cells with PBS three times for 5 minutes each. Next, the PLA probe solutions were prepared according to the manufacturer's instructions and added to the cells, which were then incubated for 1 hour at 37°C in a humidity chamber. The cells were then washed with the PBS twice for 5 minutes

each, and the ligation solution was added, with the cells incubated for 30 minutes at 37°C in a humidity chamber. Finally, the amplification solution was added, and the cells were incubated for 100 minutes at 37°C in a humidity chamber. The cells were washed with PLA buffer B twice for 10 minutes each. A final wash was performed at RT for 1 min using 0.01X PLA buffer B in ddH_2O, and the cells were mounted onto slides using a mounting medium containing DAPI. Then, the coverslips were sealed to the slides with nail polish. Slides were then analyzed under a confocal microscope (Leica TCS SP8, USA), using 405 nm to visualize the nucleus and 545 nm to detect the PLA signals. PLA signals were quantified in the maximum projection of the z-stacks over the DAPI-stained nuclei.

4.5. Alkaline Phosphatase (AP) Assay

Alkaline Phosphatase (AP) is an enzyme expressed in both prokaryotes and eukaryotes, responsible for the removal of the phosphate groups from various biomolecules such as DNA, RNA, nucleotides, and proteins. When a sample containing AP is introduced to its substrate, p-nitrophenyl phosphate (p-NPP), the p-NPP turns yellow due to the phosphatase activity of the AP enzyme (λmax = 405 nm). This property makes AP a commonly used tool in colorimetric assays in the field of molecular biology. The AP Assay method involves expressing vectors formed by adding AP to the N-terminal (extracellular part) of EGFR ligands, such as TGFα, HB-EGF, epiregulin, and amphiregulin. The amount of AP released into the medium is then analyzed using semi-quantitative colorimetrical methods, which provide insight into the shedding activity of ADAM group metalloproteases. This approach is a simple yet powerful technique for studying ADAM17-mediated ectodomain shedding (Sahin et al., 2006).

In this single-well assay, the initial sample represents the supernatant collected from a cell culture after a 1-hour conditioning period, establishing the baseline levels of constitutive ectodomain shedding, which occurs continuously at a basal level without the need for specific triggers, from a specific well. After that, a fresh medium containing a compound that either stimulates or inhibits this shedding process is added to the same well and conditioned for an additional hour. Phorbol 12-myristate 13-acetate (PMA) is a potent activator of Protein Kinase C, a known upstream regulator of ADAM17 activity (Düsterhöft,

Lokau, et al., 2019). Treatment with PMA induces a rapid and robust increase in ADAM17-mediated shedding. Conversely, BB94 serves as a broad-spectrum inhibitor of matrix metalloproteinases, including ADAM17. Each well-based assay thus generates a single data point that indicates the percent change in shedding activity observed in the second sample relative to the constitutive baseline levels measured in the first sample.

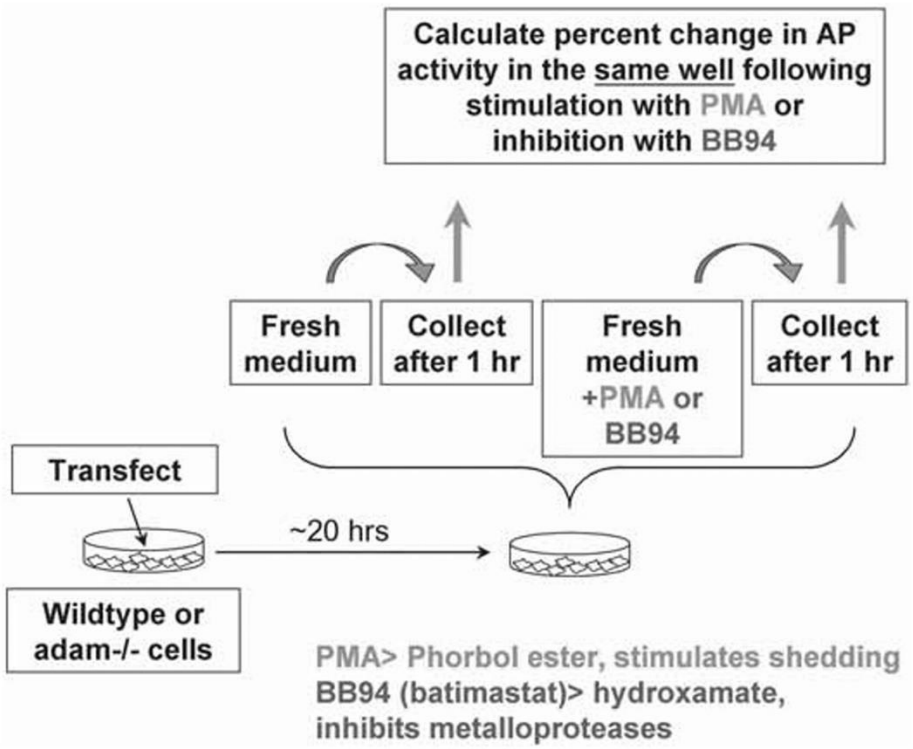

Figure 4.2. Schematic representation of Alkaline phosphatase assay (AP assay) for the semi-quantitative analysis of ADAM17-mediated protein ectodomain shedding.The figure is reprinted from Sahin et al., 2006.

HEK293 cells were transfected with 500 ng of an AP-tagged ADAM17 substrate construct (AP-TGFα, AP-HB-EGF, AP-Epiregulin). 18-20 hours after transfection, the alkaline phosphatase (AP) assay was initiated. First, the cells were starved in 500 µL of incomplete OptiMem medium for 2 hours in the incubator. Then, 500 µL of fresh OptiMem was added, and the cells were incubated for 1 hour to allow for constitutive shedding. After the incubation, the media was collected in 1.5 mL tubes and kept at 4°C. The same cells

were then incubated for an additional hour with OptiMem containing either PMA (25 ng/mL) or BB94 (2 μM), and the media was collected in 1.5 mL tubes and kept at 4°C. The cells were then lysed in 250 μL of AP Lysis Buffer and incubated at 4°C on a rotator for 20-30 minutes. The lysates were then transferred to 1.5 mL tubes. The collected media and cell lysates were centrifuged at 2,000 × g at 4°C for 10 minutes. 100 μL of the media from the unstimulated, PMA-stimulated, or BB94-inhibited conditions were transferred to 96-well plates. Additionally, 10 μL of the lysates were diluted in 90 μL of AP Assay buffer in 96-well plates. Triplicate wells of duplicate or triplicate technical replicates were analyzed. The AP substrate solution (50 mg/mL p-NPP) was diluted 1:25 in the AP Assay Buffer to create the working solution. Finally, 100 μL of this diluted working solution was added to the wells using a multichannel pipette. AP substrate (50 mg/mL p-NPP) was diluted 1:25 in AP Assay Buffer (working solution). Finally, 100 μL of the working solution was added to the wells using a multichannel pipette. The 96-well plates were then incubated at 37°C until optimal reading could be obtained. The colorimetric measurements were performed at 405 nm using a plate reader. A blank was prepared by combining 100 μL of AP Assay buffer with 100 μL of p-NPP solution.

4.6. Immunoprecipitation (IP)

HEK293 cells were seeded in 10 cm culture plates at a density of 70.000/cm^2. 18-20 hours transfection, the culture medium was discarded, and the cells were incubated with 1mL of ice-cold NEM Working Solution at room temperature for 2-3 minutes to inhibit deSUMOylation. After discarding the NEM Working solution, 5 mL PBS was added to the cells. The cells were then scraped and collected in 15 mL falcon tubes, followed by centrifugation at 300 x g for 5 minutes. The supernatant (PBS) was removed, and the pellet (the cells) were lysed in 120-150 μL of 2% SDS and Protease Inhibitor Cocktail (PIC) containing IP Lysis Buffer. The lysates were sonicated (amplitude 60%, 15 sec, 8 cycles) until they appeared homogenous. The lysates were then diluted 1:10 with PIC containing RIPA buffer to achieve a final SDS concentration of 0.2%, and centrifuged at 2000 x g for 30 minutes at +4°C. In the meantime, the protein A agarose beads were prepared by washing them 5-6 times with RIPA buffer to equilibrate them. Following centrifugation, the supernatants were transferred to clean 1.5 mL tubes, and 90 μL of the lysates were set aside

and mixed with 30 µL of the 4X Laemmli solution to and kept as a whole cell lysate. The remaining lysates were then pre-cleared by incubating them with 25 µL of equilibrated protein A agarose beads at room temperature for 45 minutes to 1 hour on a tube rotator. The lysate-bead mixture was then spun down for 1 minute, and the lysates were separated from the beads and transferred to a clean tube. Next, the pre-cleared lysates were incubated with the primary antibody against the protein of interest, either at room temperature for 1 hour or at 4°C overnight. Finally, the antibody-protein complexes were captured by adding 50 µL of the equilibrated protein A agarose beads and further incubating for 2-3 hours at 4°C on a tube rotator. After removing all the remaining PBS with the help of a 200 µL pipette tip, the immunoprecipitated proteins were then eluted from the beads by adding 40 to 75 µL of 2X Laemmli solution. Whole-cell lysate (WCL) and immunoprecipitation (IP) samples were stored at -20°C for future Western blot analysis.

4.7. Western Blot Analysis

8% or 10% SDS-PAGE gels were prepared, depending on the specific requirements of the experiment. Cas9 samples were incubated at 95°C for 5-10 minutes to denature the proteins, while ADAM17 samples were incubated at room temperature before loading onto the gels. 15-20 µL of the immunoprecipitation samples or whole-cell lysates were loaded onto the SDS-PAGE gels, along with a pre-stained protein ladder to allow for the estimation of protein sizes. The gels were run at 80V for 30 minutes to focus the samples on the stacking gel, and then at 120V for 1-2 hours to separate the proteins in the resolving gel based on their molecular weights. The separated proteins were then transferred to nitrocellulose membranes by wet transfer at 100V for 3 hours at +4°C to preserve protein integrity. Ponceau S staining was used to check the efficiency of the protein transfer, and the dye was subsequently washed off with water and TBS-T. The membranes were blocked with 5% skim milk in TBS-T for 1 hour at room temperature to prevent nonspecific binding of antibodies. Primary antibodies, prepared in the blocking solution, were then incubated with the membranes overnight at +4°C to allow for the specific binding of the target proteins. After three 10-minute washes in TBS-T to remove unbound primary antibodies, the membranes were incubated with HRP-conjugated secondary antibodies, also dissolved in the blocking solution, for 1 hour at room temperature. Finally, the membranes were washed

three times for 5 minutes each in TBS-T to remove unbound secondary antibodies, and a horseradish peroxidase solution was applied to detect the chemiluminescence signal, which indicates the presence and abundance of the target proteins. The membranes were then visualized by a visualization system (GBox Chemi, Syngene, UK).

4.8. Site-Directed Mutagenesis (SDM)

The primers carrying the desired mutations were manually designed. With the assistance of Primer3 software, the primers were evaluated for self-complementarity and potential primer-primer dimers. These primers were then ordered from Macrogen. The primer sequences were provided in the Materials section, Table 3.2. The pCW-Cas9 (addgene, #50661), and pRK5F-TACE (addgene, #31713) plasmids were utilized for the Cas9 and ADAM17 variant constructs, respectively.

A single primer was used to perform a polymerase chain reaction for 10 cycles. The ingredients and volumes for the first round of PCR are detailed in Table 4.2, while the PCR conditions are shown in Table 4.3.

Table 4.2. PCR ingredients and amounts used for site-directed mutagenesis

Ingredient	**Volume (µL)**
ddH_2O	12,25
5x Q5 Reaction Buffer	5
dNTP (10 mM)	0,5
Primer Forward or Reverse (10 µM)	1
5x Q5 Enhancer solution	5
Q5 Polymerase	0,25
Plasmid DNA (50 ng/µL)	1
Total	25

Table 4.3. PCR Conditions for the first round PCR of SDM

Temperature (^{0}C)	**Duration**	**Cycles**
95^{0}C	5 secs	1
95^{0}C	30 secs	10
55-70^{0}C gradient	30 secs	10
72^{0}C	4 mins	10

Then, reactions with 25 µL of forward and 25 µL reverse primers were mixed in a PCR tube and a second round of PCR reaction was performed for 15 cycles according to Table 4.4.

Table 4.4. PCR Conditions for the second round PCR of SDM

Temperature	Duration	Cycles
95^0C	5 secs	1
95^0C	30 secs	15
55-70^0C gradient	30 secs	
72^0C	4 min	
72^0C	5 min	1
12^0C	On hold	

To accommodate the varying annealing temperatures of each primer pair, gradient PCR was employed for the site-directed mutagenesis. The primer pairs and their corresponding annealing temperatures are provided in Table 4.5. Additionally, a negative control lacking Q5 polymerase was included in all the reactions.

Table 4.5. Annealing temperatures for the primer pairs used for site-directed mutagenesis

Primer name	Annealing Temperature
Cas9-D850A	55
ADAM17-K188R	60
ADAM17-K697R	61
ADAM17-K753R	70

Following the second round of PCR, 5 µL of PCR products were mixed with 1 µL of 6X loading dye and loaded onto a 1% agarose gel, along with a DNA ladder and negative controls. The gel was then run at 120V for 30 minutes and visualized under UV light.

After the amplification of the plasmids with the primers designed for site-directed mutagenesis, PCR clean-up was conducted following the manufacturer's instructions. Then, DpnI digestion was performed to digest the parental plasmid DNA. For this, 20 µL of the

PCR clean-up sample was mixed with 68 µL of ddH_2O, 10 µL of 10X Buffer Tango, and 2 µL of DpnI, and incubated overnight at 37°C. DpnI was then heat-inactivated by incubating the tubes at 80°C for 20 minutes.

Since DpnI is a restriction enzyme that specifically recognizes and cleaves methylated DNA, at the end of the reaction, the parental DNA which was methylated by the bacterial methyltransferases was selectively digested. In contrast, the newly amplified DNA produced during the site-directed mutagenesis process remained intact, as it was not methylated. This selective digestion of the parental DNA allowed for the isolation of the plasmids harboring the desired mutation, effectively separating them from the original, unmutated parental plasmid DNA.

The SDM products were then transformed into DH5α competent cells, and the transformed bacteria were grown on LB agar plates with ampicillin. To ensure the efficacy of the mutagenesis and transformation processes, two negative controls were included. The first negative control consisted of untransformed competent cells, while the second included DpnI-digested parental plasmid DNA. No colonies should be observed in either of these negative controls, as they serve to verify the functionality of the ampicillin selection and the effectiveness of the DpnI digestion, respectively. Following the successful transformation, a single colony was selected for each SDM plasmid and sent for Sanger sequencing to verify the presence of the desired mutation.

4.9. Generation of Stable Cell Lines

HEK293 cells were seeded on 10 cm culture plates at a density of 140,000 cells/cm2. The next day, transfection was performed with the pCW-Cas9 construct, along with the helper plasmids psPAX2 (addgene, #12260**)** and pVSV-G (addgene, #138479**)**, to facilitate virus production. 6 hours after transfection, the media was replaced with 8 mL of fresh medium. 48 hours post-transfection, the media containing the virus particles was collected and filtered through a 0.45 µm pore size filter. The filtered virus-containing media was then used to transduce HEK293 cells.

HEK293 cells were seeded at a density of 70,000 cells/cm2 in 6-well plates. The virus-containing media was then added to the seeded cells, along with 8 μg/mL polybrene to enhance the transduction efficiency. The polybrene helps to facilitate the entry of the viral particles into the cells, improving the transduction efficiency. 48 hours post-transduction, the cells were selected with 1 μg/mL puromycin for 2 weeks to obtain stable cell lines expressing Cas9. This selection process ensures that only the cells that have successfully integrated the Cas9 construct and are expressing the Cas9 protein, will survive and proliferate. The Cas9 protein expression in these stable cell lines was then assessed through Western blot analysis, utilizing an anti-FLAG antibody following overnight induction with 2 μg/mL doxycycline. The Western blot analysis allows for the detection and quantification of the Cas9 protein, which is fused to a FLAG tag, to confirm its expression in the generated stable cell lines.

5. RESULTS

5.1. Investigation of Cas9 SUMOylation and Ubiquitylation by Proximity Ligation Assay

5.1.1. Preliminary Data: Identification of SUMOylation of Cas9 Protein by SUMO1 and SUMO2/3 in Eukaryotic Cells by Immunoprecipitation and His Pulldown Methods

Previously, our lab members had been shown that Cas9 is SUMOylated with three different assays (Çelen, 2019; Ergünay, 2022). In the first assay, HEK293 cells were co-transfected with a doxycycline-inducible lentiviral construct expressing FLAG-Cas9 (pcW-Cas9) and plasmids containing GFP tagged human SUMO1 or SUMO2/3. Then immunoprecipitation (IP) was performed with anti-FLAG antibody (Sigma-Aldrich, #F1804) using agarose A/G beads (Thermo Fisher, cat 20421). After running the IP products on precast gels (8% or 4-12% gradient), Western blot analysis was performed with human anti-SUMO1 antibody (CST, #4930), human anti-SUMO2-3 antibody (Abcam, ab3742), or anti-GFP antibody (Santa Cruz, sc-9996).

The immunoblot analysis following FLAG-Cas9 pulldown revealed a smeared pattern when probed with antibodies against SUMO1, SUMO2/3, or GFP, indicating that Cas9 is modified by both SUMO1 and SUMO2/3 (Figure 5.1.A). Immunoblotting against GFP enabled a comparative evaluation of the relative conjugation levels of Cas9 by the two distinct SUMO paralogs. This analysis indicated that the Cas9 protein is more strongly modified by SUMO2/3 conjugates compared to SUMO1 conjugates (Figure 5.1.A).

In the second assay, His-pulldown was performed with Ni-NTA beads (Thermo Fisher, cat R90101) on HEK293 cells that were co-transfected with FLAG-Cas9 and histidine-tagged SUMO1 and SUMO2/3 to purify His-SUMO conjugates. Western blot analysis with anti-FLAG antibody resulted in multiple bands above 160 kDa (which is the molecular

weight of the Cas9) verifying that Cas9 is modified by both SUMO1 and SUMO2/3 (Figure 5.1.B). Notably, SUMO2/3 modification was stronger compared to SUMO1 on Cas9 protein. Controls included immunoblotting with anti-His on the His pulldown samples and anti-FLAG antibody on whole cell lysates to check the levels of His-SUMO conjugated proteins and Cas9 expression, respectively.

In a third assay, immunoprecipitation using an anti-FLAG antibody was conducted on HEK293 cells transfected with a doxycycline-inducible FLAG-Cas9 construct. Immunoblotting against human SUMO1 and SUMO2/3 antibodies demonstrated that Cas9 is endogenously SUMOylated by both SUMO1 and SUMO2/3, with the latter exhibiting stronger modification (Figure 5.1.C).

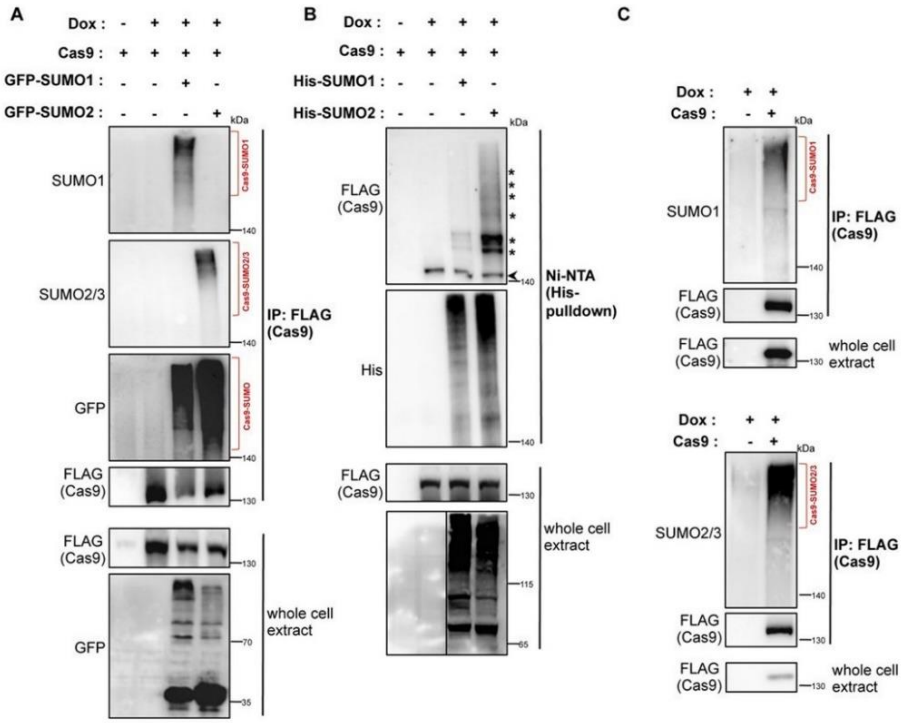

Figure 5.1. SUMO1 and SUMO2/3 modifications on Cas9 protein. (A). Immunoprecipitation experiments revealed that Cas9 is modified by both SUMO1 and SUMO2/3. (B). His pulldown assays confirmed the SUMOylation of Cas9 by SUMO1 and SUMO2/3. (C). Immunoprecipitation experiments with endogenous SUMO1 and SUMO2/3 confirmed that Cas9 is SUMOylated by SUMO1 and SUMO2/3.

5.1.2. Revealing Endogenous SUMOylation of Cas9 by Proximity Ligation Assays (PLA)

The proximity ligation assay was employed to verify the SUMOylation of Cas9 in HEK293 and HK-2 cell lines that endogenously express the SUMO peptides. Cas9-stable cells were incubated with primary antibodies targeting Cas9 (Biolegend, 7A9) and SUMO1 (CST, #4930), or SUMO2/3 (Abcam, ab3742), which are then recognized by specially designed secondary antibodies that attached to complementary DNA oligonucleotides. When the target proteins (Cas9 and SUMO) are in close proximity, the linked oligonucleotides hybridize and initiate a signal amplification process, allowing for the visualization and quantification of the Cas9-SUMO interaction as distinct fluorescent spots under a microscope.

This approach enabled the detection and analysis of the endogenous SUMOylation of Cas9 protein within the cellular context. PLA experiments were also conducted by using a UBC9 antibody (Abcam, ab75854) together with a Cas9 antibody to investigate the Cas9 and UBC9 interactions.

The proximity ligation assay on HEK293 (Figure 5.2.A) and HK-2 (Figure 5.2.B) cell lines stably expressing FLAG-Cas9 yielded similar results. Cas9 was found to be endogenously interacted by both SUMO1 and SUMO2/3, with the SUMO2/3 signals per cell being approximately twice as numerous as the SUMO1 signals. The results suggest that Cas9 is more strongly modified by endogenous SUMO2/3 than SUMO1.

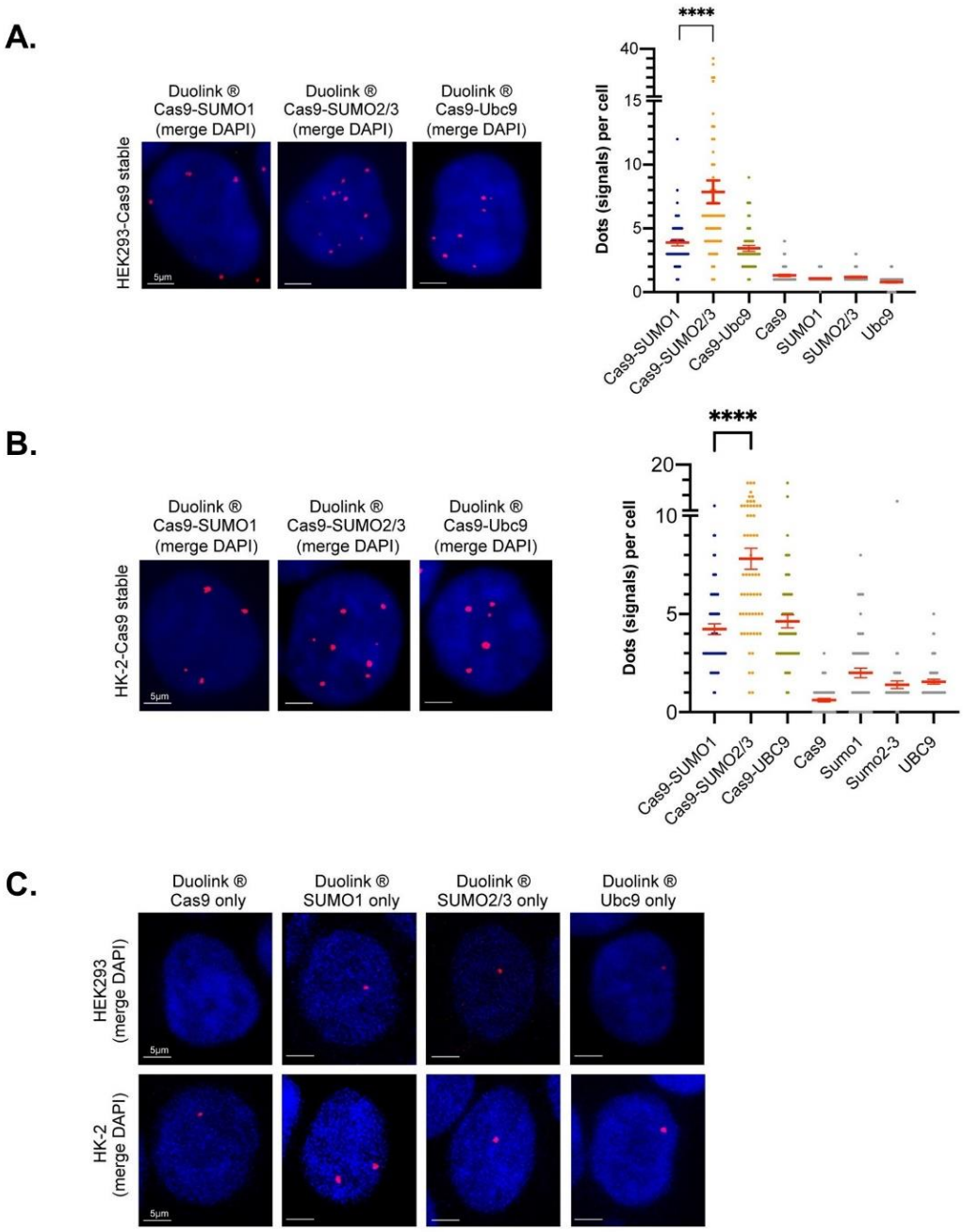

Figure 5.2. Proximity Ligation Assays (PLAs) showing Cas9 interaction by endogenous SUMO1, SUMO2/3, and UBC9 in Cas9-stable HEK293 (A) and HK-2 (B) cell lines. Mean value from two experiments per condition is represented in the graphs, including the negative controls of a given Duolink pair, ± SEM (****P < 0.0001, unpaired t test). (C). Representative images of the negative controls using a single antibody are provided.

Additionally, PLA with an anti-UBC9 antibody resulted in positive signals, demonstrating an interaction between Cas9 and UBC9 (Figure 5.2). Since UBC9 is the universal SUMO E2 conjugase, this Cas9-UBC9 interaction can be interpreted as UBC9 mediating the conjugation of SUMO peptides onto Cas9. Further examination of the z-stacks revealed that the SUMO modification of Cas9 occurred primarily in the nucleus. Notably, no considerable background signal was detected in the negative control groups, where only a single antibody was used (Figure 5.2.C).

5.1.3. Comparison of WT vs K848R Cas9 SUMOylation levels by endogenous SUMO1 and SUMO2/3 in transfection system by proximity ligation assay

Previous experiments by other lab members involving immunoprecipitations of various Cas9 mutants identified K848 on Cas9 as the major SUMO2/3 conjugation site. To further compare the endogenous SUMOylation levels of wild-type Cas9 and the K848R Cas9 mutant (K848R-Cas9), HEK293 cells were transfected with FLAG-tagged constructs of either WT-Cas9 or K848R-Cas9. Proximity ligation assay was performed using antibodies against Cas9, as well as antibodies against SUMO1 or SUMO2/3.

The results revealed that the K848R-Cas9 mutant exhibited a significant decrease in SUMO1 modification compared to the wild-type Cas9. However, the SUMO2/3 conjugation levels were markedly reduced in the K848R-Cas9 mutant relative to the WT-Cas9 protein. This further confirms that the lysine residue at position 848 is the major SUMOylation site for Cas9, particularly for the SUMO2/3 conjugation (Figure 5.3).

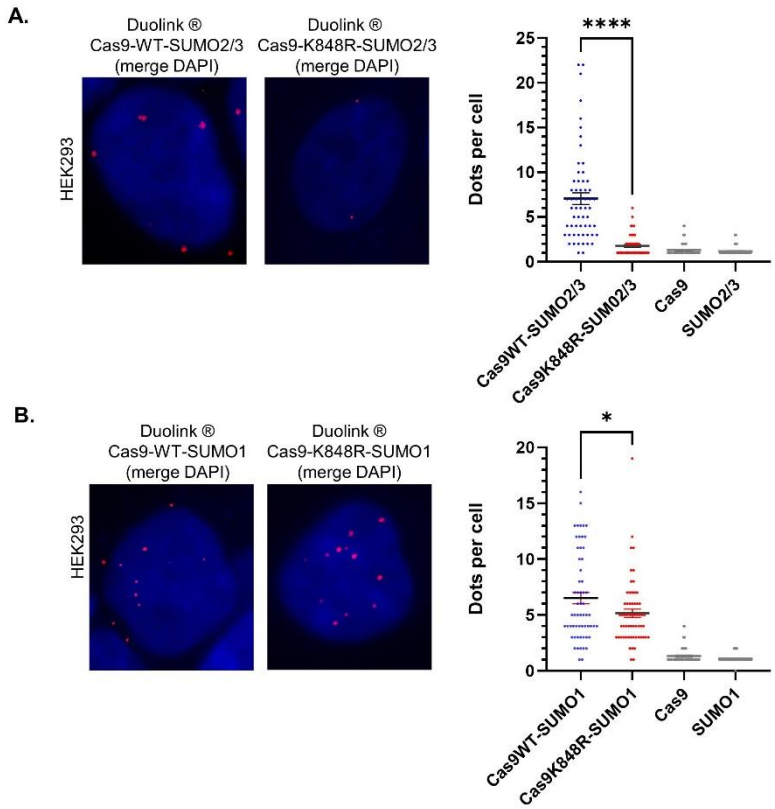

Figure 5.3. Proximity Ligation Assay (PLA) experiments comparing the SUMO modification of wild-type Cas9 and the K848R Cas9 mutant by SUMO2/3 (A) and SUMO1 (B) in the transfection system. The mean values from two experiments are represented, including the negative controls of a given Duolink pair, ± SEM (****P < 0.0001, unpaired t-test).

5.1.4. Creation of Another SUMOylation-deficient Mutant (D850A) by Site-Directed Mutagenesis (SDM)

Substituting the aspartic acid or glutamic acid residue within the SUMOylation consensus motif with the small, neutral amino acid alanine is a widely used technique to disrupt SUMOylation without substantially altering the structure or function of the target protein. This is because alanine, with its compact and uncharged side chain, can disrupt the negative charge that is essential for SUMOylation to occur while minimizing the potential for structural changes to the protein.

The SUMOylated lysine (K848) lies within the endonuclease domain of the Cas9 protein and has been shown to affect the DNA binding ability of Cas9 (Slaymaker et al., 2016). The decrease in SUMOylation observed with the K848R mutant could be attributed to the inability of this mutated form of Cas9 to efficiently bind DNA. The acidic amino acids present in SUMOylation consensus motifs are known to stabilize the interactions between the E2 SUMO conjugating enzyme and the target substrate. To further verify that K848 is the SUMO2/3-modified lysine on Cas9, we decided to create another variant, the D850A mutant, which is adjacent to K848 within the same SUMOylation consensus motif. The D850A mutation is expected to impair the binding of UBC9 to Cas9, thereby dramatically diminishing the SUMOylation of K848. This additional mutant helped confirm the importance of the K848 residue as the SUMO2/3 modification site on Cas9 and provides insights into the mechanism by which SUMOylation regulates Cas9 DNA binding and function.

Consistent with this approach, D850A mutant in pCW-Cas9 (addgene, #50661**)** construct was generated to further examine the role and importance of SUMOylation at the lysine residue located at position 848 (Figure 5.4).

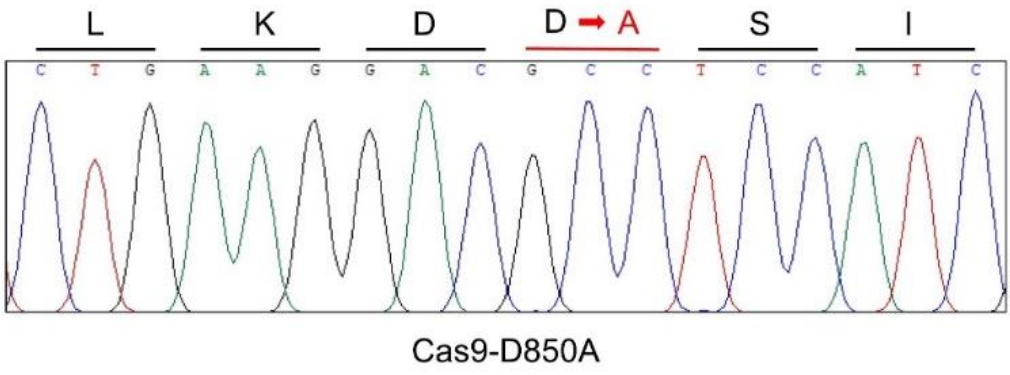

Figure 5.4. Sanger sequencing result showing D850A mutation in pCW-Cas9 plasmid. Wild-type GAC was mutated to GCC by site-directed mutagenesis to convert aspartic acid (D) residue to alanine (A) on the SUMOylation motif.

5.1.5. Generation of Stable Cell Lines Expressing WT, K848R, and D850A Cas9

HEK293 cell lines stably expressing wild-type (WT), K848R, and D850A Cas9 were generated for subsequent use in immunoprecipitation (IP) and proximity ligation assays (PLA). HEK293 cells were transfected with doxycycline-inducible lentiviral construct pCW-Cas9 carrying WT, K848R, or D850A Cas9 along with psPAX2 (addgene, #12260**)** and pVSV-G (addgene, #138479**)** helper plasmids to produce viruses. 48 hours after transfection, virus-containing media was collected and filtered, and then used to transduce HEK293 cells with the help of polybrene (4 μg/ml). The transduced cells were then selected with 1 μg/ml puromycin for 2 weeks to generate a stable cell line expressing the desired Cas9 variant. Cas9 expression levels following overnight incubation with 2 μg/mL doxycycline were analyzed by Western blot analysis using an anti-FLAG antibody (Figure 5.5).

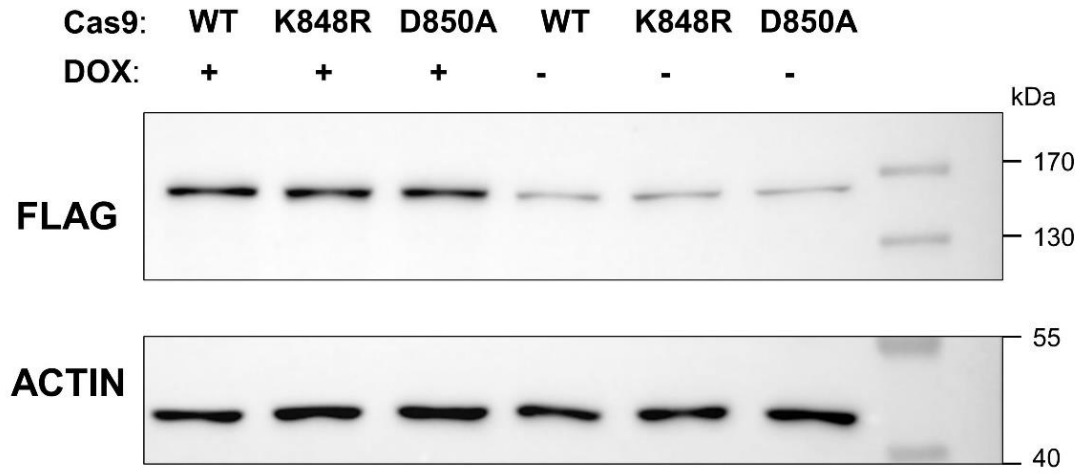

Figure 5.5. Western blot analysis of Cas9 levels in doxycycline-inducible HEK293 cells stably expressing the wild-type, K848R, and D850A Cas9 variants. HEK293 cells were transduced with viruses containing doxycycline-inducible FLAG-Cas9 and selected with puromycin. After an overnight incubation of doxycycline, the cells were lysed in 2X Laemli solution and immunoblotted against ADAM17 and Actin.

5.1.6. Investigation of the Effect of Cas9 SUMOylation in Cell Lines Stably Expressing WT, K848R, and D850A Cas9 by Proximity Ligation Assay

According to immunoprecipitation experiments conducted by Tunahan Ergünay, the substitution of the aspartic acid residue adjacent to lysine 848 with alanine (Cas9-D850 mutant) led to a substantial reduction in the enzyme's conjugation with endogenous SUMO2/3 peptides (Ergünay et al., 2022). These findings suggest that the major SUMO2/3 modification site on Cas9 is the lysine at position 848 and that the surrounding acidic residue (D850) plays a critical role in the SUMOylation process at this site.

PLA experiments were also conducted on HEK293 cells stably expressing wild-type (WT), K848R, or D850A Cas9 using the antibodies against Cas9 and SUMO1 or SUMO2/3. These experiments examined the levels of endogenous SUMO1 and SUMO2/3 modifications on the different Cas9 forms.

Consistent with the PLA results indicating that wild-type Cas9 is much more strongly modified by SUMO2/3 compared to SUMO1 (Figure 5.2), the average number of dots per cell for SUMO2/3 was approximately twice as high compared to SUMO1 in the WT-Cas9 samples (Figure 5.6). In line with the observations from the transient expression system, the cells stably expressing the K848R and D850A Cas9 variants exhibited a significant reduction in the interactions between Cas9 and SUMO2/3, in comparison to the wild-type Cas9. Furthermore, SUMOylation by SUMO2/3 was nearly abolished, especially in HEK293 cells stably expressing the K848R-Cas9 mutant, further confirming that lysine 848 is the major SUMO2/3 attachment site for Cas9 (Figure 5.6).

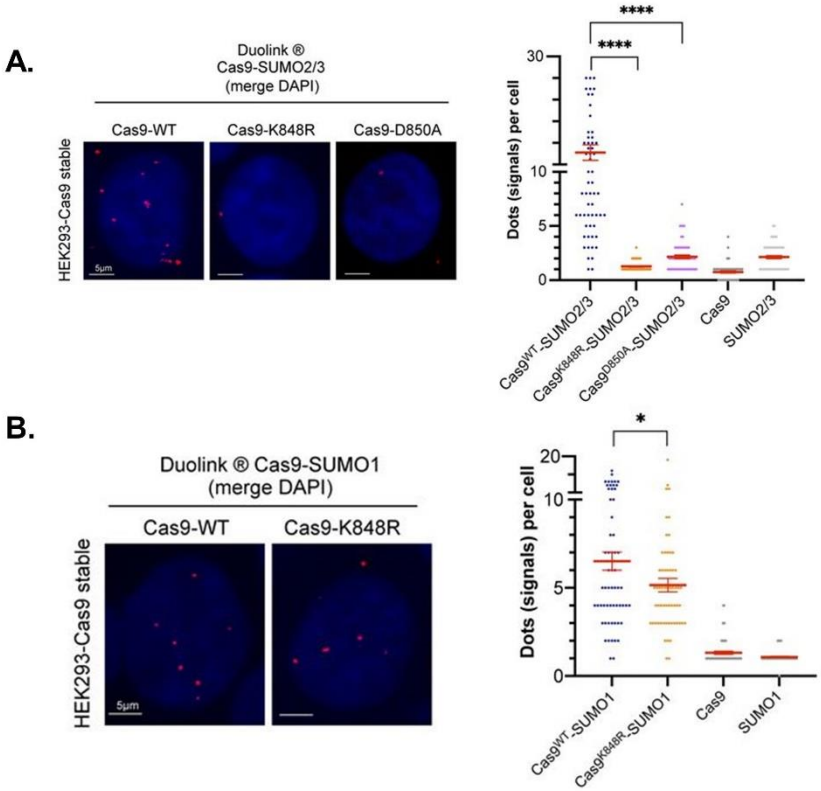

Figure 5.6. PLA experiments showing SUMO1 and SUMO2/3 interactions in the cells stably expressing WT, K848R and D850A Cas9. Representative images and dot plots of PLA showing a significant decrease on SUMOylation levels by SUMO2/3 (A) on HEK293 cells stably expressing WT, K848R, and D850A Cas9, and by SUMO1 (B) on HEK293 cells stably expressing WT and K848R Cas9.

5.1.7. Revealing Endogenous Ubiquitylation of Cas9 by Proximity Ligation Assays (PLA)

Our previous lab member (Çelen, 2019) had demonstrated that Cas9 is also ubiquitylated using similar experimental approaches as those employed for investigating Cas9 SUMOylation. Specifically, immunoprecipitation was performed using an anti-FLAG antibody to pull down FLAG-Cas9 in HEK293 cells co-transfected with FLAG-Cas9 and His-Ubiquitin. Western blot analysis was then conducted with an anti-ubiquitin antibody to detect ubiquitylated forms of Cas9. Additionally, His pull-down experiments were conducted by transfecting HEK293 cells with His-Ubiquitin construct along with FLAG-

Cas9. Immunoblotting against FLAG in His pulldown samples further verified Cas9 ubiquitylation. The cells were also treated with the proteasome inhibitor MG132 to prevent possible degradation of ubiquitylated Cas9 forms in proteasomes. DMSO was used as a carrier. The observation of high molecular weight bands in the anti-ubiquitin immunoblots of the FLAG-immunoprecipitated samples and the anti-FLAG immunoblots of the His-pulldown samples provided clear evidence that Cas9 is ubiquitylated (Çelen, 2019).

Proximity ligation assays (PLAs) were performed to reproduce these findings and investigate the endogenous ubiquitylation of Cas9. PLAs were conducted using anti-FLAG (rabbit, CST, #14793) to target Cas9 and anti-Ubiquitin (mouse, R&D Systems, Clone FK2) antibodies in HEK293 cells stably expressing FLAG-Cas9. Consistent with the previous findings, proximity ligation assays conducted on HEK293 cells stably expressing FLAG-Cas9 demonstrated robust interactions between Cas9 and ubiquitin. Notably, the number of Cas9-ubiquitin PLA signals increased significantly in cells treated with the proteasome inhibitor MG132, compared to the control group (Figure 5.7.A). This strongly suggests that Cas9 undergoes substantial modification by endogenous ubiquitin, which then targets the Cas9 protein for degradation through the proteasomal pathway following its expression in human cells.

To further investigate the interaction between Cas9 and the proteasome, proximity ligation assays were conducted utilizing an antibody against PSMA5 (rabbit, CST, #2457), which targets the 20S proteasome subunit alpha-5, along with the Cas9 antibody (Biolegend, 7A9). The presence of multiple positive PLA signals confirmed a physical interaction between Cas9 and the proteasome. Although pharmacologic blockade of the proteasome with the inhibitor MG132 inhibits its catalytic activity and the degradation of client proteins, it should not interfere with the physical interaction between the proteasome and its substrates. As expected, the number of Cas9–PSMA5 PLA signals increased significantly in MG132-treated cells, consistent with the hypothesis that ubiquitylation marks Cas9 for proteasomal degradation (Figure 5.7.A).

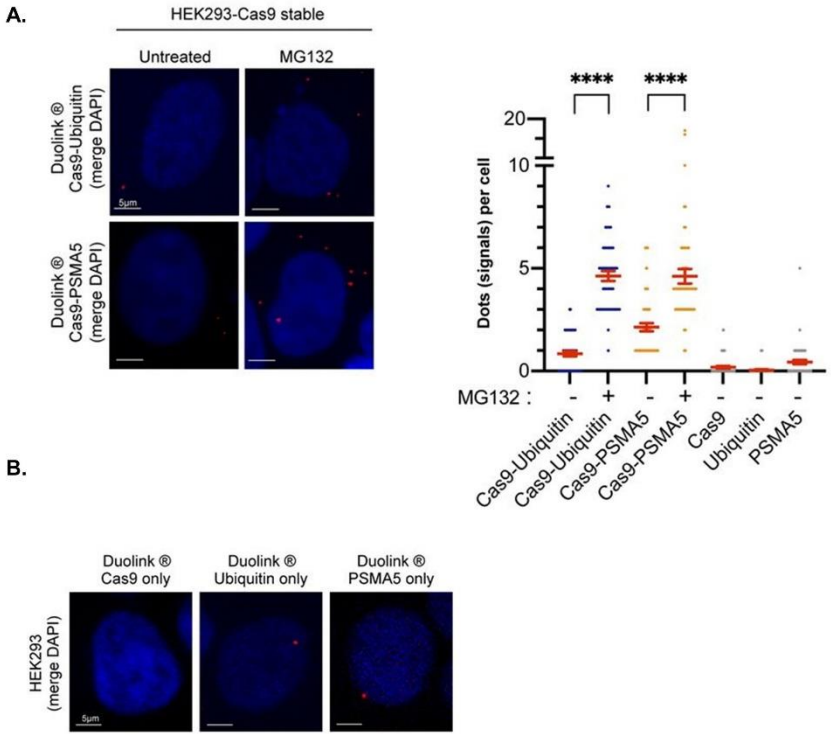

Figure 5.7. Proximity ligation assays demonstrate Cas9 interactions with ubiquitin and the proteasome subunit PSMA5 in the presence and absence of the proteasome inhibitor MG132. (A). Representative images and quantification of PLA signals in Cas9-expressing HEK293 cells using antibodies against FLAG and ubiquitin or PSMA5. (B). Negative control images showing PLA with a single antibody. (****P < 0.0001, unpaired t-test).

Examination of z-stacks from the PLA experiments revealed that the Cas9-ubiquitin and Cas9-proteasome interactions were predominantly localized in the cytoplasm, in contrast to the nuclear localization of Cas9 SUMOylation observed previously. In addition, negative control experiments using only a single primary antibody yielded negligible background signals, which confirms the specificity of the positive PLA signals observed in the dual-antibody experiments targeting the Cas9-ubiquitin and Cas9-proteasome interactions (Figure 5.7.B). Together, these findings provide further evidence that ubiquitylation is an important post-translational modification that regulates the stability and turnover of the Cas9 protein.

5.1.8. Investigation of the Effect of the SUMO2/3 Deficient Variant (K848R Cas9) on Ubiquitylation Levels of Cas9

The major SUMOylation site K848 was found to be also ubiquitylated according to the analyses of our former lab members (Ergünay, 2022), which suggests that the two post-translational modifications, SUMO and ubiquitin, may compete for the same lysine residue on Cas9. This competition between SUMO and ubiquitin for the K848 site could potentially lead to distinct functional consequences, such as differences in Cas9 stability, localization, or activity.

To investigate the effect of the SUMO2/3 deficient variant on the ubiquitylation levels of Cas9, proximity ligation assay experiments were conducted in HEK293 cells stably expressing the wild-type and K848R Cas9 variants using the antibodies against FLAG (CST, #14793) and ubiquitin (R&D Systems, Clone FK2).

The PLA results showed that the Cas9-ubiquitin interaction was significantly higher in the K848R mutant compared to the wild-type, both in the absence and presence of the proteasome inhibitor MG132. This increase was more pronounced when the proteasomes were inhibited by MG132. These findings suggest an antagonistic relationship between SUMOylation and ubiquitination at the same lysine residue of Cas9 (K848).

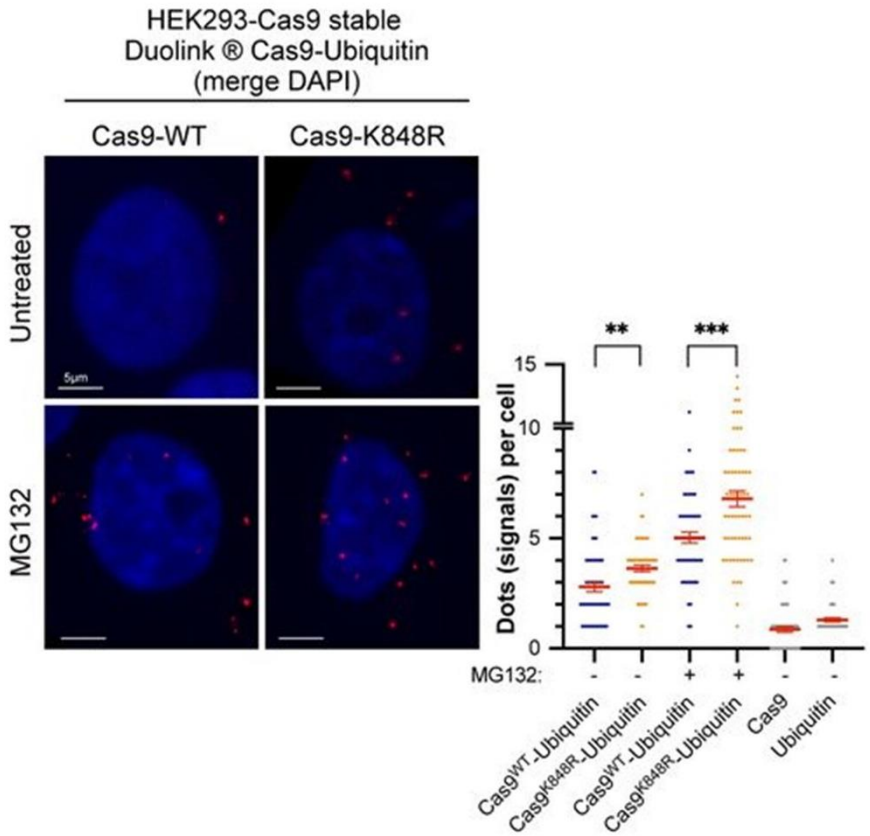

Figure 5.8. Representative images and dot plots of PLA showing Cas9-Ubiquitin interaction on WT-Cas9 and K848R-Cas9 stable HEK293 cells in the presence and absence of proteasome inhibitor MG132. Mean values from two experiments per condition is represented in the graphs, including the negative controls of a given Duolink pair, ± SEM (****P < 0.0001, unpaired t test).

5.1.9. The effects of Cas9 SUMOylation on Its Localization

In our recent study (Ergünay et al., 2022), we have identified the complex post-translational modifications of the Cas9 protein, particularly its SUMOylation and ubiquitination, and how these changes affect Cas9's stability, localization, and DNA binding abilities. Our findings indicated that Cas9 is primarily modified by SUMO2/3 compared to SUMO1, as demonstrated through various experimental techniques such as immunoprecipitation (IP), His pulldown, and Proximity Ligation Assay (PLA).

The proximity ligation assay (PLA) method, which is a powerful and ultra-sensitive technique, was used to further verify that Cas9 has undergone SUMO modification **endogenously**. In line with the immunoprecipitation results of our former lab members, it was shown that Cas9 was endogenously SUMOylated by predominantly SUMO2/3 rather than SUMO1 by PLA.

Notably, PLA experiments further confirmed that lysine 848 is a critical site for SUMO2/3 conjugation in accordance with the IP results conducted by other lab members. When this lysine was altered to arginine (K848R), a significant reduction in PLA signals showing Cas9 and SUMO2/3 interaction was observed, confirming the significant role of this residue. Disrupting the SUMOylation of this site by changing the adjacent aspartic acid residue at position 850 to alanine (D850A) also confirmed its significance in SUMO2/3 modification.

According to previous results of our former lab members, Cas9 was also ubiquitylated. Those results were also replicated by PLA experiments showing the interaction between Cas9 and ubiquitin. Furthermore, proximity ligation assays revealed that Cas9 and proteasome subunits interact with each other indicating its degradation through the proteasomal pathway after its ubiquitylation. Moreover, an antagonistic relationship between SUMOylation and ubiquitylation at K848 was observed. The SUMOylation-deficient K848R mutant showed increased ubiquitylation levels especially in the presence of proteasome inhibitor MG-132, suggesting a model where SUMOylation at K848 protects it from ubiquitylation and subsequent proteasomal degradation. The antagonistic relationship between SUMOylation and ubiquitylation of K848 affects its stability and turnover.

Importantly, PLA experiments clearly showed that SUMOylation of Cas9 was mostly nuclear whereas its ubiquitylation was mostly cytoplasmic, suggesting different regulation by SUMO and ubiquitin modifications on the localization of the Cas9.

5.2. Investigation of ADAM17 SUMOylation and Ubiquitinylation and The Effect of SUMOylation on ADAM17-mediated Protein Ectodomain Shedding

5.2.1. Bioinformatic Analysis of SUMOylation Consensus Motifs on ADAM17

Bioinformatic analysis using the GPS-SUMO tool, which predicts SUMO-interaction motifs and SUMOylation sites (Zhao et al., 2014), revealed a total of 4 SUMOylation consensus and non-consensus sites in the ADAM17 protein, with 3 of these located in the cytosolic domain. (Table 5.1). These findings suggest that ADAM17 might undergo SUMOylation within the cell, and this post-translational modification may influence ADAM17-mediated ectodomain shedding. Additionally, the 724-727 amino acid region of ADAM17 contains a SUMO-interaction motif (SIM), which may enable interactions with SUMO peptides that bind to the lysine residue at position 753 which is located near the SIM (723-VRII-728, not shown). Additionally, this SIM on ADAM17 could potentially interact with SUMO groups on other SUMOylated proteins. Furthermore, bioinformatic analysis identified SUMO-interaction motifs in some of the ADAM17 substrate proteins such as TGFα, amphiregulin, epiregulin, HB-EGF, and TNFα, indicating that SUMOylation may regulate the activity and substrate specificity of ADAM17 through both direct modification and indirect interactions. Given the key role of ADAM17 in various critical cellular processes, the potential regulation of ADAM17 by SUMOylation warrants further investigation to elucidate its impact on ADAM17-mediated ectodomain shedding and downstream signaling pathways.

Table 5.1. Potential SUMOylation sites identified on the ADAM17 protein by GPS-SUMO. The lysine residues (K) in the SUMOylation motif were shown in red. ***: end of the sequence.

Position	Peptide	Type	Domain
188	PKVCGYLKVDNEELL	SUMOylation consensus	Prodomain
697	LVHCVDKKLDKQYES	SUMOylation consensus	Cytoplasmic tail
753	PSAPAAPKLDHQRMD	SUMOylation consensus	Cytoplasmic tail
820	RQNRVDSKETEC***	SUMOylation nonconsensus	Cytoplasmic tail

Furthermore, the analysis of COSMIC (Catalog Of Somatic Mutations In Cancer), a comprehensive database that catalogs somatic mutations found in human cancers, revealed that two of the mutations located at the predicted SUMOylation sites of ADAM17 disrupt the SUMOylation site (Table 5.2). This finding suggests that the disruption of ADAM17 SUMOylation may potentially contribute to the development or progression of certain cancer types. However, further research is needed to elucidate the precise molecular mechanisms underlying the impact of altered ADAM17 SUMOylation on oncogenesis.

Table 5.2. Mutations in the COSMIC database, located within the predicted SUMOylation sites of ADAM17, and disrupt the SUMOylation motif.

Mutation	Count	Cancer type	Tissue	Affected pathway	Pubmed / COSMIC link
p.D190Y	1	Renal cell carcinoma	Kidney	Notch and Delta Notch	29088767
p.D695V	1	Hepatocellular carcinoma	Liver	Notch and Delta Notch	COSU381

5.2.2. Impact of Reduced Cellular SUMOylation on ADAM17-mediated Ectodomain Shedding

To investigate the impact of reduced global SUMOylation on ADAM17-mediated protein ectodomain shedding, a SUMOylation inhibitor compound, ML792, was utilized. ML792 is a SAE1/SUMO E1 inhibitor commonly used in this research field to block SUMOylation (Brackett and Blagg, 2020). In those experiments, cells were initially transfected with AP-tagged ADAM17 substrates such as AP-TGFα, AP-HB-EGF, and AP-Epiregulin. The overall SUMOylation levels of the cells were then reduced by ML792 treatment (2 μM). Twenty-four hours after ML792 treatment, both control cells and the cells with decreased global SUMOylation were subjected to an AP Assay. All experiments were set up as technical triplicates.

As shown in Figure 5.9, a significant increase in ADAM17-mediated TGFα shedding was observed in the group treated with ML792 compared to the control group, in both PMA-stimulated and BB94-inhibited conditions.

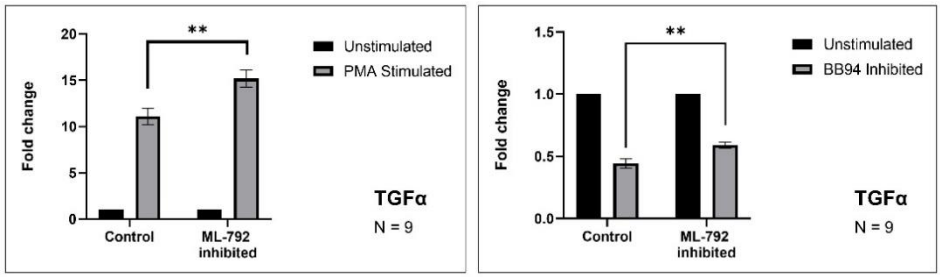

Figure 5.9. Analysis of ADAM17-mediated TGFα shedding by AP Assay in the cells that global SUMOylation level was reduced by SUMOylation inhibitor ML792. Statistical analyses were performed with the unpaired nonparametric t-test. **: $p < 0.01$, n=9

Similar experiments were conducted with other ADAM17 substrates, HB-EGF and epiregulin. Just like the TGFα experiments, cells were initially transfected with plasmids containing AP-HB-EGF or AP-Epiregulin. The global SUMOylation level was then

inhibited using ML792 (2 μM for 22-24 hours). The ADAM17-mediated ectodomain shedding was calculated using the AP Assay in both control cells and cells where the global SUMOylation level was inhibited by ML792. No significant difference was observed between the control group and the cells where SUMOylation was inhibited by ML792, either for HB-EGF or epiregulin ectodomain shedding (Figure 5.10).

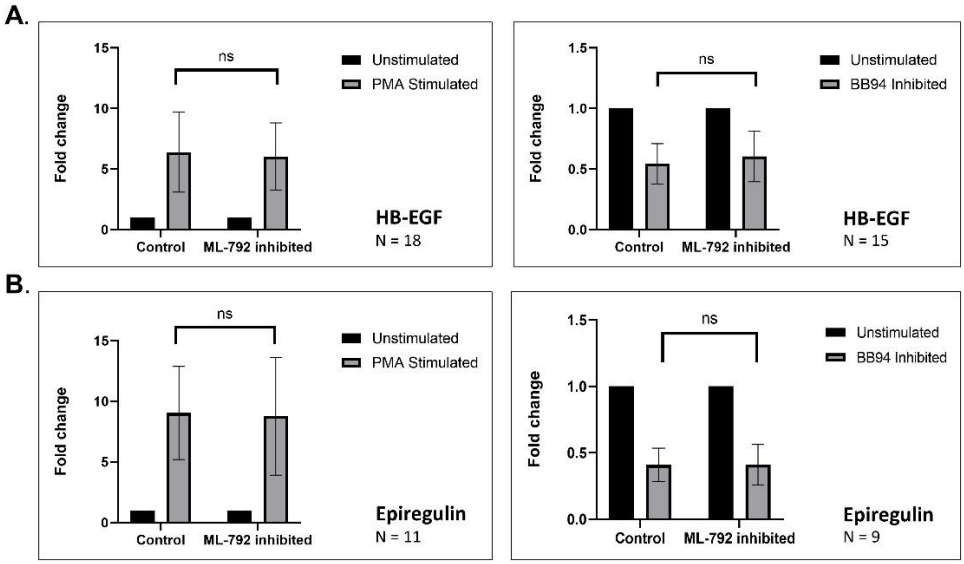

Figure 5.10. Analysis of ADAM17-mediated HB-EGF (A) and Epiregulin (B) shedding by AP Assay in the cells that global SUMOylation level was inhibited by SUMOylation inhibitor ML792.Statistical analyses were performed with the unpaired nonparametric t-test. ns: not significant.

Western blot analyses were also conducted to verify the effect of ML792 on SUMOylation. The samples were lysed in 2X Laemli solution before they were run on polyacrylamide gels and immunoblotted with anti-SUMO1 antibody. As shown in Figure 5.11, a decrease in global SUMOylation levels was evident in the samples. Based on these findings, it was concluded that the ML792 molecule successfully inhibits global SUMOylation in cells.

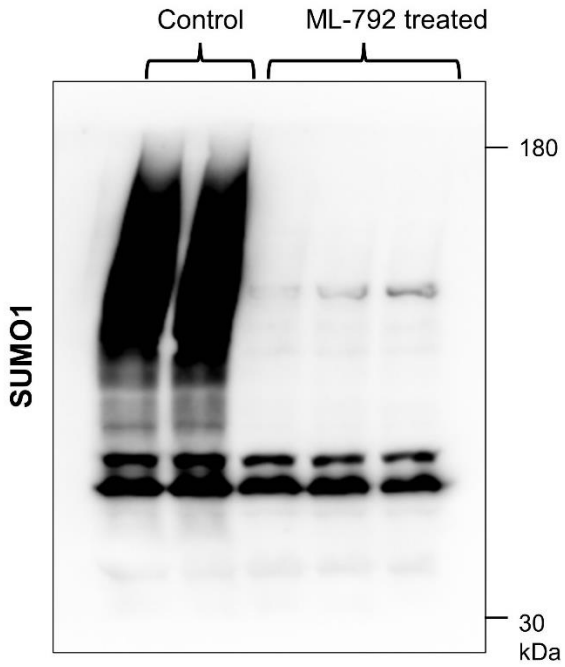

Figure 5.11. Western blot analysis of global SUMOylation levels of the control (untreated) and ML792 treated AP Assay samples using SUMO1 antibody.

5.2.3. ADAM17-mediated Protein Ectodomain Shedding in the Cells with Increased Global SUMOylation

To investigate the effect of the global increase of SUMOylation on ADAM17-mediated protein ectodomain shedding, HEK293 cells were transfected with one of the AP-tagged ADAM17 substrates like AP-TGFα, AP-HB-EGF or AP-Epiregulin, along with GFP-SUMO1, GFP-SUMO2/3 and GFP-UBC9 (SUMO E2 conjugation enzyme) containing plasmids. All experiments were set up as technical triplicates. AP Assay was performed 16-18 hours after transfection.

Increasing the global SUMOylation level by overexpressing SUMO paralogs did not result in any significant change in the ADAM17-mediated shedding activity of all three ADAM17 substrates that were tested, specifically TGFα (Figure 5.12), HB-EGF (Figure 5.13), and epiregulin (Figure 5.14).

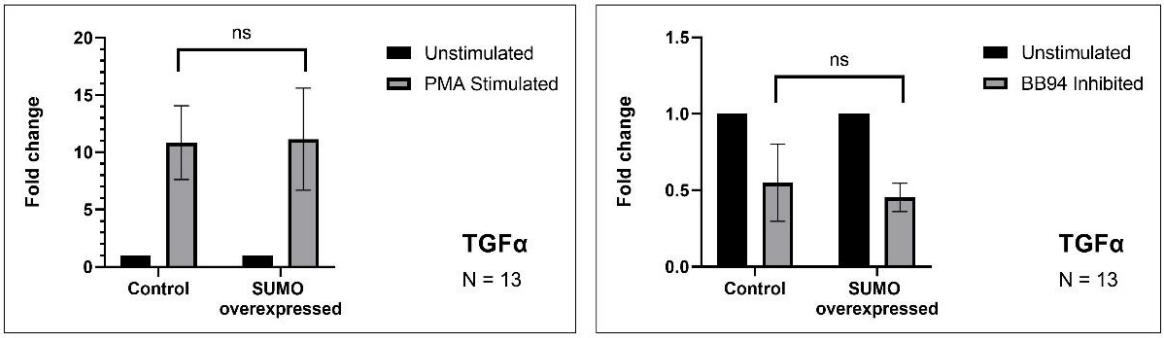

Figure 5.12. Analysis of ADAM17-mediated TGFα shedding by AP Assay in the cells that global SUMOylation level was increased with overexpression of SUMO1 and SUMO2/3. Statistical analyses were performed with the unpaired nonparametric t-test. ns: not significant.

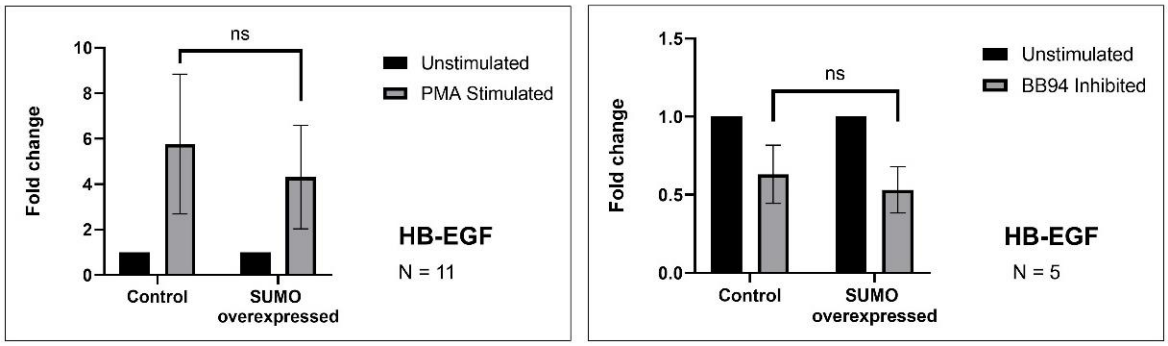

Figure 5.13. Analysis of ADAM17-mediated HB-EGF shedding by AP Assay in the cells that global SUMOylation level was increased with the overexpression of SUMO1 and SUMO2/3.Statistical analyses were performed with the unpaired nonparametric t-test. ns: not significant.

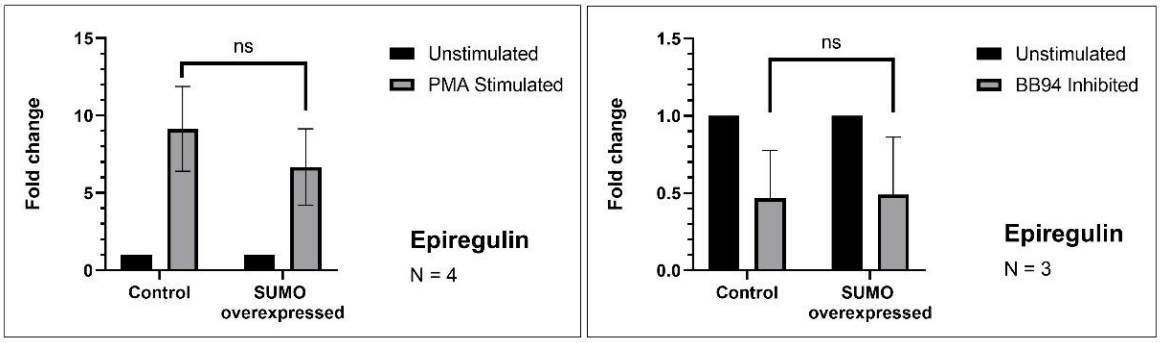

Figure 5.14. Analysis of ADAM17-mediated Epiregulin shedding by AP Assay in the cells that global SUMOylation level was increased with the overexpression of SUMO1 and SUMO2/3. Statistical analyses were performed with the unpaired nonparametric t-test. ns: not significant.

5.2.4. Optimization of Immunoprecipitation (IP) and Western Blot Analysis Conditions for ADAM17

As previously mentioned, the ADAM17 protein exists in two forms: an inactive proform and an active mature form. Multiple experiments were performed to optimize the immunoprecipitation conditions for isolating the active form (mature form) of ADAM17. Different methods, including adjusting the detergents in the lysis buffer or RIPA, and changing the antibody for immunoprecipitation, were tested. Unfortunately, none of these attempts were successful in isolating mature ADAM17 through immunoprecipitation (data not provided).

Before running the samples on polyacrylamide gels for Western blot analysis, the samples are incubated at 95°C for 5-10 minutes. However, studies have shown that transmembrane proteins precipitate at 95°C, so these proteins should be loaded at room temperature when analyzed by Western blot analysis (Tsuji, 2020).

To optimize the IP conditions in the hopes of immunoprecipitating mature form of ADAM17, IP experiments were conducted using two different antibodies anti-FLAG (Sigma Aldrich, F1804) and anti-ADAM17 (Santa Cruz, sc-390859) in HEK293 cells that were

overexpressing FLAG-ADAM17. Considering that ADAM17 is also a transmembrane protein, the IP samples and whole cell lysate (WCL) samples were either incubated at 95°C for 5 mins or at room temperature before loading on polyacrylamide gels. Western blot analysis was performed by probing with anti-ADAM17 antibody (Figure 5.15).

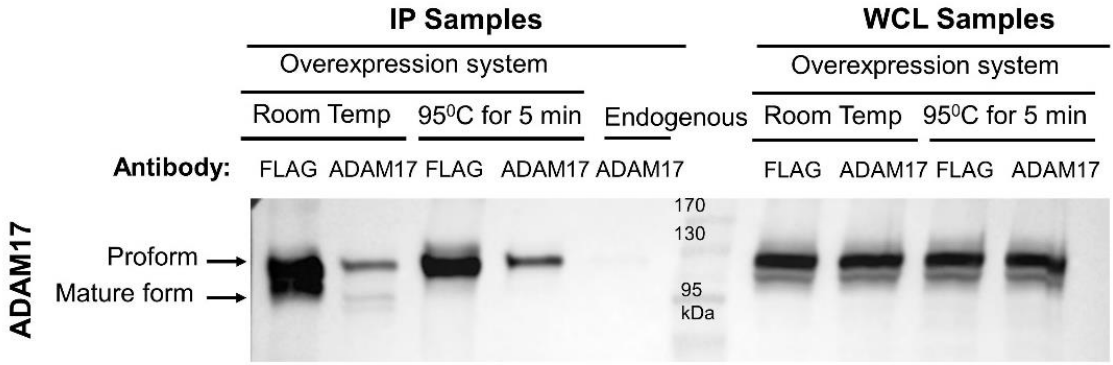

Figure 5.15. Optimization of Western blot analysis conditions for immunoprecipitation (IP) experiments. Two different antibodies, anti-FLAG and anti-ADAM17, were used in IP experiments in the cells overexpressing FLAG-ADAM17. Samples were run on polyacrylamide gel under two different conditions - incubating at 95°C for 5 minutes or at room temperature before loading and then immunoblotted against ADAM17.

The results in Figure 5.15 show that the mature form is visible in the immunoprecipitation samples incubated at room temperature before loading onto polyacrylamide gels, but not in the same samples incubated at 95°C for 5 minutes.

In this optimization experiment, two different antibodies were tested during immunoprecipitation. Since the overexpressed ADAM17 protein in cells was FLAG-tagged, one of the antibodies used was the monoclonal anti-FLAG antibody and the other was the monoclonal anti-ADAM17 antibody that had been used in previous immunoprecipitation experiments of endogenous ADAM17. As shown in Figure 5.16, the anti-FLAG antibody proved to be much more efficient in immunoprecipitation compared to the monoclonal anti-ADAM17 antibody. A sample from our previous immunoprecipitation experiments, where endogenous ADAM17 had been precipitated, was also included in the Western blot analysis

as a positive control. Based on the results of this optimization experiment, it was decided to perform immunoprecipitation using the anti-FLAG antibody after overexpressing FLAG-tagged ADAM17 in HEK293 cells and then incubating the samples at room temperature before loading polyacrylamide gels for Western blot analysis. This approach successfully allowed for the precipitation and visualization of both the active mature form and the proform of the ADAM17.

5.2.5. Investigation of ADAM17 SUMOylation by Two Different IP Methods

To investigate whether ADAM17 is SUMOylated, two different immunoprecipitation (IP) approaches were used.

In the first approach, HEK293 cells were co-transfected with FLAG-tagged ADAM17 and GFP-tagged SUMO1 or SUMO2/3 together with GFP-tagged UBC9. 18-20 hours post-transfection, IP was performed with the anti-FLAG antibody (Sigma Aldrich, F1804) to immunoprecipitate the ADAM17 protein. IP and whole cell lysate (WCL) samples were incubated at room temperature before loading and running on polyacrylamide gels and then immunoblotted against ADAM17 to determine transfection and pull-down efficiencies, respectively. IP samples were immunoblotted against SUMO1 and SUMO2/3 to detect SUMOylated forms of ADAM17 which corresponds to a smear pattern.

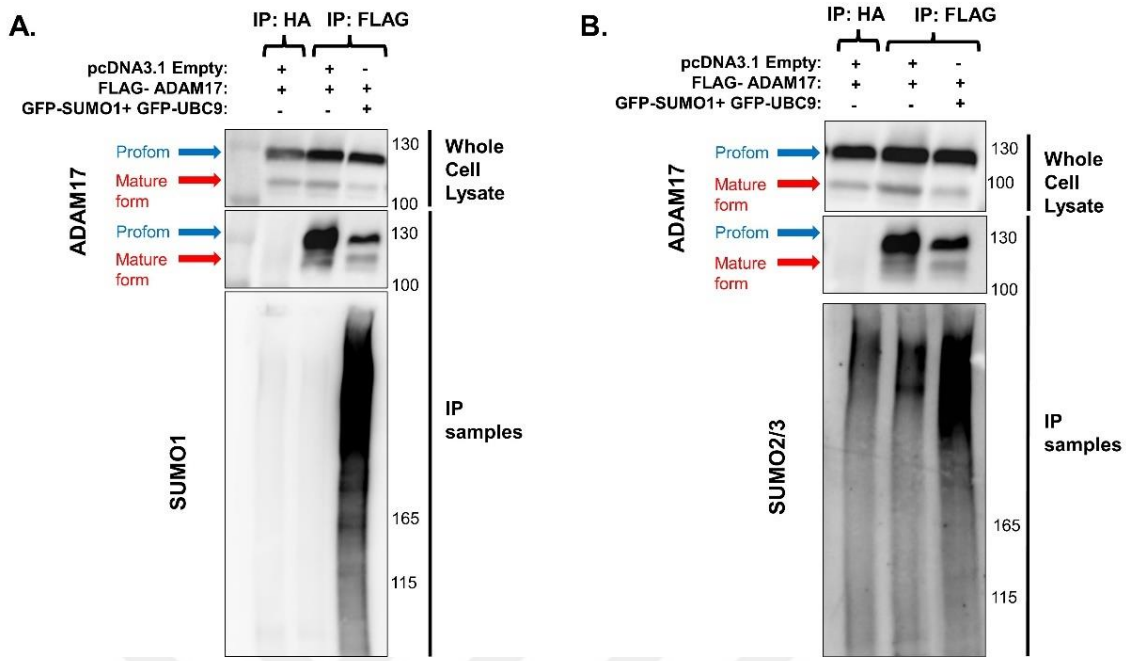

Figure 5.16. The immunoprecipitation experiment showing that ADAM17 undergoes SUMO modification with both SUMO1 (A) and SUMO2/3 (B). HEK293 cells were transfected with FLAG-tagged ADAM17 along with GFP-tagged SUMO1 or SUMO2/3 plasmids. Immunoprecipitation (IP) was performed with the anti-FLAG antibody. Whole cell lysate (WCL) and IP samples were then immunoblotted against ADAM17.

As shown in Figure 5.16, both the proform and the mature form of ADAM17 were immunoprecipitated using the FLAG antibody. The amount of transfected DNA was consistent across groups expressing only FLAG-tagged ADAM17 and those expressing FLAG-tagged ADAM17 in combination with GFP-tagged SUMO paralogs. However, a decrease in both forms of ADAM17, particularly in the mature form, was observed in the latter group. In other words, the level of the mature form of ADAM17 decreased when FLAG-tagged ADAM17 was expressed alongside GFP-tagged SUMO paralogs. This decrease was evident in Figure 5.16 through immunoblotting against ADAM17 in whole-cell lysate samples, explaining the higher pull-down of ADAM17 in the former group. Immunoblots against SUMO1 and SUMO2/3 revealed a smear pattern corresponding to SUMOylated forms of ADAM17. The same experiments were repeated three times for SUMO1 and SUMO2/3, yielding similar results each time.

Another IP approach was performed to further validate that ADAM17 was SUMOylated by both SUMO1 and SUMO2/3. Unlike in the first approach, the anti-GFP antibody (Santa Cruz, sc-9996) was used to pull down all the SUMOylated proteins since HEK293 cells were transfected with GFP-tagged SUMO paralogs together with FLAG-tagged ADAM17. Subsequently, Western blot analysis using an anti-ADAM17 antibody was carried out to determine if ADAM17 is indeed one of those SUMOylated proteins. In the first approach shown in Figure 5.16, a smear band on SUMO1 or SUMO2/3 immunoblots was a representation of SUMOylated ADAM17 proteins. In the second IP approach, sharp ADAM17 mature and proform bands are the representation of SUMOylated ADAM17 forms (Figure 5.17).

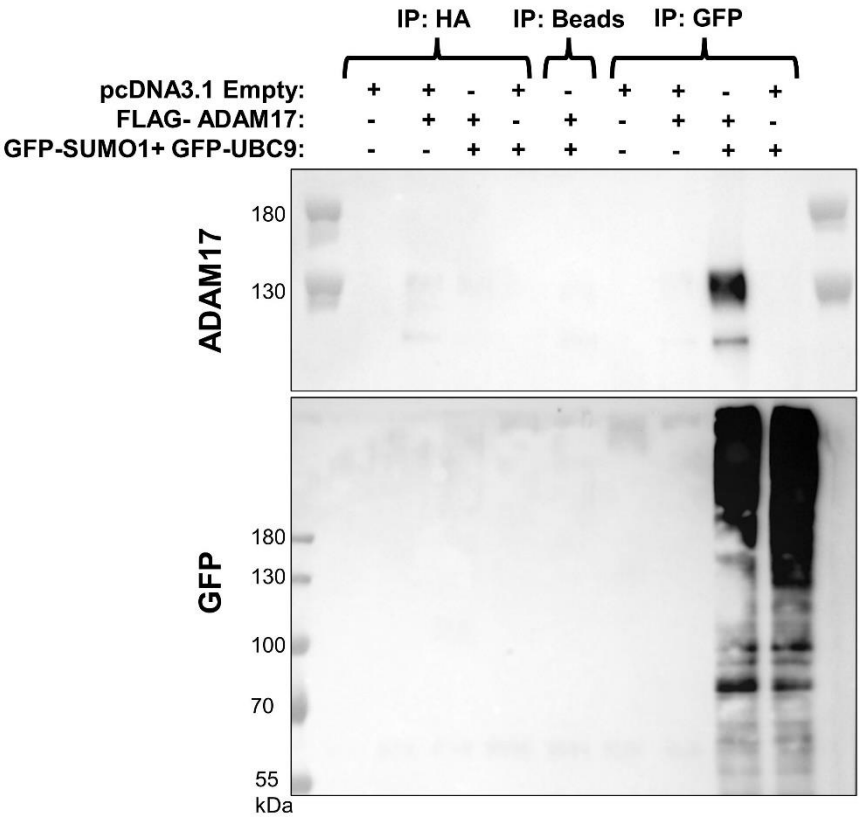

Figure 5.17. Demonstration of ADAM17 undergoing SUMO1 modification. HEK293 cells were transfected with FLAG-ADAM17 and GFP-tagged SUMO1 and UBC9 plasmids.All proteins undergoing SUMO modification were immunoprecipitated using an anti-GFP antibody. SUMOylated ADAM17 forms were then detected by Western blot analysis using ADAM17 antibody. Anti-HA antibody was used as a negative control.

Other control groups were also included in those experiments. IP was also performed with an anti-HA antibody (Biolegend, 901502) on the same groups to validate the specificity of the anti-GFP antibody used in IP experiments. As seen in Figures 5.17 and 5.18, any protein was not detected by the pull-down of the anti-HA antibody, highlighting the specificity of the anti-GFP antibody. Another sample was also included incubating with the beads only without using any antibody ("IP: Beads" groups) to demonstrate that the proteins are not bound to the beads nonspecifically.

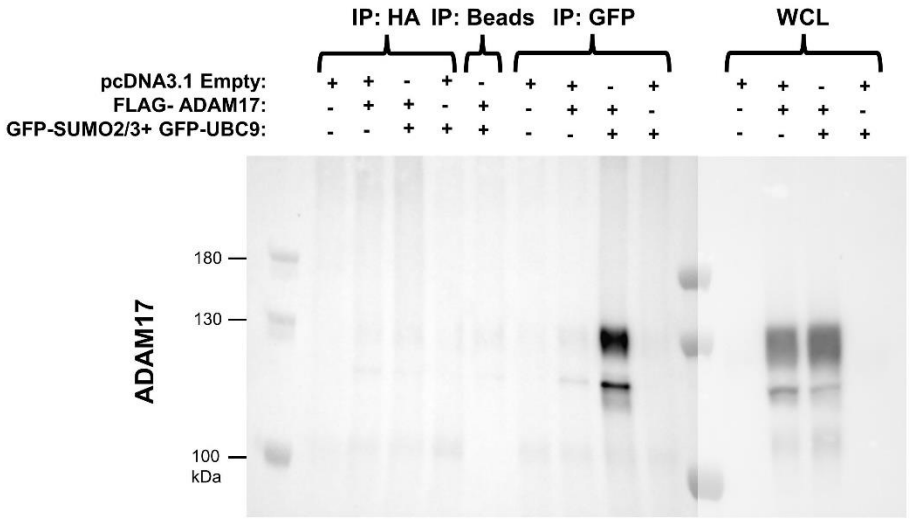

Figure 5.18. Demonstration of ADAM17 undergoing SUMO2/3 modification. HEK293 cells were transfected with FLAG-ADAM17 and GFP-tagged SUMO2/3 and UBC9 plasmids. All proteins undergoing SUMO modification were precipitated using an anti-GFP antibody. SUMOylated ADAM17 forms by SUMO2/3 were then detected by immunoblotting against ADAM17. Anti-HA antibody was used as a negative control.

5.2.6. Investigation of ADAM17 SUMOylation by Proximity Ligation Assay (PLA) Method

The proximity ligation assay (PLA) method, known for its high sensitivity, was utilized to confirm that ADAM17 undergoes SUMO modification endogenously. This

method, developed recently, can detect peptide modifications like Ubiquitin and SUMO on proteins (Sahin et al., 2016).

Since ADAM17 (and also SUMO peptides) is ubiquitously expressed in all cell lines, proximity ligation assay (PLA) can be used to analyze the interaction between ADAM17 and SUMO proteins in cells without the need for transfection. HeLa cells that were fixed, as in the immunofluorescence method, were treated with an anti-ADAM17 antibody which is raised against amino acids 1-300 mapping at the N-terminus of ADAM17 (Santa Cruz, sc-390859) and anti-SUMO primary antibodies (human anti-SUMO1 (CST, #4930), human anti-SUMO2/3 (Abcam, ab3742). Since the sensitivity of the PLA method is at a single molecule level, every positive signal (dot) represents one ADAM17-SUMO interaction (Figure 5.19).

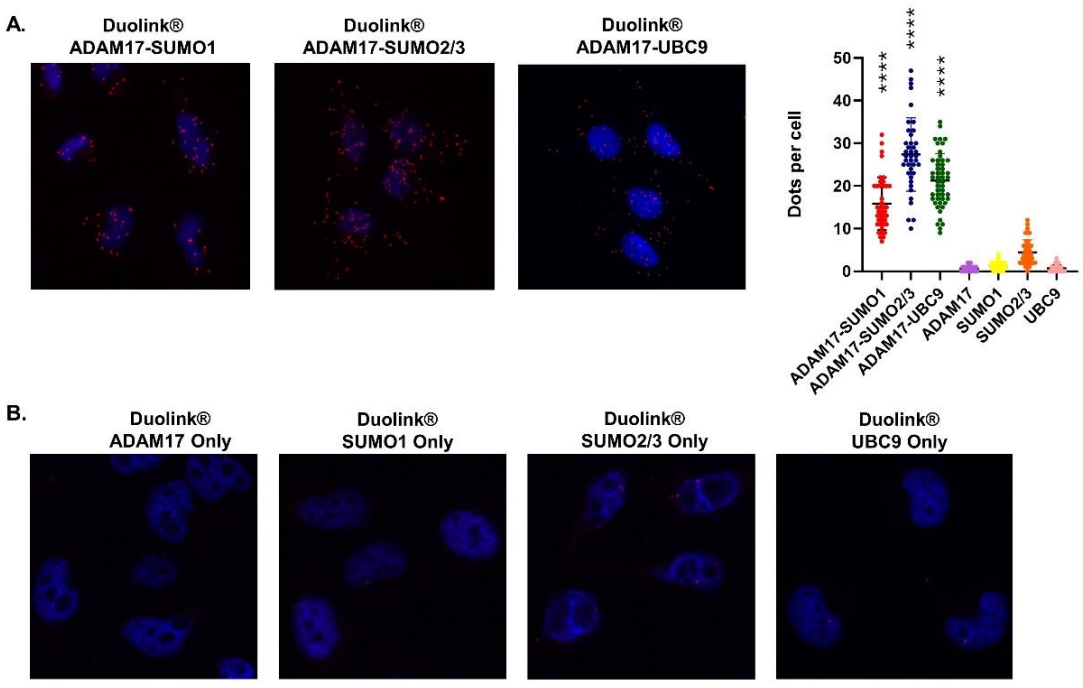

Figure 5.19. Representative images and dot plots showing ADAM17 modification by endogenous SUMO1 and SUMO2/3 peptides, as well as physical interaction with the UBC9 in HeLa cells. (A). PLA was performed using anti-ADAM17 antibody together with anti-SUMO1, anti-SUMO2/3, or anti-UBC9 antibodies. (B). Negative controls with a single antibody of a given Duolink pair. (****P<0.00001, unpaired t-test).

According to PLA experiments, ADAM17 was endogenously SUMOylated with both SUMO1 and SUMO2-3 (Figure 5.19) where SUMO2-3 signals per cell were twice as many as SUMO1 signals per cell. However, the background signal when using only SUMO2/3 antibody was also higher compared to other negative controls where only a single antibody was used. Thus, it is hard to tell whether this phenomenon stems from higher SUMO modification levels of ADAM17 by SUMO2/3 or because of a higher background. PLA experiments should be further optimized to reduce the background signal for SUMO2/3 antibody.

Moreover, examination of z-stacks revealed that although most of the ADAM17-SUMO interaction was predominantly cytoplasmic, some of the SUMO modification of ADAM17 was nuclear (Figure 5.19).

5.2.7. Investigation of The Effect of SUMOylation on ADAM17 Protein Stability

While analyzing Western blot images of the immunoprecipitation experiments, a decrease in the level of the mature form of ADAM17 was observed in cells that had increased SUMOylation levels in 3 independent experiments. This finding can be seen in Figure 5.16 in whole-cell lysate samples transfected with FLAG-ADAM17 and GFP-SUMO1 or GFP-SUMO2/3. It implies that the mature form of ADAM17 might be degraded upon SUMO overexpression. It is known that some proteins that undergo SUMO modification are subsequently ubiquitylated and degraded in proteasomes by a SUMO-dependent ubiquitylation mechanism (Celen and Sahin, 2020).

To investigate the effect of SUMOylation on ADAM17 protein stability, HEK293 cells were transfected with plasmids expressing FLAG-ADAM17 alone (control), or together with either SUMO1 or SUMO2/3, or with a combination of SUMO1 and SUMO2/3. 18-20 hours post-transfection, cells were lysed in 2X Laemmli solution and loaded onto polyacrylamide gels at room temperature for Western blot analysis. Immunoblotting was performed using an anti-FLAG (or anti-ADAM17) and anti-Actin antibodies (Figure 5.20).

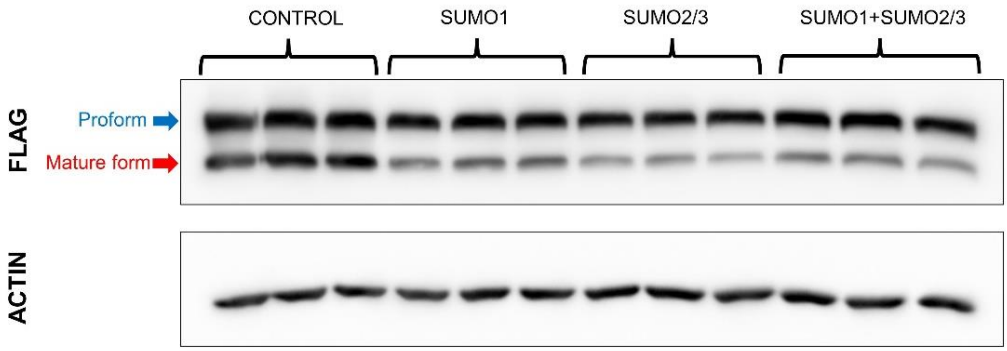

Figure 5.20. Representative Western blot images of the analysis of changes in ADAM17 proform and mature form levels in the cells with increased SUMOylation. HEK293 cells transfected with FLAG-ADAM17 alone (control), or together with SUMO1, SUMO2/3, or a combination of SUMO1 and SUMO2/3.

The differences in ADAM17 proform and mature form levels were quantified with the help of the Image-J program and normalized to Actin levels. An unpaired t-test was applied to these experiments, which were repeated 3 times. As shown in Figure 5.20, the proform of ADAM17 was significantly reduced only when SUMO2/3 was overexpressed together with FLAG-ADAM17. Importantly and interestingly, a significant decrease in the mature form levels of ADAM17 was evident in all groups, with the greatest decrease seen in cells transfected with SUMO2/3. So, it can be concluded that the mature (or active) form of ADAM17 was significantly reduced upon an increase in the global SUMOylation, pointing to the antagonistic effect of SUMOylation on the maturation of ADAM17.

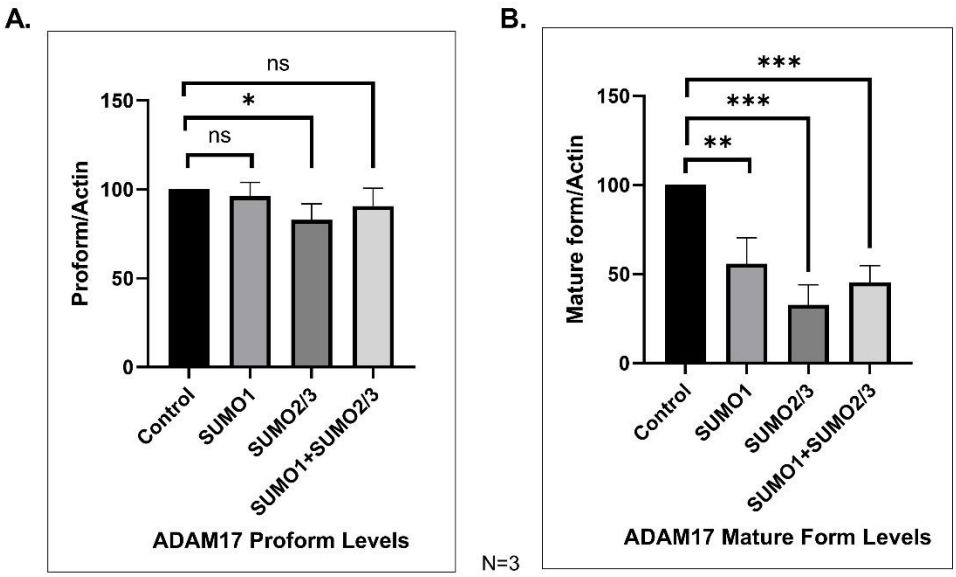

Figure 5.21. Statistical analysis of ADAM17 proform (A) and mature form (B) levels in the cells with increased global SUMOylation levels by overexpression of SUMO peptides. N=3, unpaired t-test, ***P < 0.001, **P < 0.01, *P < 0.05, ns: not significant.

Further experiments were also conducted using the protein synthesis inhibitor cycloheximide (CHX) and/or the SUMOylation inhibitor ML792 to investigate the effect of inhibition of SUMOylation on ADAM17 protein stability. HEK293 cells were transfected with FLAG-ADAM17. 18 hours after transfection, cells were treated with cycloheximide (CHX, 50 μg/ml) to stop the protein synthesis and ML792 (1 μM) to inhibit global SUMOylation. 4, 8, and 12 hours after treatments, cells were collected and lysed in 2X Laemli solution. Western blot analysis was performed with an anti-FLAG and anti-Actin antibodies. ADAM17 proform and mature form levels were quantified and normalized to Actin levels with the help of ImageJ program. Cells at the time of treatments (t=0, untreated) were used as controls to determine the percentage decrease in the proform and mature form of ADAM17 protein.

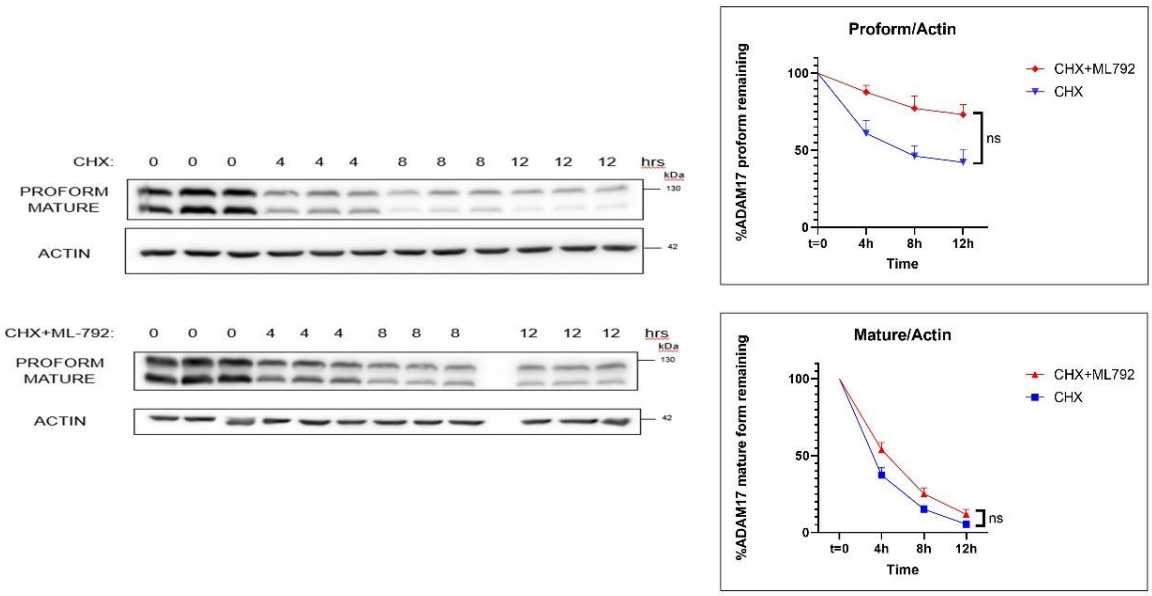

Figure 5.22. Analysis of the effect of reduced SUMOylation on ADAM17 protein stability. HEK293T cells transfected with FLAG-ADAM17.18 h post-transfection, cells were treated with protein synthesis inhibitor cycloheximide (CHX) and/or SUMOylation inhibitor ML792 at specific time points (0, 4, 8, 12 h). Western blot analysis was performed with anti-FLAG and anti-Actin antibodies to detect the changes in ADAM17.

As demonstrated in Figure 5.22, the simultaneous administration of SUMOylation inhibitor ML792 also led to an increase in the stability of ADAM17. This was evidenced by the protein levels that remained after 12 hours of exposure to cycloheximide, although this increase was not statistically significant. This result was consistent with the experiments shown in Figure 5.21.

To sum up, the stability of the mature form of ADAM17 decreased when global protein SUMOylation levels were increased by the overexpression of SUMO peptides (Figure 5.21). However, the stability of ADAM17 increased when global SUMOylation was inhibited by ML792 even though this increase was not statistically significant (Figure 5.22).

5.2.8. Identification of ADAM17 Ubiquitylation by Immunoprecipitation (IP) Method

Immunoprecipitation (IP) experiments were conducted to investigate the ADAM17-ubiquitin relationship like IP experiments conducted for SUMO groups. HEK293 cells were transfected with FLAG-tagged ADAM17 and His-tagged ubiquitin constructs. IP was performed in similar conditions to SUMOylation experiments but with an anti-His (Santa Cruz, sc-8036) antibody to pull down all the ubiquitinylated proteins. Then, whole cell lysate (WCL) and IP samples were run on polyacrylamide gels and immunoblotted against ADAM17 to analyze ubiquitinylated ADAM17 forms. Figure 5.23 shows that ADAM17 may also get ubiquitylated.

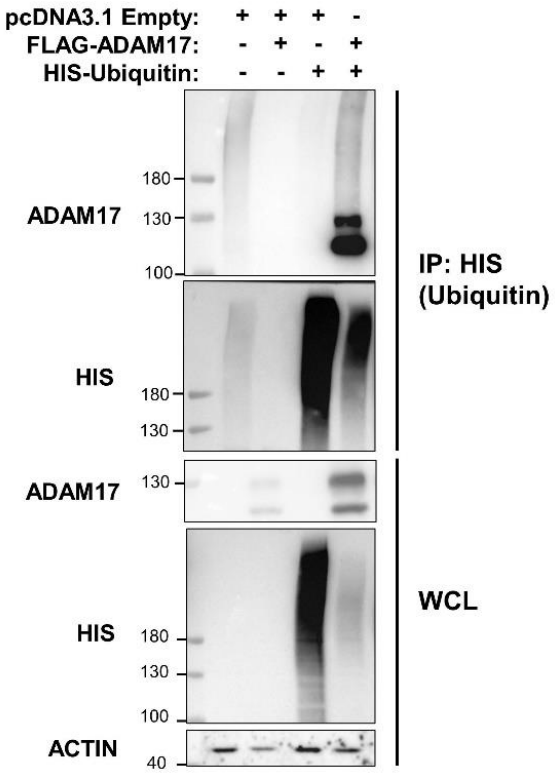

Figure 5.23. Demonstration of ADAM17 ubiquitylation. HEK293 cells were transfected with FLAG-ADAM17 and His-Ubiquitin. All the ubiquitylated proteins were pulled down using an anti-His antibody. Ubiquitylated ADAM17 forms were then detected by immunoblotting against ADAM17.

After showing that ADAM17 is ubiquitylated, it was investigated whether the ubiquitination of ADAM17 is SUMOylation-dependent. For this purpose, a group that was treated with a SUMOylation inhibitor (ML792) was included in the immunoprecipitation experiments. In those experiments, HEK293 cells were transfected with FLAG-ADAM17 and His-Ubiquitin plasmids in the absence or presence of a SUMOylation inhibitor (ML792, 1 μM for 16 hours). Immunoprecipitation was performed under similar conditions shown in Figure 5.24 using an anti-His (Santa Cruz, sc-8036) antibody to pull down all the ubiquitinylated proteins. Then, whole cell lysate and immunoprecipitation samples were run on polyacrylamide gels, and Western blot analysis was performed with anti-ADAM17 antibody to analyze the levels of ubiquitylated ADAM17 forms (Figure 5.24).

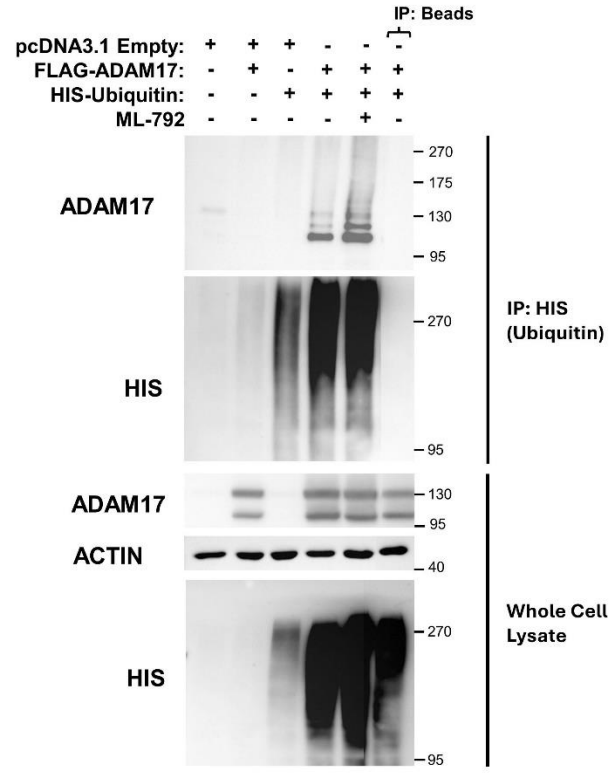

Figure 5.24. Representative Western blot images showing the effect of SUMOylation inhibitor ML792 on ADAM17 ubiquitylation. HEK293 cells were transfected with FLAG-ADAM17 and His-Ubiquitin plasmids in the presence or absence of the SUMOylation inhibitor ML792. Ubiquitylated proteins were pulled down using an anti-His antibody, and ubiquitylated ADAM17 forms were detected by immunoblotting against ADAM17.

As shown in Figure 5.24, the levels of ubiquitylated ADAM17 forms increased when SUMOylation was inhibited by ML792. Also, negative controls verified the specificity of the approach. The experiments were conducted at least three times, and similar results were obtained. These results suggest that ubiquitination and SUMOylation might have antagonistic effects on ADAM17.

Importantly, a sharp increase in both ADAM17 forms with a smeared pattern was observed when FLAG-ADAM17 and His-ubiquitin were overexpressed in whole cell lysate samples, indicating a significant increase in ubiquitylated ADAM17 forms (Figure 5.25). These results contrast with what was observed in SUMO overexpression, where a significant decrease was evident in both the proform and the mature form levels of ADAM17. Again, this highlights that ubiquitylation and SUMOylation might have antagonistic effects on ADAM17 protein stability. Also, the levels of ubiquitylated ADAM17 forms were not affected by the inhibition of global SUMOylation by ML792 in whole-cell lysate samples (Figure 5.25).

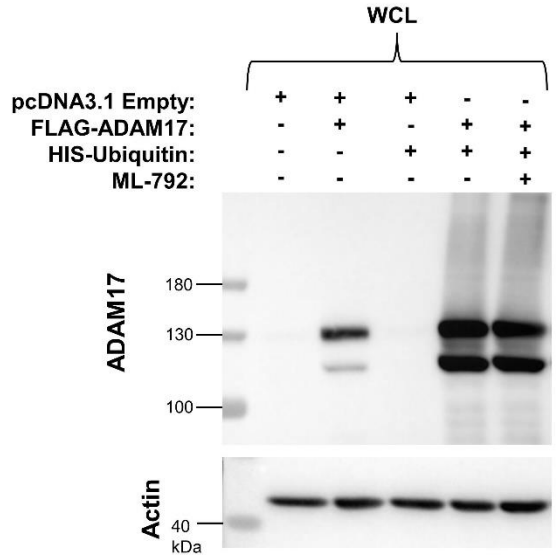

Figure 5.25. Western blot analysis of ADAM17 proform and mature form levels in whole cell lysates (WCL) upon increased ubiquitylation by overexpressing His-Ubiquitin together with FLAG-ADAM17. SUMOylation inhibitor ML792 was also used to elucidate the relationship between ubiquitylation and SUMOylation.

5.2.9. Identification of ADAM17 Ubiquitylation by Proximity Ligation Assay (PLA) Method

Proximity ligation assay (PLA) experiments were also performed using anti-ADAM17 and anti-ubiquitin antibodies to detect endogenous ADAM17-Ubiquitin interactions. HeLa cells were treated with the proteasome inhibitor (MG132, 2 μM for 16 h) to prevent possible ADAM17 degradation upon ubiquitylation (Figure 5.28).

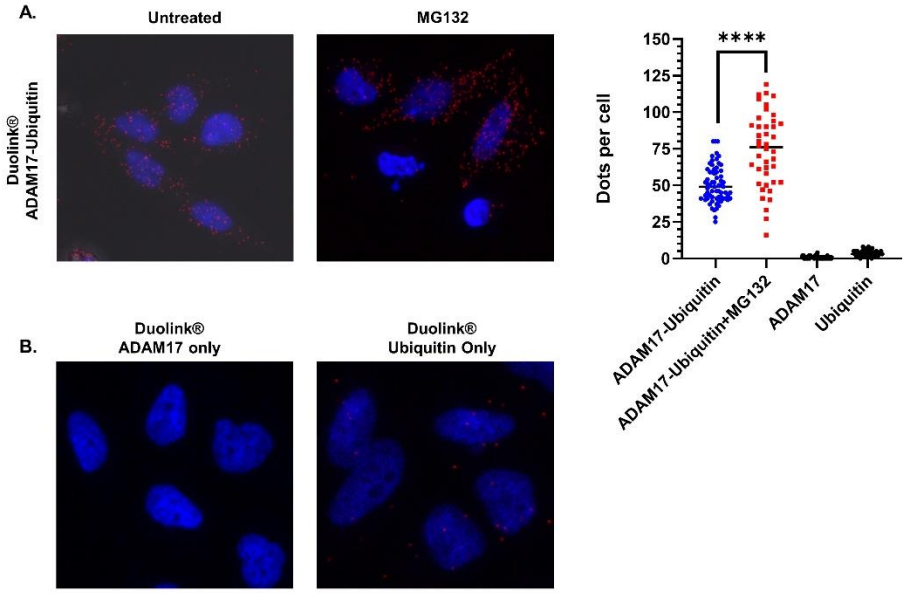

Figure 5.26. Representative images and dot plots showing endogenous ADAM17 ubiquitinylation in HeLa cells. (A). Proximity Ligation Assay (PLA) was performed using anti-ADAM17 and anti-ubiquitin antibodies in the absence and presence of proteasome inhibitor MG132. (B). Negative controls with a single antibody of a given Duolink pair. (****P<0.00001, unpaired t-test).

PLA experiments demonstrated that ADAM17 undergoes massive ubiquitylation endogenously. Moreover, although positive PLA signals were evident in untreated samples, treatment with the proteasome inhibitor MG132 significantly increased the positive PLA signals, suggesting that some of the ubiquitylated ADAM17 forms might have undergone proteasomal degradation (Figure 5.26). Although quantification of positive PLA signals in both untreated and MG132-treated samples gave significant results compared to the negative

controls where a single antibody was used, a background was observed when only ubiquitin antibody was used as a negative control. Thus, further experiments are needed to decrease this background to negligible levels in the future. Additionally, examination of z-stacks revealed that ADAM17-ubiquitin interaction was predominantly cytoplasmic (Figure 5.26) like ADAM17-SUMO interaction (Figure 5.19).

5.2.10. Generation of Potential SUMOylation-Deficient ADAM17 Mutants by Site-Directed Mutagenesis

As stated in the previous section, there are four potential SUMOylation motifs on ADAM17 (K188, K697, K753 and K820). Since K188, K697, and K753 are strong consensus motifs, they are the best candidates for SUMO conjugation. Although lysine residue at position 820 appears to be "solvent accessible", the fact that it is located in a non-consensus motif slightly reduces the possibility of this residue undergoing a SUMO modification. Considering ADAM17 domains and the functions of those domains, it was expected that SUMOylation would occur on the cytosolic tail of ADAM17 which was shown to be post-translationally modified (phosphorylated) in the previous studies (Díaz-Rodríguez et al., 2002). Two of the lysine residues of ADAM17 (K697 and K753) are both on the cytosolic tail and in the consensus SUMOylation motif, suggesting they are the strongest candidate SUMO conjugation sites on ADAM17.

Site-directed mutagenesis (SDM) was performed on those lysine residues to create FLAG-ADAM17-K188R, FLAG-ADAM17-K693R, and FLAG-ADAM17-K753R variants. Those two cytosolic cites (K693R and K753R) were also double mutated and will be referred to as FLAG-ADAM17-2KR. On the other hand, one of the lysine residues that is also in the SUMO consensus motif (K188) is on the pro-domain of ADAM17. To eliminate the probability that SUMOylation occurs before ADAM17 is maturated, the relevant variant (K188R) was also included. Chromatograms showing successful disruption of these residues by site-directed mutagenesis can be seen in Figure 5.27.

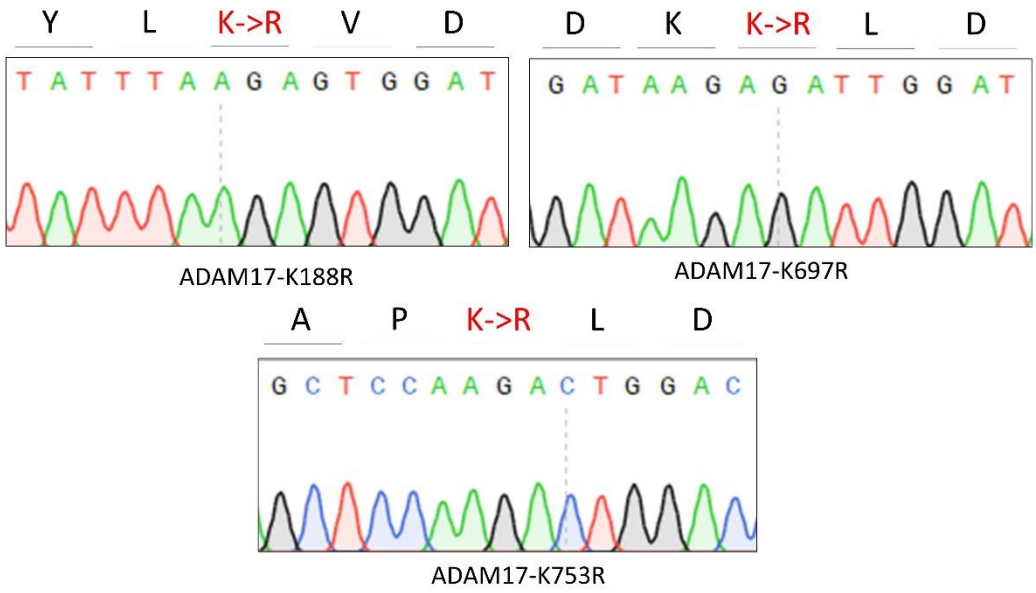

Figure 5.27. Chromatograms showing that three potential SUMOylation sites on ADAM17 are converted to arginine by site-directed mutagenesis.In this way, three separate ADAM17 variants were obtained: ADAM17-K188R, ADAM17-K697R, and ADAM17-K753R.

Although immunoprecipitation and proximity ligation assays were conducted with those variants to elucidate the major SUMOylation sites on ADAM17, the experiments failed mostly due to the problems related to their transfection. Thus, IP and PLA conditions with those variants are needed to optimize to reveal the major SUMOylation sites on ADAM17.

6. DISCUSSION

6.1. SUMOylation and Ubiquitylation of Cas9

CRISPR-Cas9 system has revolutionized the field of genome editing enabling significant applications such as curing human diseases and improving crops (Wang and Doudna, 2024). Cas9 is the key enzyme in this system and *S. pyogenes* Cas9 has been extensively employed as a genome editor despite its limitations such as its big size and other drawbacks. Researchers worldwide have been trying to develop strategies to enhance the on-target effect and reduce the off-target effect of Cas9 (Kovalev et al., 2024). Thus, understanding the regulation of this prokaryotic protein within eukaryotic systems is crucial for designing more reliable and efficient CRISPR-Cas9 genome editing tools.

In this study, post-translational modifications, specifically SUMOylation and ubiquitinylation on Cas9 protein in eukaryotic systems were studied by proximity ligation assays. Proximity ligation assay (PLA) is a powerful technique to determine protein-protein interactions and post-translational modifications in cells (Sahin et al., 2016). Together with the immunoprecipitation results of our former lab member (Ergünay, 2022), the quantification of positive PLA signals demonstrated that Cas9 is endogenously SUMOylated by SUMO1 and SUMO2/3, with a stronger interaction of the latter (Figure 5.2). Moreover, PLA results also demonstrated that Cas9 physically interacts with UBC9, the universal SUMO E2 conjugase, suggesting SUMOylation of this critical enzyme. Noteworthy, the positive PLA signals showing Cas9 interaction with SUMO1, SUMO2/3, and UBC9 were mostly nuclear.

SUMOylation typically occurs on lysine residues within consensus or non-consensus SUMOylation motifs of proteins, and mutating these residues to arginine is a common approach to disrupt SUMOylation. *In silico* analysis which was performed to detect SUMOylation consensus motifs (ψKxD/E) on Cas9 protein revealed 10 consensus motifs on SpCas9, 9 of which are located on the solvent-accessible surface of the protein. Our previous

lab member performed site-directed mutagenesis (SDM) converting lysine residues to arginine on SUMOylation consensus motifs to create 10 different FLAG-Cas9 constructs that each is one consensus motif defective (Yeşildağ, 2019). Immunoprecipitation experiments using those potential SUMOylation-deficient variants revealed that the lysine residue at position 848 is the major SUMOylation site for SUMO2/3 modification. This was demonstrated by the abolishment of SUMO2/3 modification when using the K848R Cas9 mutant, in which the lysine at position 848 was replaced with an arginine residue (Ergünay, 2022). In contrast, none of the 10 lysine residues located within a SUMOylation consensus motif, including lysine 848, were found to significantly contribute to the enzyme's SUMO1 modification (Ergünay et al., 2022). This suggests that the primary SUMO1 attachment site on Cas9 lies outside the canonical SUMOylation motifs described previously.

PLAs by transfecting HEK293 cells with wild-type (WT) or K848R Cas9 also verified endogenous SUMOylation of K848R by SUMO2/3. Positive PLA signals were nearly abolished in Cas9-SUMO2/3 interaction whereas a significant reduction was observed in endogenous interaction of this variant with SUMO1 (Figure 5.3).

Another strategy to disrupt the SUMOylation motif is altering the aspartic acid or glutamic acid residues to neutral alanine present in SUMOylation consensus motifs. The acidic amino acids present in SUMOylation consensus motifs are known to stabilize the interactions between the E2 SUMO conjugating enzyme and the target substrate (Gareau and Lima, 2010). To assess the role of K848 in SUMOylation, another Cas9 variant was created by changing the aspartic acid residue adjacent to this lysine residue to alanine (D850A) by site-directed mutagenesis (Figure 5.4). This construct was further used not only in immunoprecipitation and PLA experiments but also in the generation of stable cell lines expressing wild-type, K848R, and D850A Cas9 which is a more relevant system for CRISPR-based applications (Figure 5.5).

Proximity ligation assays conducted by using cell lines stably expressing wild-type (WT), K848R, and D850A Cas9 yielded similar results where a significant reduction in the interactions between Cas9 and SUMO2/3 was observed (Figure 5.6). Together with the immunoprecipitation experiments, and proximity ligation assays conducted in the transient

expression systems confirmed the importance of the lysine residue at position 848 on Cas9 for SUMO2/3 conjugation.

Ubiquitylation of the Cas9 protein was also shown by our former lab member (Çelen, 2019). PLAs shown in this study also verified a robust endogenous interaction with endogenous ubiquitin and Cas9. Moreover, this interaction was significantly enhanced in the presence of proteasome inhibitor MG-132, suggesting Cas9 might have undergone a proteasomal degradation pathway and subsequently its ubiquitinylation (Figure 5.7). PLA experiments conducted by proteasome subunits PSMA5 also showed strong interaction with Cas9, especially in the presence of proteasome inhibitor MG132, confirming this hypothesis (Figure 5.7). Although inhibition of the proteasomes by MG132 suppresses its catalytic activity and the degradation of client proteins, the physical interaction between the proteasome and its substrates should not be affected. Thus, proximity ligation assays suggest that ubiquitylation marks Cas9 for proteasomal degradation.

Furthermore, lysine residue at position 848 was also shown to be one of the ubiquitylation sites of Cas9 (Ergünay, 2022). PLA results indicated that the K848R Cas9 variant, which is unable to be SUMOylated at this site, displayed higher ubiquitylation levels compared to the wild-type Cas9 (Figure 5.8). This suggests an antagonistic relationship between SUMOylation and ubiquitination at the K848 site of Cas9. The increased ubiquitylation of the K848R Cas9 variant implies that the lack of SUMO2/3 modification at this lysine residue leads to greater ubiquitin conjugation, potentially marking the protein for proteasomal degradation. This finding highlights the intricate interplay between these two post-translational modifications in regulating Cas9 stability and turnover.

Indeed, the experiments conducted to determine the half-lives of wild-type, K848R, or D850A Cas9 by using protein synthesis inhibitor cycloheximide in HEK293 cells stably expressing those variants revealed that K848R and D850 variants of Cas9 have an increased turnover rate compared to the wild-type. Furthermore, those SUMOylation-deficient variants were stabilized upon treatment with proteasome inhibitor MG132, suggesting a protective role of SUMOylation from ubiquitylation and subsequent proteasomal degradation (Ergünay et al., 2022). So, it can be concluded that SUMOylation and

ubiquitylation compete for the same lysine residue at position 848 on Cas9, and SUMOylation increases Cas9 stability by preventing its degradation in proteasomes upon ubiquitylation.

Importantly, the proximity ligation assays revealed that the Cas9-ubiquitin interactions were predominantly localized in the cytoplasm, in contrast to the nuclear localization of Cas9 SUMOylation. This observation indicates that SUMOylation and ubiquitylation may have distinct, compartment-specific functions in regulating Cas9.

6.2. Identification of ADAM17 SUMOylation and Ubiquitylation and Their Effect on ADAM17-mediated Ectodomain Shedding

ADAM17, known as the TNFα converting enzyme, is a critical metalloproteinase responsible for shedding of many ligands such as growth factors, adhesion proteins, immune mediators, and signaling molecules, contributing to diverse cellular and physiological processes ranging from immunity to regeneration and development (Düsterhöft, Lokau, et al., 2019). Given its pivotal role in these distinct processes, it is not surprising that ADAM17 is tightly regulated through various mechanisms to maintain balanced protein levels and enzymatic activation.

This study investigated post-translational modifications of the ADAM17 protein, specifically SUMOylation and ubiquitylation, and their effects on ADAM17 stability and ADAM17-mediated ectodomain shedding. Immunoprecipitation (IP) and proximity ligation assays (PLA) revealed, for the first time, that ADAM17 is subject to SUMOylation and ubiquitylation, adding another level of regulation of this critical protein.

ADAM17-mediated ectodomain shedding of TGFα, HB-EGF, and epiregulin was investigated under conditions of increased or decreased global SUMOylation levels, using alkaline phosphatase assays. In these experiments, the phorbol ester PMA was used to activate ADAM17, while the metalloproteinase inhibitor batimastat (BB94) was used to inhibit ADAM17 in cells transfected with AP-tagged ADAM17 substrates. The fold changes

in the PMA-stimulated and BB94-inhibited shedding activity were calculated and normalized to constitutive shedding, with untreated conditions serving as the basal shedding level. The AP assays showed that ADAM17-mediated TGFα shedding was significantly increased under both PMA-stimulated and BB94-inhibited conditions when global SUMOylation levels were reduced by the SUMOylation inhibitor ML792 (Figure 5.9). However, no changes were observed in ADAM17-mediated shedding of HB-EGF and epiregulin under the same conditions (Figure 5.10). These results suggest that decreased global SUMOylation levels specifically enhance ADAM17-mediated TGFα shedding. In contrast, when global SUMOylation levels were increased by overexpressing SUMO1, SUMO2/3, and the universal SUMO conjugase UBC9, no significant changes were observed in the ADAM17-mediated shedding of TGFα, HB-EGF, or epiregulin, despite a non-significant decrease in HB-EGF and epiregulin shedding (Figures 5.12, 5.13, and 5.14).

Changing the global SUMOylation levels within cells may alter the SUMOylation of numerous proteins including the ones upstream or downstream of ADAM17 regulation. One significant example is SUMOylation of protein kinase C (PKC), a critical activator of ADAM17. A recent study showed that SUMOylation enhances the stability of protein kinase C delta by suppressing its ubiquitinylation (Gao et al., 2021). Many other proteins involved in the regulation of ADAM17 or the substrate-specific ADAM17-mediated ectodomain shedding might be affected by the changes in global SUMOylation levels. This could explain why some of the ADAM17-mediated ectodomain shedding substrates, such as HB-EGF and epiregulin, were unaffected by induced or reduced global SUMOylation, while a significant increase was observed in ADAM17-mediated TGFα shedding in the conditions where the SUMOylation was inhibited by ML792 (Figure 5.9). Another possible explanation is that AP assays were performed with endogenous ADAM17 and endogenous ADAM17 levels were not altered by SUMO overexpression, although a significant decrease was seen in the overexpression system. To better understand the effect of ADAM17 SUMOylation on its stability and ADAM17-mediated ectodomain shedding, similar experiments should be performed using SUMOylation-deficient ADAM17 variants. This would allow for the inhibition of ADAM17 SUMOylation without altering global SUMOylation levels, providing a more reliable system to investigate the specific effects of ADAM17 SUMOylation.

The best way to show the protein-specific SUMO modification in cell lines is to apply methods such as immunoprecipitation, and affinity precipitation by overexpressing both the protein of interest and the SUMO1 or SUMO2/3 peptides. However, when ADAM17 is overexpressed, there is only an increase in its inactive form, the proform, and the level of its mature form cannot be increased (Düsterhöft et al., 2019). This situation makes isolating mature ADAM17 challenging in overexpression systems. Since immunoprecipitation experiments were conducted in overexpression systems, the mature form of ADAM17 could not be detected in the first IP experiments. However, by optimizing the conditions for the detection and visualization of IP experiments, mature ADAM17 forms were successfully isolated in overexpression systems (Figure 5.15).

SUMOylation of ADAM17 was demonstrated using two different immunoprecipitation methods. In the first approach, a FLAG antibody was used to immunoprecipitate ADAM17 forms from HEK293 cells transfected with FLAG-tagged ADAM17 and GFP-tagged SUMO peptides. Immunoblotting against SUMO1 and SUMO2/3 revealed a smeared band pattern, indicating that ADAM17 is SUMOylated (Figure 5.16). In the second method, all SUMO-modified proteins were pulled down using an anti-GFP antibody in HEK293 cells overexpressing FLAG-ADAM17 together with GFP-SUMO1 or GFP-SUMO2/3. Western blot analysis with anti-FLAG or anti-ADAM17 antibodies confirmed the SUMOylation of ADAM17 by both SUMO1 (Figure 5.17) and SUMO2/3 (Figure 5.18). Together, these two complementary approaches demonstrated that ADAM17 is a target for SUMOylation.

Importantly, proximity ligation assays revealed endogenous interactions of ADAM17 with SUMO1, SUMO2/3, and UBC9, suggesting potential SUMO modification of ADAM17 (Figure 5.19). Although the PLA signals indicating ADAM17-SUMO2/3 interactions were nearly double those of ADAM17-SUMO1 interactions, a slight background signal was observed in the negative control group with only SUMO2/3 antibody (Figure 5.19). This makes it challenging to definitively determine the relative levels of SUMO1 and SUMO2/3 modification on ADAM17. Thus, the PLA experiments should be repeated in the future with improved conditions to reduce the background noise. However, the experiments examining ADAM17 stability upon overexpression of SUMO peptides

revealed that the degradation of overexpressed ADAM17 forms was more pronounced with SUMO2/3 overexpression, suggesting a higher level of ADAM17 modification by SUMO2/3 (Figure 5.21), in line with the PLA findings.

The results indicate that when ADAM17 is overexpressed together with SUMO peptides, there is a significant decline in the levels of the mature form of ADAM17. This suggests that ADAM17 may be degraded upon increased global SUMOylation. Consistent with these findings, experiments showed that treating cells with the protein synthesis inhibitor cycloheximide resulted in higher levels of remaining ADAM17 protein when global SUMOylation was inhibited by ML792 compared to the control group. However, when the same experiments were performed without overexpressing ADAM17 in the cells to examine the change in levels of endogenous ADAM17 forms, the levels of the proform and mature ADAM17 were unaffected, regardless of whether SUMOylation was increased by overexpressing SUMO peptides or inhibited by ML792. Taken together, these results suggest that the stability of the mature form of overexpressed ADAM17 decreases in response to an increase in the global SUMOylation levels, while the endogenous levels of ADAM17 forms are not affected. Considering the tight regulation of ADAM17 protein levels in the cell, the processes of SUMOylation and subsequent degradation of ADAM17 could potentially be leveraged to modulate the increased expression of ADAM17 in the cell.

ADAM17 harbors four potential SUMO conjugation sites (K188, K697, K753, and K820). While the lysine residue at position 188 lies within the prodomain of ADAM17, the other three lysine residues are located in the cytoplasmic domain. However, one of those cytoplasmic sites (K820) lies within a non-consensus SUMOylation motif, reducing the likelihood of it being the major SUMOylation site. Moreover, since the cytoplasmic domain of ADAM17 is known to be post-translationally modified by phosphorylation (Düsterhöft, Babendreyer, et al., 2019), SUMOylation, another post-translational modification, would likely occur through the cytoplasmic tail of ADAM17. This makes the lysine residues at positions 697 and 753 the strongest candidates for SUMO conjugation sites on ADAM17. In a study conducted by Schwarz et al. (2013), the complete deletion of ADAM17 cytoplasmic tail resulted in a complete loss of ADAM17-mediated TNFα shedding under PMA-stimulated conditions. Interestingly, partial deletion of the ADAM17 cytoplasmic

domain (ADAM17Δ700) was sufficient to rescue the phenotype observed with complete cytoplasmic domain deletion (ADAM17ΔCT). ADAM17Δ700 and ADAM17ΔCT variants differ only 6 amino acids and the lysine residue at position 697 was located within this sequence (N-VDKKLD-C, K697 is shown in red), highlighting the importance of this candidate lysine residue in the ADAM17 cytoplasmic tail. SUMOylation of this specific lysine residue could potentially explain the phenotypic differences observed in this study (Schwarz et al., 2013).

Although the lysine residues at positions 697 and 753 are the strongest candidates for SUMO conjugation sites on ADAM17, the possibility that SUMOylation may occur before the maturation of ADAM17 cannot be ruled out, making the lysine residue at position 188 another potential site. To identify the major SUMOylation sites, site-directed mutagenesis was performed to generate three FLAG-tagged ADAM17 variants, each harboring a single mutation where the lysine residue was replaced with arginine (K188R, K697R, and K753R). Additionally, another variant was created with a double mutation (K697R and K753R) on the cytoplasmic tail, to account for potential compensatory mechanisms in case ADAM17 is SUMOylated at multiple sites.

Immunoprecipitation and proximity ligation assays were performed using the potential SUMO-defective variants of ADAM17. HEK293 cells were transfected with either wild-type FLAG-ADAM17 or the FLAG-ADAM17 variants, and immunoprecipitation and proximity ligation assays were performed to identify the major SUMOylation sites on ADAM17. Unfortunately, the experiments encountered some technical problems, primarily related to the transfection process. Therefore, the IP and PLA experiments using these constructs need to be repeated to successfully identify the major SUMOylation sites on the ADAM17 protein. Once the major SUMOylation site on ADAM17 is identified, the SUMOylation-defective ADAM17 variant could be utilized to elucidate the effect of ADAM17 SUMOylation on its stability and ADAM17-mediated ectodomain shedding.

Immunoprecipitation and proximity ligation assays demonstrated that ADAM17 is also subject to ubiquitylation. Similar experimental approaches were employed to investigate ADAM17 ubiquitylation as were used to examine its SUMOylation. HEK293 cells were co-

transfected with FLAG-ADAM17 and His-ubiquitin, and immunoprecipitation was performed with an anti-His antibody to pull down all the ubiquitylated proteins. Immunoblotting against the FLAG tag revealed a laddered pattern above 100 kDa, an indication of ubiquitylated ADAM17 forms (Figure 5.23). Additionally, proximity ligation assays verified the endogenous interaction of ADAM17 with ubiquitin, with significantly increased PLA signals in the presence of the proteasome inhibitor MG132 (Figure 5.26).

Moreover, the ubiquitylation levels of ADAM17 in the presence and absence of the SUMOylation inhibitor ML792 were compared by immunoprecipitation experiments to investigate the crosstalk between SUMOylation and ubiquitylation of ADAM17. These experiments revealed an increase in the ubiquitylated ADAM17 forms in the presence of SUMOylation inhibitor ML792, suggesting an antagonistic relationship between SUMOylation and ubiquitylation of ADAM17 (Figure 5.24). Additionally, examination of proform and mature form levels of ADAM17 in whole cell lysates upon increased global ubiquitylation revealed an increase in both forms of ADAM17, in contrast to the significant reduction of ADAM17 forms upon increased global SUMOylation, highlighting the antagonistic effects of SUMOylation and ubiquitylation of ADAM17 on its stability. However, those results may be attributed to the indirect effects of changing SUMOylation and ubiquitylation globally in the cells. Therefore, those experiments should be repeated using SUMOylation-defective ADAM17 variants to fully elucidate the crosstalk between SUMOylation and ubiquitylation of ADAM17.

Various post-translational modifications on ADAM17, including phosphorylation reported previously and SUMOylation and ubiquitylation reported here, can influence the stability and function of ADAM17 in numerous ways. SUMOylation and ubiquitylation can compete for the same lysine residue as in the case of Cas9 protein, and this could explain the increased levels of ADAM17 ubiquitylation upon SUMOylation inhibition by ML792. Alternatively, ADAM17 SUMOylation can trigger its ubiquitylation and subsequent degradation by SUMOylation-dependent ubiquitylation pathway, explaining the decreased level of ADAM17 forms observed upon increased global SUMOylation. Ubiquitylation of ADAM17 can also mark this critical metalloprotease for its internalization by endocytosis. In a recent study, it was shown that ADAM17 is degraded in lysosomes rather than

proteasomes (Zhang et al., 2021). Ubiquitylation can also target proteins for lysosomal degradation (Clague and Urbé, 2010). Considering that ADAM17 is internalized via clathrin-mediated endocytosis followed by lysosomal degradation (Lorenzen et al., 2016), ubiquitylation may be an important mechanism for regulating the active ADAM17 levels at the cell membrane. Furthermore, given the fact that ADAM17 is also phosphorylated on its cytoplasmic domain, phosphorylation-dependent SUMOylation can also occur in the cytoplasmic domain of ADAM17. Therefore, further research is needed to elucidate the complex crosstalk of post-translational modifications on ADAM17 protein, and the effect of those modifications on its stability, localization, and enzymatic activity. The crosstalk of those modifications can add another layer to the regulation of ADAM17-mediated ectodomain shedding, making them significant therapeutic targets for the various diseases stemming from the dysregulation of ADAM17-mediated ectodomain shedding.

To sum up, this study revealed SUMOylation and ubiquitylation of ADAM17 for the first time known. Experimental evidence suggests an antagonistic relationship between SUMOylation and ubiquitylation, with SUMOylation inhibition leading to increased ADAM17 ubiquitylation. While increased global ubiquitylation elevates ADAM17 levels, increased global SUMOylation decreases them, hinting at opposing roles in protein stability. Furthermore, reduced global SUMOylation led to a significant increase in ADAM17-mediated TGFα shedding. However, further investigation using SUMOylation-defective ADAM17 variants is needed to confirm these findings. Identifying the major SUMOylation sites on ADAM17 is also crucial for elucidating how SUMOylation affects the stability, localization, and function of ADAM17, as well as its crosstalk with ubiquitylation. Gaining these insights into the regulation of ADAM17 by post-translational modifications could uncover novel therapeutic targets for diseases where dysregulated ADAM17 activity is implicated, such as cancer, arthritis, and cardiovascular disorders.

REFERENCES

Adrain, C., M. Zettl, Y. Christova, N. Taylor, and M. Freeman, 2012, "Tumor Necrosis Factor Signaling Requires IRhom2 to Promote Trafficking and Activation of TACE", *Science*, Vol. 335, No. 6065, pp. 225–228.

Anders, C., O. Niewoehner, A. Duerst, and M. Jinek, 2014, "Structural Basis of PAM-Dependent Target DNA Recognition by the Cas9 Endonuclease", *Nature*, Vol. 513, No. 7519, pp. 569–573.

Anjum, R., and J. Blenis, 2008, "The RSK Family of Kinases: Emerging Roles in Cellular Signalling", *Nature Reviews. Molecular Cell Biology*, Vol. 9, No. 10, pp. 747–758.

Arribas, J., and C. Esselens, 2009, "ADAM17 as a Therapeutic Target in Multiple Diseases", *Current Pharmaceutical Design*, Vol. 15, No. 20, pp. 2319–2335.

Barrangou, R., C. Fremaux, H. Deveau, M. Richards, P. Boyaval, S. Moineau, D. A. Romero, and P. Horvath, 2007, "CRISPR Provides Acquired Resistance against Viruses in Prokaryotes", *Science (New York, N.Y.)*, Vol. 315, No. 5819, pp. 1709–1712.

Bayer, P., A. Arndt, S. Metzger, R. Mahajan, F. Melchior, R. Jaenicke, and J. Becker, 1998, "Structure Determination of the Small Ubiquitin-Related Modifier SUMO-1", *Journal of Molecular Biology*, Vol. 280, No. 2, pp. 275–286.

Black, R. A., C. T. Rauch, C. J. Kozlosky, J. J. Peschon, J. L. Slack, M. F. Wolfson, B. J. Castner, K. L. Stocking, P. Reddy, S. Srinivasan, N. Nelson, N. Boiani, K. A. Schooley, M. Gerhart, R. Davis, J. N. Fitzner, R. S. Johnson, R. J. Paxton, C. J. March, and D. P. Cerretti, 1997, "A Metalloproteinase Disintegrin That Releases Tumour-Necrosis Factor-α from Cells", *Nature*, Vol. 385, No. 6618, pp. 729–733.

Blaydon, D. C., P. Biancheri, W.-L. Di, V. Plagnol, R. M. Cabral, M. A. Brooke, D. A. van Heel, F. Ruschendorf, M. Toynbee, A. Walne, E. A. O'Toole, J. E. Martin, K. Lindley, T. Vulliamy, D. J. Abrams, T. T. MacDonald, J. I. Harper, and D. P. Kelsell, 2011, "Inflammatory Skin and Bowel Disease Linked to ADAM17 Deletion", *The New England Journal of Medicine*, Vol. 365, No. 16, pp. 1502–1508.

Blobel, C. P., 2005, "ADAMs: Key Components in EGFR Signalling and Development", *Nature Reviews Molecular Cell Biology*, Vol. 6, No. 1, pp. 32–43.

Bolotin, A., B. Quinquis, A. Sorokin, and S. D. Ehrlich, 2005, "Clustered Regularly Interspaced Short Palindrome Repeats (CRISPRs) Have Spacers of Extrachromosomal Origin", *Microbiology (Reading, England)*, Vol. 151, No. Pt 8, pp. 2551–2561.

Brackett, C. M., and B. S. J. Blagg, 2020, "Current Status of SUMOylation Inhibitors", *Current Medicinal Chemistry*, Vol. 28, No. 20, pp. 3892–3912.

Cavadas, M., I. Oikonomidi, C. J. Gaspar, E. Burbridge, M. Badenes, I. Félix, A. Bolado, T. Hu, A. Bileck, C. Gerner, P. M. Domingos, A. von Kriegsheim, and C. Adrain, 2017, "Phosphorylation of IRhom2 Controls Stimulated Proteolytic Shedding by the Metalloprotease ADAM17/TACE", *Cell Reports*, Vol. 21, No. 3, pp. 745–757.

Celen, A. B., and U. Sahin, 2020, "Sumoylation on Its 25th Anniversary: Mechanisms, Pathology, and Emerging Concepts", *FEBS Journal*, Vol. 287, No. 15, pp. 3110–3140.

Clague, M. J., and S. Urbé, 2010, "Ubiquitin: Same Molecule, Different Degradation Pathways", *Cell*, Vol. 143, No. 5, pp. 682–685.

Cong, L., F. A. Ran, D. Cox, S. Lin, R. Barretto, N. Habib, P. D. Hsu, X. Wu, W. Jiang, L. A. Marraffini, and F. Zhang, 2013, "Multiplex Genome Engineering Using CRISPR/Cas Systems", *Science (New York, N.Y.)*, Vol. 339, No. 6121, pp. 819–823.

Çelen, A.B., 2019, *A Novel Post-translational Modification on the Central CRISPR enzyme: Discovery of CAS9 Ubiquitylation*, M.S. Thesis, Boğaziçi University.

Díaz-Rodríguez, E., J. C. Montero, A. Esparís-Ogando, L. Yuste, and A. Pandiella, 2002, "Extracellular Signal-Regulated Kinase Phosphorylates Tumor Necrosis Factor Alpha-Converting Enzyme at Threonine 735: A Potential Role in Regulated Shedding", *Molecular Biology of the Cell*, Vol. 13, No. 6, pp. 2031–2044.

Drag, M., and G. S. Salvesen, 2008, "DeSUMOylating Enzymes - SENPs", *IUBMB Life*, Vol. 60, No. 11, pp. 734–742.

Düsterhöft, S., A. Babendreyer, A. A. Giese, C. Flasshove, and A. Ludwig, 2019, "Status Update on IRhom and ADAM17: It's Still Complicated", *Biochimica et Biophysica Acta - Molecular Cell Research*, Vol. 1866, No. 10, pp. 1567–1583.

Düsterhöft, S., S. Jung, C.-W. Hung, A. Tholey, F. D. Sönnichsen, J. Grötzinger, and I. Lorenzen, 2013, "Membrane-Proximal Domain of a Disintegrin and Metalloprotease-17 Represents the Putative Molecular Switch of Its Shedding Activity Operated by Protein-Disulfide Isomerase", *Journal of the American Chemical Society*, Vol. 135, No. 15, pp. 5776–5781.

Düsterhöft, S., J. Lokau, and C. Garbers, 2019, "The Metalloprotease ADAM17 in Inflammation and Cancer", *Pathology Research and Practice*, Vol. 215, No. 6, pp. 152410.

Ergünay, T., 2022, *Investigation of The Effects of Sumo Modification on Two Critical Proteins: A Pathogenic Nek1 Mutant That Drives Als Pathogenesis and The CRISPR-Associated Cas9 Protein*, M.S. Thesis, Boğaziçi University.

Ergünay, T., Ö. Ayhan, A. B. Celen, P. Georgiadou, E. Pekbilir, Y. T. Abaci, D. Yesildag, M. Rettel, U. Sobhiafshar, A. Ogmen, N. T. Emre, and U. Sahin, 2022, "Sumoylation of Cas9 at Lysine 848 Regulates Protein Stability and DNA Binding", *Life Science Alliance*, Vol. 5, No. 4, pp. e202101078.

Fan, H., C. W. Turck, and R. Derynck, 2003, "Characterization of Growth Factor-Induced Serine Phosphorylation of Tumor Necrosis Factor-α Converting Enzyme and of an Alternatively Translated Polypeptide", *Journal of Biological Chemistry*, Vol. 278, No. 20, pp. 18617–18627.

Gao, S., X. Zhao, L. Hou, R. Ma, J. Zhou, M. X. Zhu, S. J. Pan, and Y. Li, 2021, "The Interplay between SUMOylation and Phosphorylation of PKCδ Facilitates Oxidative Stress-Induced Apoptosis", *FEBS Journal*, Vol. 288, No. 22, pp. 6447–6464.

Gareau, J. R., and C. D. Lima, 2010, "The SUMO Pathway: Emerging Mechanisms That Shape Specificity, Conjugation and Recognition", *Nature Reviews Molecular Cell Biology*, Vol. 11, No. 12, pp. 861–871.

Gooz, P., Y. Dang, S. Higashiyama, W. O. Twal, C. J. Haycraft, and M. Gooz, 2012, "A Disintegrin and Metalloenzyme (ADAM) 17 Activation Is Regulated by A5β1 Integrin in Kidney Mesangial Cells", *PLoS ONE*, Vol. 7, No. 3, pp. 1–9.

Grieve, A. G., H. Xu, U. Künzel, P. Bambrough, B. Sieber, and M. Freeman, 2017, "Phosphorylation of IRhom2 at the Plasma Membrane Controls Mammalian TACE-Dependent Inflammatory and Growth Factor Signalling", *ELife*, Vol. 6, pp. e23968.

Grötzinger, J., I. Lorenzen, and S. Düsterhöft, 2017, "Molecular Insights into the Multilayered Regulation of ADAM17: The Role of the Extracellular Region", *Biochimica et Biophysica Acta - Molecular Cell Research*, Vol. 1864, No. 11, pp. 2088–2095.

Hall, K. C., and C. P. Blobel, 2012, "Interleukin-1 Stimulates ADAM17 through a Mechanism Independent of Its Cytoplasmic Domain or Phosphorylation at Threonine 735", *PloS One*, Vol. 7, No. 2, pp. e31600.

Hartmann, D., B. de Strooper, L. Serneels, K. Craessaerts, A. Herreman, W. Annaert, L. Umans, T. Lübke, A. Lena Illert, K. von Figura, and P. Saftig, 2002, "The Disintegrin/Metalloprotease ADAM 10 Is Essential for Notch Signalling but Not for Alpha-Secretase Activity in Fibroblasts", *Human Molecular Genetics*, Vol. 11, No. 21, pp. 2615–2624.

Horiuchi, K., S. Le Gall, M. Schulte, T. Yamaguchi, K. Reiss, G. Murphy, Y. Toyama, D. Hartmann, P. Saftig, and C. P. Blobel, 2007, "Substrate Selectivity of Epidermal Growth Factor-Receptor Ligand Sheddases and Their Regulation by Phorbol Esters and Calcium Influx", *Molecular Biology of the Cell*, Vol. 18, No. 1, pp. 176–188.

Huang, C. J., D. Wu, F. A. Khan, and L. J. Huo, 2015, "DeSUMOylation: An Important Therapeutic Target and Protein Regulatory Event", *DNA and Cell Biology*, Vol. 34, No. 11, pp. 652–660.

Jiang, F., and J. A. Doudna, 2017, "CRISPR-Cas9 Structures and Mechanisms", *Annual review of biophysics*, Vol. *46*, pp. 505–529.

Jiang, F., K. Zhou, L. Ma, S. Gressel, and J. A. Doudna, 2015, "STRUCTURAL BIOLOGY. A Cas9-Guide RNA Complex Preorganized for Target DNA Recognition", *Science (New York, N.Y.)*, Vol. 348, No. 6242, pp. 1477–1481.

Jinek, M., K. Chylinski, I. Fonfara, M. Hauer, J. A. Doudna, and E. Charpentier, 2012, "A Programmable Dual-RNA-Guided DNA Endonuclease in Adaptive Bacterial Immunity", *Science (New York, N.Y.)*, Vol. 337 No. 6096, pp. 816–821.

Jinek, M., F. Jiang, D. W. Taylor, S. H. Sternberg, E. Kaya, E. Ma, C. Anders, M. Hauer, K. Zhou, S. Lin, M. Kaplan, A. T. Iavarone, E. Charpentier, E. Nogales, and J. A. Doudna, 2014, "Structures of Cas9 Endonucleases Reveal RNA-Mediated Conformational Activation", *Science (New York, N.Y.)*, Vol. 343, No. 6176, pp. 1247997.

Kato, T., M. Hagiyama, and A. Ito, 2018, "Renal ADAM10 and 17: Their Physiological and Medical Meanings", *Frontiers in Cell and Developmental Biology*, Vol. 6, 153.

Killock, D. J., and A. Ivetić, 2010, "The Cytoplasmic Domains of TNFα-Converting Enzyme (TACE/ADAM17) and L-Selectin Are Regulated Differently by P38 MAPK and PKC to Promote Ectodomain Shedding", *Biochemical Journal*, Vol. 428, No. 2, pp. 293–304.

Kovalev, M. A., A. I. Davletshin, and D. S. Karpov, 2024, "Engineering Cas9: Next Generation of Genomic Editors", *Applied Microbiology and Biotechnology*, Vol. 108, No. 1, 209.

Le Gall, S. M., T. Maretzky, P. D. A. Issuree, X. Da Niu, K. Reiss, P. Saftig, R. Khokha, D. Lundell, and C. P. Blobel, 2010, "ADAM17 Is Regulated by a Rapid and Reversible Mechanism That Controls Access to Its Catalytic Site", *Journal of Cell Science*, Vol. 123, No. 22, pp. 3913–3922.

Leonard, J. D., F. Lin, and M. E. Milla, 2005, "Chaperone-like Properties of the Prodomain of TNFα-Converting Enzyme (TACE) and the Functional Role of Its Cysteine Switch", *Biochemical Journal*, Vol. 387, No. 3, pp. 797–805.

Lichtenthaler, S. F., M. K. Lemberg, and R. Fluhrer, 2018, "Proteolytic Ectodomain Shedding of Membrane Proteins in Mammals-Hardware, Concepts, and Recent Developments", *The EMBO Journal*, Vol. 37, No. 15, pp. 1–24.

Lorenzen, I., J. Lokau, Y. Korpys, M. Oldefest, C. M. Flynn, U. Künzel, C. Garbers, M. Freeman, J. Grötzinger, and S. Düsterhöft, 2016, "Control of ADAM17 Activity by Regulation of Its Cellular Localisation", *Scientific Reports*, Vol. 6, 35067.

Makarova, K. S., Y. I. Wolf, O. S. Alkhnbashi, F. Costa, S. A. Shah, S. J. Saunders, R. Barrangou, S. J. J. Brouns, E. Charpentier, D. H. Haft, P. Horvath, S. Moineau, F. J. M. Mojica, R. M. Terns, M. P. Terns, M. F. White, A. F. Yakunin, R. A. Garrett, J. van der Oost, … E. V. Koonin, 2015, "An Updated Evolutionary Classification of CRISPR-Cas Systems", *Nature reviews. Microbiology*, Vol. 13, No 11, pp. 722–736.

Makarova, K. S., F. Zhang, and E. V. Koonin, 2017, "SnapShot: Class 2 CRISPR-Cas Systems", *Cell*, Vol. 168, No. 1–2, pp. 328- 328.e1.

Mali, P., K. M. Esvelt, and G. M. Church, 2013, "Cas9 as a Versatile Tool for Engineering Biology", *Nature Methods*, Vol. 10, No. 10, pp. 957–963.

Matthews, A. L., P. J. Noy, J. S. Reyat, and M. G. Tomlinson, 2017, "Regulation of A Disintegrin and Metalloproteinase (ADAM) Family Sheddases ADAM10 and ADAM17: The Emerging Role of Tetraspanins and Rhomboids", *Platelets*, Vol. 28 No. 4, pp. 333–341.

Milla, M. E., M. A. Leesnitzer, M. L. Moss, W. C. Clay, H. L. Carter, A. B. Miller, J. L. Su, M. H. Lambert, D. H. Willard, D. M. Sheeley, T. A. Kost, W. Burkhart, M. Moyer, R. K. Blackburn, G. L. Pahel, J. L. Mitchell, C. R. Hoffman, and J. D. Becherer, 1999, "Specific Sequence Elements Are Required for the Expression of Functional Tumor Necrosis Factor-Alpha-Converting Enzyme (TACE)", *The Journal of Biological Chemistry*, Vol. 274, No. 43, pp. 30563–30570.

Mojica, F. J. M., C. Díez-Villaseñor, J. García-Martínez, and E. Soria, 2005, "Intervening Sequences of Regularly Spaced Prokaryotic Repeats Derive from Foreign Genetic Elements", *Journal of Molecular Evolution*, Vol. 60, No. 2, pp. 174–182.

Murthy, A., Y. W. Shao, S. R. Narala, S. D. Molyneux, J. C. Zúñiga-Pflücker, and R. Khokha, 2012, "Notch Activation by the Metalloproteinase ADAM17 Regulates Myeloproliferation and Atopic Barrier Immunity by Suppressing Epithelial Cytokine Synthesis", *Immunity*, Vol. 36, No. 1, pp. 105–119.

Nacerddine, K., F. Lehembre, M. Bhaumik, J. Artus, M. Cohen-Tannoudji, C. Babinet, P. P. Pandolfi, and A. Dejean, 2005, "The SUMO Pathway Is Essential for Nuclear Integrity and Chromosome Segregation in Mice", *Developmental Cell*, Vol. 9, No. 6, pp. 769–779.

Nishimasu, H., F. A. Ran, P. D. Hsu, S. Konermann, S. I. Shehata, N. Dohmae, R. Ishitani, F. Zhang, and O. Nureki, 2014, "Crystal Structure of Cas9 in Complex with Guide RNA and Target DNA", *Cell*, Vol. 156, No. 5, pp. 935–949.

Oikonomidi, I., E. Burbridge, M. Cavadas, G. Sullivan, B. Collis, H. Naegele, D. Clancy, J. Brezinova, T. Hu, A. Bileck, C. Gerner, A. Bolado, A. von Kriegsheim, S. J. Martin, F. Steinberg, K. Strisovsky, and C. Adrain, 2018, "ITAP, a Novel IRhom Interactor, Controls TNF Secretion by Policing the Stability of IRhom/TACE", *ELife*, Vol. 7, e35032.

Palermo, G., J. S. Chen, C. G. Ricci, I. Rivalta, M. Jinek, V. S. Batista, J. A. Doudna, and J. A. McCammon, 2018, "Key Role of the REC Lobe during CRISPR-Cas9 Activation by “Sensing”, “Regulating”, and “Locking” the Catalytic HNH Domain". *Quarterly Reviews of Biophysics*, Vol. 51, e91.

Peschon, J. J., J. L. Slack, P. Reddy, K. L. Stocking, S. W. Sunnarborg, D. C. Lee, W. E. Russell, B. J. Castner, R. S. Johnson, J. N. Fitzner, R. W. Boyce, N. Nelson, C. J. Kozlosky, M. F. Wolfson, C. T. Rauch, D. P. Cerretti, R. J. Paxton, C. J. March, and R. A. Black, 1998, "An Essential Role for Ectodomain Shedding in Mammalian Development", *Science (New York, N.Y.)*, Vol. 282, No. 5392, pp. 1281–1284.

Pourcel, C., G. Salvignol, and G. Vergnaud, 2005, "CRISPR Elements in Yersinia Pestis Acquire New Repeats by Preferential Uptake of Bacteriophage DNA, and Provide Additional Tools for Evolutionary Studies", *Microbiology (Reading, England)*, Vol. 151, No. Pt 3, pp. 653–663.

Reddy, P., J. L. Slack, R. Davis, D. P. Cerretti, C. J. Kozlosky, R. A. Blanton, D. Shows, J. J. Peschon, and R. A. Black, 2000, "Functional Analysis of the Domain Structure of Tumor Necrosis Factor-Alpha Converting Enzyme", *The Journal of Biological Chemistry*, Vol. 275, No. 19, pp. 14608–14614.

Robb, G. B, 2019, "Genome Editing with CRISPR-Cas: An Overview", *Current Protocols in Essential Laboratory Techniques*, Vol. 19 No. 1.

Sahin, U., H. de Thé, and V. Lallemand-Breitenbac, 2022, "Sumoylation in Physiology, Pathology and Therapy", *Cells*, Vol. 11, No 5, 814.

Sahin, U., F. Jollivet, C. Berthier, H. de Thé, and V. Lallemand-Breitenbach, 2016, "Detection of Protein SUMOylation In Situ by Proximity Ligation Assays", *Methods in molecular biology (Clifton, N.J.)*, Vol. 1475, pp. 139–150.

Sahin, U., G. Weskamp, K. Kelly, H. M. Zhou, S. Higashiyama, J. Peschon, D. Hartmann, P. Saftig, and C. P. Blobel, 2004, "Distinct Roles for ADAM10 and ADAM17 in Ectodomain Shedding of Six EGFR Ligands", *Journal of Cell Biology*, Vol. 164, No. 5, pp. 769–779.

Sahin, U., G. Weskamp, Y. Zheng, V. Chesneau, K. Horiuchi, and C. P. Blobel, 2006, "A Sensitive Method to Monitor Ectodomain Shedding of Ligands of the Epidermal Growth Factor Receptor". *Methods in Molecular Biology (Clifton, N.J.)*, Vol. 327, No. 5, pp. 99–113.

Salas-Lloret, D., and R. González-Prieto, 2022, "Insights in Post-Translational Modifications: Ubiquitin and SUMO", *International Journal of Molecular Sciences*, Vol. 23, No 6, 321.

Schlöndorff, J., J. D. Becherer, and C. P. Blobel, 2000, "Intracellular Maturation and Localization of the Tumour Necrosis Factor Alpha Convertase (TACE)", *The Biochemical Journal*, Vol. 347 Pt 1, No. Pt 1, pp. 131–138.

Schwarz, J., C. Broder, A. Helmstetter, S. Schmidt, I. Yan, M. Müller, D. Schmidt-Arras, C. Becker-Pauly, F. Koch-Nolte, H. W. Mittrücker, B. Rabe, S. Rose-John, and A. Chalaris, 2013, "Short-Term TNFα Shedding Is Independent of Cytoplasmic Phosphorylation or Furin Cleavage of ADAM17", *Biochimica et Biophysica Acta - Molecular Cell Research*, Vol. 1833, No. 12, pp. 3355–3367.

Schwarz, J., S. Schmidt, O. Will, T. Koudelka, K. Köhler, M. Boss, B. Rabe, A. Tholey, J. Scheller, D. Schmidt-Arras, M. Schwake, S. Rose-John, and A. Chalaris, 2014, "Polo-like Kinase 2, a Novel ADAM17 Signaling Component, Regulates Tumor Necrosis Factor α Ectodomain Shedding", *Journal of Biological Chemistry*, Vol. 289, No. 5, pp. 3080–3093.

Slaymaker, I. M., L. Gao, B. Zetsche, D. A. Scott, W. X. Yan, and F. Zhang, 2016, "Rationally Engineered Cas9 Nucleases with Improved Specificity", *Science (New York, N.Y.)*, Vol. 351, No. 6268, pp. 84–88.

Sommer, A., F. Kordowski, J. Büch, T. Maretzky, A. Evers, J. Andrä, S. Düsterhöft, M. Michalek, I. Lorenzen, P. Somasundaram, A. Tholey, F. D. Sönnichsen, K. Kunzelmann, L. Heinbockel, C. Nehls, T. Gutsmann, J. Grötzinger, S. Bhakdi, and K. Reiss, 2016, "Phosphatidylserine Exposure Is Required for ADAM17 Sheddase Function", *Nature Communications*, Vol. 7, pp. 11523.

Spoel, S. H., 2018, "Orchestrating the Proteome with Post-Translational Modifications", *Journal of Experimental Botany*, Vol. 69, No. 19, pp. 4499–4503.

Villiger, L., J. Joung, L. Koblan, J. Weissman, O. O. Abudayyeh, and J. S. Gootenberg, 2024, "CRISPR Technologies for Genome, Epigenome and Transcriptome Editing", *Nature Reviews Molecular Cell Biology*, Vol. 25, No. 6, pp. 464–487.

Wang, J. Y., and J. A. Doudna, 2024, "CRISPR Technology: A Decade of Genome Editing Is Only the Beginning", *Science (New York, N.Y.)*, Vol. 379, No. 6629, pp. eadd8643.

Wasik, U., and A. Filipek, 2014, "Non-Nuclear Function of Sumoylated Proteins", *Biochimica et Biophysica Acta*, Vol. 1843, No. 12, pp. 2878–2885.

Wilkinson, R. A., C. Martin, A. A. Nemudryi, and B. Wiedenheft, 2019, "CRISPR RNA-Guided Autonomous Delivery of Cas9", *Nature Structural & Molecular Biology*, Vol. 26, No. 1, pp. 14–24.

Xu, P., and R. Derynck, 2010, "Direct Activation of TACE-Mediated Ectodomain Shedding by P38 MAP Kinase Regulates EGF Receptor-Dependent Cell Proliferation", *Molecular Cell*, Vol. 37, No. 4, pp. 551–566.

Xu, P., J. Liu, M. Sakaki-Yumoto, and R. Derynck, 2012, "TACE Activation by MAPK-Mediated Regulation of Cell Surface Dimerization and TIMP3 Association", *Science Signaling*, Vol. 5, No. 222, pp. ra34.

Yeşildağ, D., 2019, *Identification of The Major Sumoylation Site on CRISPR Cas9 Protein*, M.S. Thesis, Boğaziçi University.

Yoda, M., T. Kimura, T. Tohmonda, H. Morioka, M. Matsumoto, Y. Okada, Y. Toyama, and K. Horiuchi, 2013, "Systemic Overexpression of TNFα-Converting Enzyme Does Not Lead to Enhanced Shedding Activity In Vivo", *PLoS ONE*, Vol. 8, No. 1.

Zhang, X., L. Tang, and Z. Zhang, 2021, "ADAM10 and ADAM17 Are Degraded by Lysosomal Pathway via Asparagine Endopeptidase", *Biochemical and Biophysical Research Communications*, Vol. 537, pp. 15–21.

Zhao, Q., Y. Xie, Y. Zheng, S. Jiang, W. Liu, W. Mu, Z. Liu, Y. Zhao, Y. Xue, and J. Ren, 2014, "GPS-SUMO: A Tool for the Prediction of Sumoylation Sites and SUMO-Interaction Motifs", *Nucleic Acids Research*, Vol. 42, No. W1, pp. W325–W330.

Zunke, F., and S. Rose-John, 2017, "The Shedding Protease ADAM17: Physiology and Pathophysiology", *Biochimica et Biophysica Acta - Molecular Cell Research*, Vol. 1864, No. 11 Pt B, pp. 2059–2070.

APPENDIX: PERMISSIONS FROM QUOTED FIGURES

Figure 1.1 is reprinted from Salas-Lloret, D., and R. González-Prieto, 2022, "Insights in Post-Translational Modifications: Ubiquitin and SUMO", *International Journal of Molecular Sciences*, Vol. 23, No 6, 321., with open access by MDPI. For more information, please visit “MDPI Open Access Information and Policy”.

Figure 1.2 is reprinted from Sahin, U., H. de Thé, and V. Lallemand-Breitenbac, 2022, "Sumoylation in Physiology, Pathology and Therapy", *Cells*, Vol. 11, No 5, 814., with open access by MDPI. For more information, please visit “MDPI Open Access Information and Policy”.

Figure 1.3 is reprinted from Celen, A. B., and U. Sahin, 2020, "Sumoylation on Its 25th Anniversary: Mechanisms, Pathology, and Emerging Concepts", *FEBS Journal*, Vol. 287, No. 15, pp. 3110–3140., with permission from John Wiley and Sons.

Figure 1.4 and Figure 1.5 are reprinted from Wang, J. Y., and J. A. Doudna, 2024, "CRISPR Technology: A Decade of Genome Editing Is Only the Beginning", *Science (New York, N.Y.)*, Vol. 379, No. 6629, pp. eadd8643. These figures are used under a Creative Commons Attribution License (CC-BY 4.0) or Creative Commons Attribution-NonCommercial License (CC BY-NC 4.0), which permits sharing and adaptation with attribution to the authors and the published article details.

Figure 1.6 is reprinted from Blobel, C. P., 2005, "ADAMs: Key Components in EGFR Signalling and Development", *Nature Reviews Molecular Cell Biology*, Vol. 6, No. 1, pp. 32–43., with permission from Springer Nature.

Figure 1.7 is reprinted from Zunke, F., and S. Rose-John, 2017, "The Shedding Protease ADAM17: Physiology and Pathophysiology", *Biochimica et Biophysica Acta* -

Molecular Cell Research, Vol. 1864, No. 11 Pt B, pp. 2059–2070, with permission from Elsevier.

Figure 1.8 is reprinted from Düsterhöft S., A. Babendreyer, A. A. Giese, C. Flasshove, and A. Ludwig, 2019, "Status Update on IRhom and ADAM17: It's Still Complicated". *Biochimica et Biophysica Acta - Molecular Cell Research,* Vol. 1866, No. 10, pp. 1567–1583, with permission from Elsevier.

Figure 1.9 is reprinted from Grötzinger, J., I. Lorenzen, and S. Düsterhöft, 2017, "Molecular Insights into the Multilayered Regulation of ADAM17: The Role of the Extracellular Region", *Biochimica et Biophysica Acta - Molecular Cell Research,* Vol. 1864, No. 11, pp. 2088–2095, with permission from Elsevier.

Figure 4.1 is reprinted from Sahin, U., F. Jollivet, C. Berthier, H. de Thé, and V. Lallemand-Breitenbach, 2016, "Detection of Protein SUMOylation In Situ by Proximity Ligation Assays", *Methods in molecular biology (Clifton, N.J.),* Vol. 1475, pp. 139–150., with permission from Springer Nature.

Figure 4.2 is reprinted from Sahin, U., G. Weskamp, Y. Zheng, V. Chesneau, K. Horiuchi, and C. P. Blobel, 2006, "A Sensitive Method to Monitor Ectodomain Shedding of Ligands of the Epidermal Growth Factor Receptor". *Methods in Molecular Biology (Clifton, N.J.),* Vol. 327, No. 5, pp. 99–113, with permission from Springer Nature.

Figures from this thesis research, for which the publishing house held the copyrights, were included in the thesis book according to the publisher's policy for reusing the author's text and graphics. Similarly, figures originating from this thesis and whose copyrights were transferred to the publishers were also incorporated, as per the "publishing policy valid for the re-use of the text and graphics produced by the author" stated on the publishers' websites. Figures 5.1, 5.2, 5.6, 5.7, and 5.8 were published by Life Sciences Alliance in the 2022 article "Sumoylation of Cas9 at Lysine 848 Regulates Protein Stability and DNA Binding" by Ergünay, T., Ö. Ayhan, A. B. Celen, P. Georgiadou, E. Pekbilir, Y. T. Abaci, D. Yesildag, M. Rettel, U. Sobhiafshar, A. Ogmen, N. T. Emre, and U. Sahin, which appeared in Life

Science Alliance, Vol. 5 No. 4, pp. e202101078. The author of this thesis is also a co-author of the published article.